Robustness of steel structures - study of the applicability of innovative methods on real structures.

Auteur : Vermeylen, Maxime
Promoteur(s) : Demonceau, Jean-Francois
Faculté : Faculté des Sciences appliquées
Diplôme : Master en ingénieur civil des constructions, à finalité spécialisée en "civil engineering"
Année académique : 2020-2021
URI/URL : http://hdl.handle.net/2268.2/11550

Liege University
Faculty of Applied sciences
Academic year 2020-2021

Robustness of steel structures - study of the applicability of innovative methods on real structures.

Master's thesis carried out to obtain the degree of Master of Science in Civil Engineering

by Maxime Vermeylen

Jury members
Jean-François Demonceau (promoter)
Jean-Pierre Jaspart (co-promoter)
Jean-Marc Franssen
Tudor Golea
Freddy Wertz
Klauss Weynand

Acknowledgements

Ce travail de fin d'études représente le fruit d'un long parcours. Il est l'aboutissement de plusieurs années passées sur les bancs de l'Université à apprendre, comprendre et étudier. Par le biais de ces quelques lignes, je tiens à remercier toutes les personnes qui ont été présentes pour moi, durant ces derniers mois.

En particulier, je tiens à exprimer toute ma reconnaissance à monsieur Demonceau et monsieur Jaspart qui m'ont guidés pendant ce travail. Malgré leur agenda chargé et une situation particulière, ils ont fait de leur mieux pour me fournir des informations de qualité et ce, rapidement. Je remercie également un de leur doctorant; Tudor.

J'adresse, également, mes remerciements à monsieur Wertz du bureau Feldman + Weynand qui m'a accompagné et transmis toutes les informations nécessaires au début de ce travail de fin d'études.

Je remercie aussi les membres de mon jury; monsieur Franssen et monsieur Weynand pour l'intérêt qu'ils portent à mon travail.

Je remercie André d'avoir pris le temps de relire attentivement mon travail de fin d'études.

Ma famille et mes amis ont également été très encourageant durant ce travail et je les en remercie.

Je suis très reconnaissant envers mes parents qui ont tout mis en oeuvre pour que je puisse effectuer mon travail de fin d'études dans de bonnes conditions.

J'adresse également tout mon courage à mon petit frère Clément, pour ces belles études qui l'attendent.

Finalement je remercie Adeline pour sa présence et ses mots reconfortants.

Maxime

Résumé

La demande de robustesse des structures est un sujet récent visant à assurer l'intégrité structurelle d'une structure en cas d'événements exceptionnels. Des recommandations générales de conception sont fournies dans les codes et normes modernes mais elles sont loin d'être satisfaisantes car il a été démontré que le respect de ces recommandations ne permet pas nécessairement de garantir la robustesse d'une structure. C'est la raison pour laquelle des activités de recherche sont toujours en cours dans ce domaine en vue (i) de maîtriser la réponse des structures lorsqu'elles sont soumises à des événements exceptionnels et, sur cette base, (ii) d'en déduire des règles pour les praticiens.
Ce travail de fin d'études s'inscrit dans ce contexte.

L'objectif de ce travail de fin d'études est d'étudier et d'appliquer des méthodes pour les structures de bâtiments en acier permettant d'atteindre un niveau de robustesse approprié. Ces recherches seront réalisées dans le cadre d'un projet européen RFCS en cours intitulé "FailNoMore".

En particulier, une structure métallique 3D, initialement dimensionnée par un bureau d'études allemand pour des conditions de chargement "classiques", sera étudiée en vue (i) de caractériser son comportement lorsqu'elle est soumise à un événement exceptionnel spécifique, à savoir la perte d'une colonne, et (ii) d'étudier l'efficacité des méthodes de conception existantes pour assurer la robustesse.
A la fin du travail, une analyse critique des résultats obtenus avec les différentes méthodes sera fournie en vue de faire des recommandations pour le practicien.

Ces objectifs seront atteints en utilisant des approches numériques et analytiques. Les recherches numériques seront réalisées à l'aide du logiciel FINELG.

Ce travail de fin d'études mettra en évidence que la méthode des tirants, telle qu'elle est présente dans l'Eurocode ne permet pas d'assurer une robustesse suffisante dans le cas du scénario considéré de la perte d'une colonne.

Il est aussi montré que, à la suite d'une étude numérique, la faiblesse de la structure se situe au niveau des assemblages. Une structure avec des assemblages articulés n'est pas robuste lorsqu'une perte de colonne est envisagée.

Par l'utilisation d'assemblages partiellement résistant, et au moyen d'une approche analytique innovante, il est montré que la structure considérée peut être robuste sous le scenario exceptionnelle envisagée de la perte de la colonne, en modifiant légérement les propriétés de la structure.

Summary

The request for robustness of structures is a recent topic aiming at ensuring the structural integrity of a structure in case of exceptional events. General design recommendations are provided in modern codes and standards but they are far from being satisfactory as it has been demonstrated that the respect of these recommendations do not necessarily allow to guarantee a sufficient robustness to a structure. It is the reason why research activities are still ongoing in this field in view of (i) mastering the response of structures when subjected to exceptional events and, on this basis, (ii) to derive rules for practitioners. This master thesis takes place in this context.

The objective of this master thesis is to study and apply methods for steel building structures allowing to reach an appropriate level of robustness. These research will be performed in the framework of an ongoing European RFCS project entitled "FailNoMore".

In particular, a 3D steel structures, initially designed by a German design office for "classical" loading conditions, will be studied in view of (i) characterising its behaviour when subjected to a specific exceptional event, i.e. the loss of a supporting member, and of (ii) investigating the efficiency of existing design methods for robustness. At the end of the work, a critical analysis of the results obtained with the different methods will be provided in view of making recommendations for practice.

These objectives will be achieved using numerical and analytical approaches. The numerical investigations will be realised using the FINELG software.

This master thesis will show that the tying method, such as it is present in the Eurocode, does not make it possible to ensure a sufficient robustness in the case of the scenario considered of the loss of a column.
It is also shown that, following a numerical study, the weakness of the structure is in the connections. A structure with hinged connections is not robust when column loss is considered. By using partially resistant connections, and by means of an innovative analytical approach, it is shown that the considered structure can be robust under the exceptional scenario of column loss by slightly modifying the properties of the structure.

Contents

1 Introduction

1 Introduction to robustness

The robustness of structure is a fairly new concept aimed at ensuring the structural integrity of a structure under an exceptional event. It is a subject that has been developing for several years and on which a lot of research has already been conducted and is being conducted.

Uncommon terms, linked to the robustness, have been cited, namely, structural integrity and exceptional event.
The structural integrity of a building is about ensuring that, under exceptional events, a building remains globally stable, even if some of its structural members failed.
An exceptional event is an event with major consequences but with a low probability of occurrence. So low, that the event is not taken into account in the design.

The first time the concept of robustness was mentioned was after the Ronan Point disaster in 1968. The structure consisted of prefabricated concrete slabs and walls that were joined together with mortar, without additional reinforcement. Following a gas explosion in a corner flat on the 18th floor, the load-bearing walls of the floor were destroyed, which resulted in the ruin of the last 4 floors above. Subsequently, due to an overload of the weight of the broken floors on the 18th floor, the whole corner of the building collapsed, causing the death of 4 people. The collapse of the building took place progressively. First the floors above the explosion collapsed one after the other. Then the lower floors collapsed, starting with the highest floor and going down to the lowest. This type of collapse is called a progressive collapse.

Figure 1.1: Ronan point collapse [1].

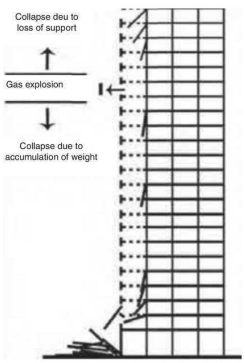

Figure 1.2: Ronan point collapse [2].

[2] https://www.designingbuildings.co.uk/wiki/File:Ronan_Point.jpg

[2] https://www.elsevier.es/es-revista-hormigon-acero-394-articulo-robustness-the-quality\-ribera-missed-S0439568917300992

As a result of this accident, the design rules for UK buildings were changed. A clause was added covering disproportionate failure, stating that "*a building shall be constructed in such a way that in the event of an accidental event, the building does not suffer disproportionate failure due to the cause*". In addition, an accidental load design value has been developed. Subsequently, the design codes of other countries were based on the British one.

The second major event that also played a role in the development of robustness was the collapse of the Twin Towers on 11 September 2001. Following a terrorist attack, where two planes collided in two towers, the buildings collapsed. The scenario for the two towers is the same. The planes collided with the towers on high floors, between the 77th and 85th floor for one tower and between the 93rd and 95th floor for the other tower. When the planes collided with the towers, the buildings remained intact and did not collapse. However, following the impact and the presence of a large quantity of kerosene in the planes, a fire started and then spread to the tower.

The structural system of the tower consisted of facade columns connected by steel beams to a very rigid central core. The steel beams were simply placed on legs attached to the columns. The structural diagram is shown in Figure 1.3. However, due to the increase in temperature following the fire, the steel beams expanded. The central core being very rigid, the beams pushed on the facade columns which deformed strongly. With the onset of these displacements, second order effects were induced in the facade columns, which led to their failure. Since the facade columns were broken, the beams over the entire height of the building were no longer connected and the ruin of the building occurred.

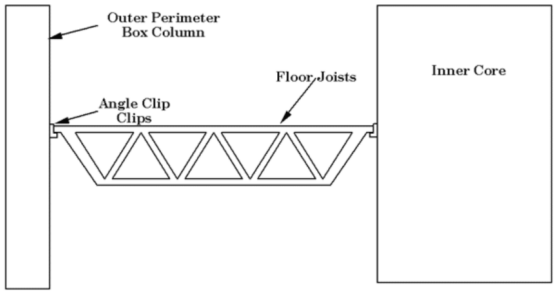

Figure 1.3: Structural scheme of the tower (Demonceau and Dewals, 2020).

Figure 1.4: Towers after the collapse [3].

At the time of its design, given the proximity of the towers to New York's John F. Kennedy International Airport, it was decided to take into account the impact of an aircraft on the tower. In addition, the beams were covered with flocking to limit the impact of a fire in the tower. On September 11, following the impact, the towers remained in place. However, as the aircraft removed the fireproofing during the impact, the beams were no longer protected against fire, and the fire caused the building to collapse.

[3] `https://www.thekongblog.com/2014/09/911-timeline-timeline-on-september-11th.html`

It is therefore a succession of events that in this case caused the ruin of the building and the death of 3000 people. In addition to the direct damage, these events led to indirect damage, such as the impossibility of using the area around the towers, which led to the temporary closure of several buildings.

Between these two events, 33 years have passed, but there are several points in common. The first is that a rather local damage, compared to the size of the building, caused the disproportionate collapse of the building. Secondly, the number of victims in both cases is significant. Finally, the ruin was caused by an insufficient design of the details, in this case the connections.

So, ensuring the robustness of a structure has several objectives:

1. to save lives by delaying the collapse of the structure.
2. if total collapse of the building can be avoided, to limit collateral damage.
3. to reduce the risk to the emergency teams.

2 Definitions

In this section, some definitions linked to the robustness of structure are proposed.

- Robustness
  According to Eurocode EN1991-1-7 (2006), *robustness is the ability of a structure to withstand events like fire, explosions, impact or the consequences of human error, without being damaged to an extent disproportionate to the original cause.*

- Exceptionnal loadings
  An exceptional load is a load with a low occurrence, so low that it is not taken into account in the design.

- Consequences classes
  A consequence class gives the consequences in terms of human lives lost. The Eurocode EN1991-1-7 (2006) defines 3 consequence classes with the second class divided into two subclasses. The consequence classes range from 1 to 3, with class 1 having the lowest consequence (e.g. a single family house) and class 3 having the highest consequence (e.g. a hospital). Depending on these consequence classes, different methods are used to ensure the robustness of the building.

- Progressive collapse
  The progressive collapse is the chain collapse of the structure, when one floor collapses after another, like the collapse of a house of cards for example.

- Key elements
  There are two distinct definitions for the key elements.
  The first one, it is an element that must resist the exceptional event and therefore be designed as such.
  The second version, it is an element designed to break first to avoid the propagation of damage and thus ensure structural integrity.

3 State of the art

3.1 Normative approach

Currently, it is the Eurocode EN1991-1-7 (2006) that deals with the robustness of structures. The aim of this design standard is to give rules and strategies to protect buildings or structures against exceptional actions, whether identifiable or not.

The strategies given by the Eurocode can be divided into two categories

1. those based on the identification of the exceptional event.
2. those based on limiting the extent of local failure.

These two strategies are themselves divided into three sub-categories, Figure 1.5 shows this subdivision.

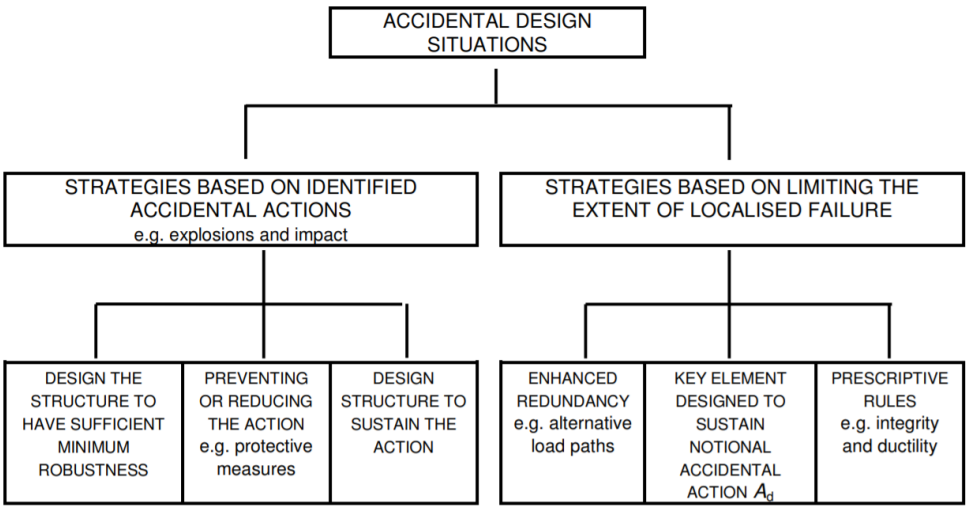

Figure 1.5: Strategies for accidental design situations (EN1991-1-7, 2006).

3.1.1 Based on identified actions

This strategy aims to identify the event beforehand and take measures to protect the building accordingly. It should be noted that only two types of events are covered by the Eurocode, explosions and impacts.

This strategy is subdivided into 3 possible approaches.

The first sub-division consists of designing the structure to provide a minimum level of robustness. But to do so, it is necessary to limit the extension of the local failure. This means following the second strategy which will be discussed in part 3.1.2.

The second sub-division, *preventing or reducing the action*, consists in implementing means to prevent or greatly reduce the effect of the action on the building. Since by definition risk is the product of occurrence and consequence, by implementing protective measures, the occurrence decreases and therefore the risk decreases as well.
To give some examples, to reduce the risk of fire, fire alarms can be used, or fire extinguishers can be placed in the building. To limit the risk of impact, protective elements (concrete blocks, steel barriers, etc.) could be placed to prevent impact on the building.

Finally for the last sub-division, *design structure to sustain the action*, this consists of considering the impact or explosion load and designing the structure so that it can resist the event. For this, the Eurocode gives values for the loads and how to apply them.

3.1.2 Limitation of the failure

The second strategy, on the right in Figure 1.5, consists in *limiting the extent of localised failure*. This strategy is divided into three sub-groups which can consist in a direct method, where a certain event is considered, or an indirect method.

The first sub-strategy is a direct method which consists in considering a certain event, applying it to the structure and checking if there is another structural path by which the forces can be transmitted to the foundations. This method is called the alternative load path method. But, it is heavy to apply, it requires a lot of calculations resources and sometimes the use of nonlinear models.
A representation of the method is given in Figure 1.6. In this figure, a column has been lost, and the forces that need to be transferred to another path are shown in red dashed lines. These mainly pass through the columns on either side of the lost column. Since the force passing through these columns is greater, their resistance must be calculated accordingly.

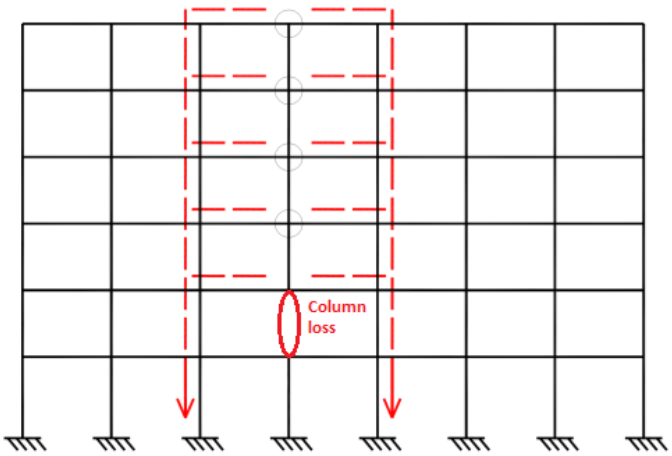

Figure 1.6: Alternative load path method (Demonceau and Dewals, 2020).

The second sub-strategy, the so-called key element method, is the second direct method. As said before there are two versions.
The first version consists in identifying the critical elements of the structure and ensuring that they can withstand the exceptional event. This can be done either by designing them to withstand the event or by protecting the sensitive elements.
The second version is the opposite of the first, i.e. the critical elements will be designed so that they break first. This may seem contradictory, but by ensuring that some elements break, the propagation of local failure to the whole structure is prevented.

In order to clearly distinguish the two versions, Figure 1.7 shows the key elements in its first version. Here, the facade columns and the roof beam have been designed to resist the column loss scenario. In contrast, Figure 1.8 shows the key element in its second version. Here, the beam connections have been designed to be brought to failure when column loss is considered. This results in the collapse of all the upper floors but allows the structure to remain in place on either side of the collapsed zone.

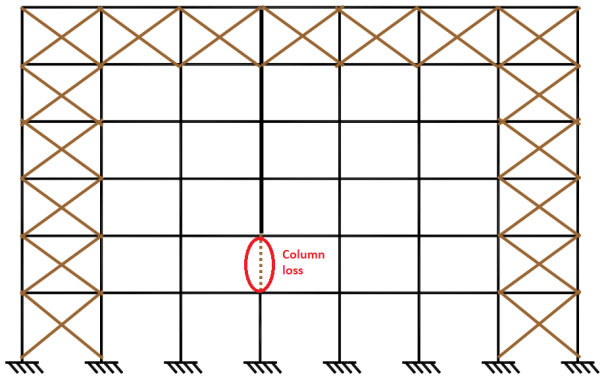

Figure 1.7: Version 1 of the key elements method (Demonceau and Dewals, 2020).

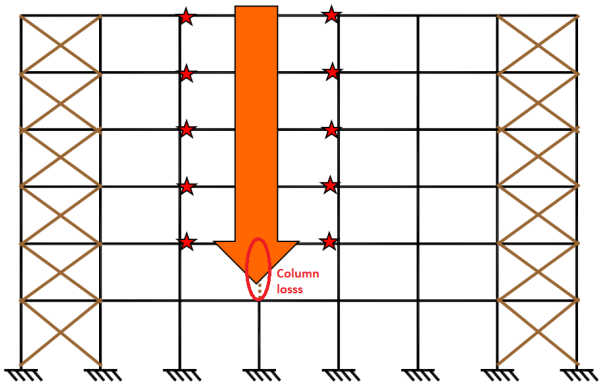

Figure 1.8: Version 2 of the key elements method (Demonceau and Dewals, 2020).

Finally, the third sub-strategy is the indirect method, the tying method. It consists of placing horizontal and vertical ties in the structure to ensure a continuity in the horizontal plane. The method calculates by empirical formulas a tensile force which the horizontal ties must resist. The method will be explained in more detail in part 3 section 4 of this master thesis.
This method is very controversial because it is empirical, it does not consider any specific scenario and it does not take into account ductility criteria.

3.2 Research carried out at the university of Liege

For several years, the University of Liege has been working on the field of robustness, and more particularly on the scenario of the loss of a column. The principle of this research is to study the behaviour of the building when one of its columns is brought to failure, to observe the redistribution of the forces in the structure and to find an alternative path of forces such that these can be brought down safely to the foundations.

A number of studies have been carried out to develop an analytical model that predicts the behaviour of a 2D structure subjected to a quasi-static column loss. When considering this scenario, the structure can be divided into two distinct parts;

1. the Directly Affected Part (DAP) which includes the beams, the column immediately above the lost column and the connections between the beams and columns, of the part affected by the event.

2. the Indirectly Affected Part (IAP) which includes the rest of the structure.

These two parts are distinguished in Figure 1.9.

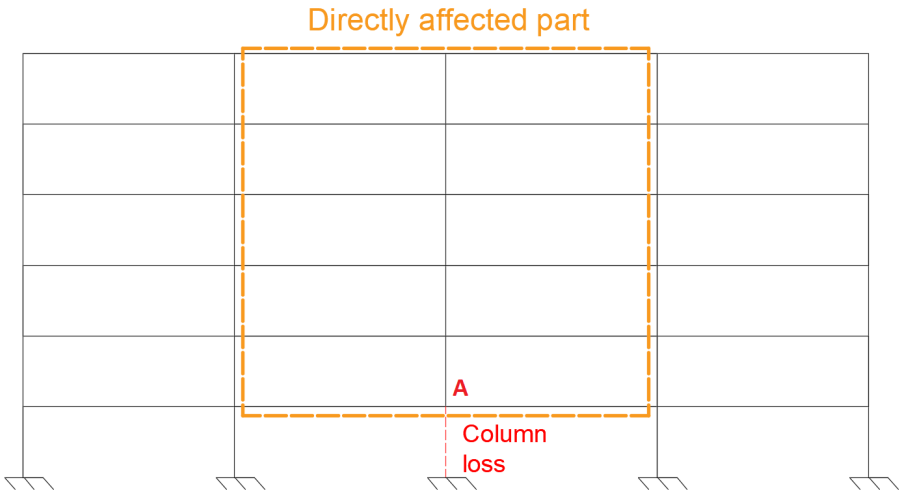

Figure 1.9: Localisation of the directly affected part.

Using the analytical model it is possible to plot the displacement of the lower part of the DAP (point A in Figure 1.9), where the top of the column is lost, as a function of the axial force in the lost column. The analytical model is based on the assumption of a quasi-static column loss. The potential dynamic effects induced by the column loss are not taken into account. In addition, other assumptions are made such as

- plastic hinges can develop either in the connections or in the beams.
- all the beams have the same cross-section.
- all columns have the same cross-section.
- the supports of the columns are assumed to be perfectly fixed.
- only an internal column loss is considered.

The vertical displacement u of the bottom of the DAP (point A in Figure 1.9) as a function of the axial force N_{AB} in the lost column is shown in Figure 1.10.

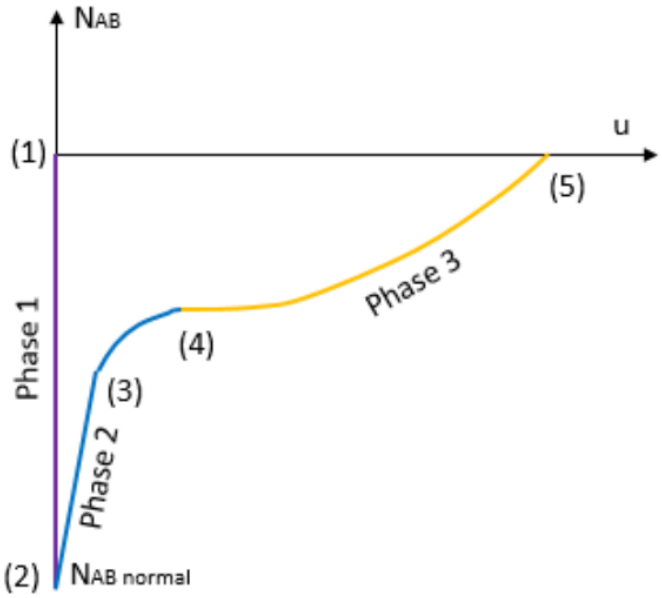

Figure 1.10: Vertical displacement u of the bottom of the DAP (point A Figure 1.9) as a function of the internal axial force N in the lost column (Huvelle et al., 2015).

This graph can be divided into 3 distinct phases :

1. Phase 1, which goes from point 1 to point 2, corresponds to the classical loading of the column.
   Point 1 represents the situation where the structure is not subjected to any load. Therefore the axial force is zero (if the selfweight is not considered).
   Point 2 corresponds to the case when all columns are present and the structure is loaded with a load combination. The column is therefore subjected to an axial force $N_{Ab,normal}$. There is also a shear force and a bending moment, but these are not of interest in the study of this graph.

2. Phase 2 can be divided into two sub-phases,

   - from point 2 to point 3. From point 2, the column starts to be removed in a quasi-static manner. From point 2 to point 3, the response of the structure is in the elastic range, no sections have yielded. As the column is progressively withdrawn, the axial force decreases and the vertical displacement increases.
   - from point 3 to point 4. From point 3, a break in the slope appears. This break corresponds to a loss of stiffness in the structure which is caused by the formation of a plastic hinge in the DAP. There will be as many slope breaks as there are plastic hinges. When they have all developed, this marks the end of phase 2, at point 4. A plastic mechanism therefore develops during this phase.

3. Phase 3 starts from point 4 to point 5. During this phase, there is no more first order stiffness, the plastic mechanism in the DAP has fully developed. Consequently, the vertical displacement u becomes significant. As the displacement increases, membrane forces begin to appear in the DAP of the structure. The appearance of these membrane forces provides a second order stiffness to the structure. Nonetheless, to withstand these tensile forces, the indirectly affected part has to exhibit adequate levels of resistance and ductility. The IAP serves as an anchor for the tensile forces transferred from the DAP.

Point 5, where the column is fully removed, can only be reached if it has been possible to find an alternative path for the forces that resists them. Indeed, since the column has been lost, part of the gravity actions must pass through another path to the foundations.

Phase 1 and 2 can be predicted easily by means of known analytical models. For phase 3, however, due to the large displacement and second order effects, a more complex analytical model had to be developed. The details of this one can be found in Huvelle et al. (2015).
Without going into details, this model takes into account a sub-structure composed of a DAP beam, whose behaviour is generalised to the others. The influence of the indirectly affected part is represented by means of springs at the extremities of the substructure. Another row of springs is also used to represent the yielding of the end of the beam, which can occur either in the beam in the case of full strength joints or in the joints if they are partial strength.

Over the last few years, a number of master thesis have been carried out on the robustness topic. Their content and results are presented briefly hereunder.

Kulik (2014) showed that the response of a steel frame 3D structure can be taken as the sum of the responses of the two perpendicular frames. In other words, there is no 3D coupling in the case of a column loss scenario in a steel structure.

Hjeir (2015) showed, by performing a parametric study, that for a 2D ULS-dimensioned frame with infinitely resistant and stiff joints, an increase in the cross-section of the roof beams was required to ensure the robustness of the steel structure. For a structure with simple joints, it was shown that for the ULS-dimensioned structure to be robust, the bracing and columns on either side of the lost column had to be reinforced.

During her research, Jacques (2019) improved Huvelle's model by taking into account more easily the influence of the IAP on the DAP. In addition, she also implemented the yielding of the IAP during phase 3 in the model.

Finally, Gemoets (2020) found from his research on a 2D steel frame that the tying method could not ensure the robustness of a 2D structure, as the empirical defined force was too small compared to that obtained by means of a nonlinear analysis. Furthermore, simple joints cannot ensure the robustness of a 2D structure.

4 Scope of the master thesis

This master thesis is part of a European project on robustness, the FailNoMore project. The aim of this project is to provide recommendations on the design of a steel or composite structure subjected to an exceptional event such as an explosion or an impact.

In this master thesis, the column loss scenario will be applied to a reference steel structure, studied in the FailNoMore project, previously designed by the German engineering office Feldman+Weynand.

In this work, the tying method will be studied with this reference structure. A critical analysis of the robustness provided by this method will be made. The relevance of its presence, as it is, in the Eurocode will be evaluated.

In order to test the validity of the prescriptive tying method, a nonlinear analysis of the structure under the scenario of a column loss will be performed. Several conclusions will be drawn from this comparison.

Then, an innovative model will be applied in order to assess the possibility to use it as an alternative and effective method for design aiming at robustness.

The master thesis will be organised as follows.

Firstly, the reference structure will be modelled and its design will be assessed by means of a linear elastic analysis with the `Finelg` software. This should allow the validation of the `Finelg` model by comparing the results of the analysis with those obtained by the Feldman+Weynand office.
After that, a short section will explain the parameters taken into account to perform nonlinear analysis. Several analyses will also be performed to check the validity of the nonlinear model.

Then, the scenario of the loss of the column will be studied with the previously validated nonlinear model. This study will allow to know the behaviour of the structure when a column is lost.

In order to find out whether the structure is robust or not, the tying method will be applied and the resistance of the different elements will be studied.

Afterwards, the results of the nonlinear analysis will be studied, in particular the internal forces in the DAP beams. The resistance of the beams will be investigated and an analysis of the connections under tensile forces will be performed in detail.

The last study will consist in analysis of the beams of the DAP with semi-rigid connections by means of a new analytical model that it can ensure the robustness of the structure.

A critical analysis of the different methods studied to ensure the robustness of the structure will conclude the master thesis.

2 Presentation of the reference structure

1 Introduction

In this section, the reference structure designed by the design office FELDMAN+WEYNAND will first be presented.

After that, the loads applied to the structure will be detailed and explained.

Then, the structure will be modelled in `Finelg` software. A design check will be performed based on a first order linear elastic analysis.

Finally, a comparison will be made between the results obtained with the FELDMAN+WEYNAND design with the `RSTAB` software and the results obtained with the `Finelg` software.
This will allow the `Finelg` numerical model to be validated.

2 Detailing of the structure

The reference structure that will be studied throughout this master thesis is a steel structure, with all the joints hinged and an inner core that serves as a lateral force resisting system. The function of the building is offices. The structure has already been designed by the German design office FELDMAN+WEYNAND which made use of the software `RSTAB`.

The steel structure consists of 3 spans of 12 m each, 6 bays of 8 m and 6 storeys of 4 m height. Therefore, the structure is 48 m long, 36 m wide and 24 m high. An inner core, consisting of inverted V-braces in both directions is used to ensure the lateral bracing.

A 3D representation of the steel structure and its dimensions is shown in Figure 2.1.

In order to transmit the horizontal forces to the inner core and the vertical forces to the beams, a 20 cm thick concrete slab is present on each floor of the structure. The slab works independently of the steel beams, in other words, there is no composite action. However, in view of the slab above the beams, it is assumed that this prevents the instability of the beams. Moreover, the assumption of an infinitely rigid slab in the horizontal plane is made.
In the model, the slab is modelled by X-bracings in the horizontal plane linking the columns together. The stiffness of the connecting rods of the crosses has a very high axial stiffness to respect the hypothesis of an infinitely rigid slab. For this purpose, the area of the connecting rod is $A = 0.1$ m^2 and its Young's modulus is $E = 2.1 \cdot 10^8$ Mpa. The slab model is shown in Figure 2.2 for one rectangle.

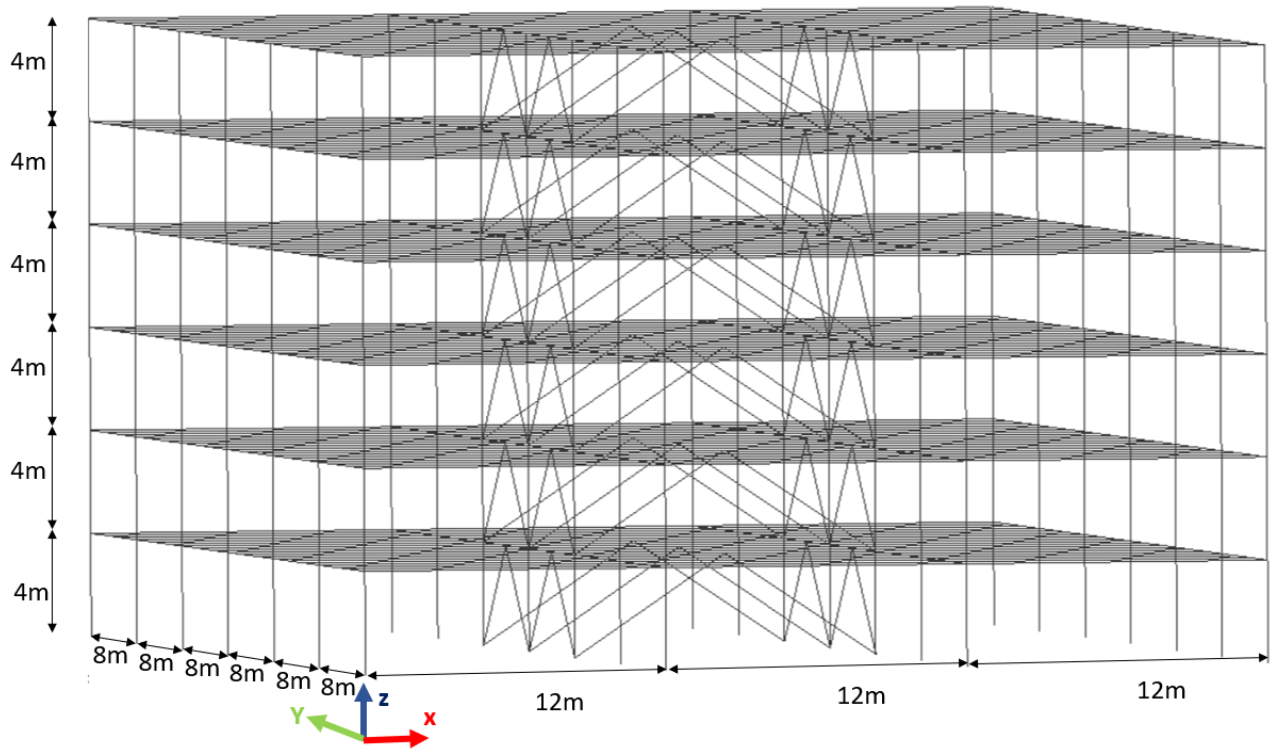

Figure 2.1: 3D view of the structure.

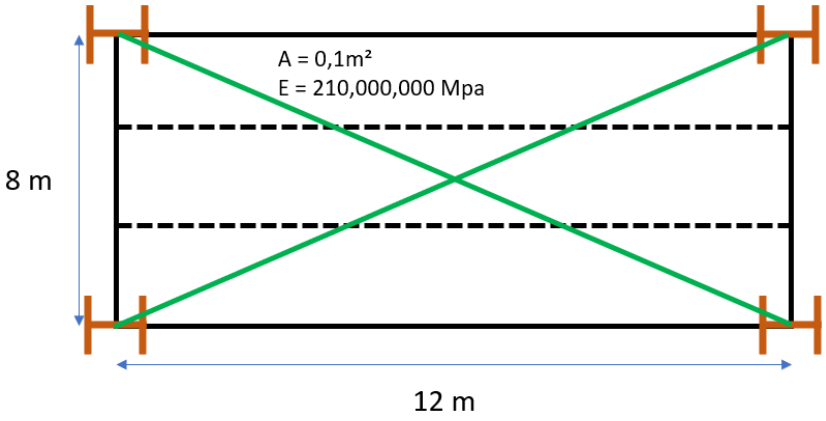

Figure 2.2: Modelling of the slab.

All structural beam members are considered to be made in one piece. This means that the beams are either 8 m or 12 m long. However it's not possible to obtain the column in a single piece. But in this master thesis, the splicing joints are not taken into account.

All the connections between elements are hinged. The supports are also hinges. Moreover, all beams elements work along their strong axis and the strong axis of the columns is directed along the global X-axis.
About the steel material, the steel grade is S355, the young modulus is taken equal to $E = 210000$ MPa and the poisson's ratio is equal to $\nu = 0.3$.

The bearing system of the structure is as follows,

1. the slab transmits the surface loads to the secondary beams which are 12 m long and spaced by 2.66 m in the Y-direction,
2. each secondary beam is supported by primary beam of 8 m length,
3. finally, the load is transferred by the primary beam to the column.

A scheme of the load descent is presented in Figure 2.3.

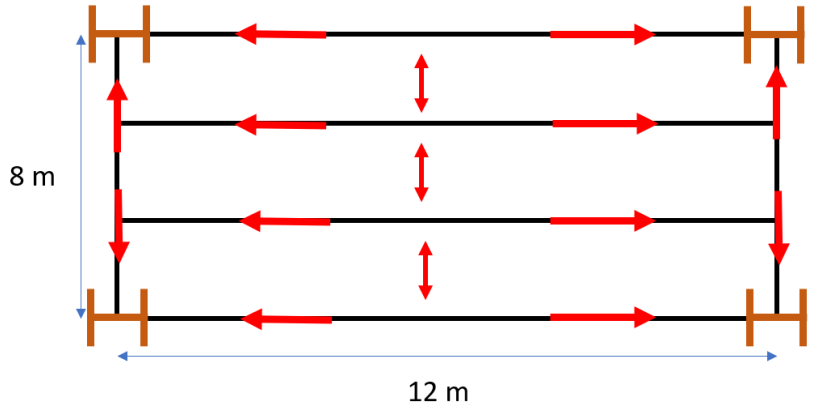

Figure 2.3: Load bearing descent.

Since the structure has already been designed, the cross-section of the different elements is known. These are presented in Figure 2.4 and Figure 2.5 for facade frames according to X-direction (short frame) and Y-direction (long frame) respectively.
The elements composing the internal frame according to X-direction without the inner core are presented in Figure 2.6, while frame with the inner core are presented in Figure 2.7.
Finally, the frame according to Y-direction is presented in Figure 2.8.

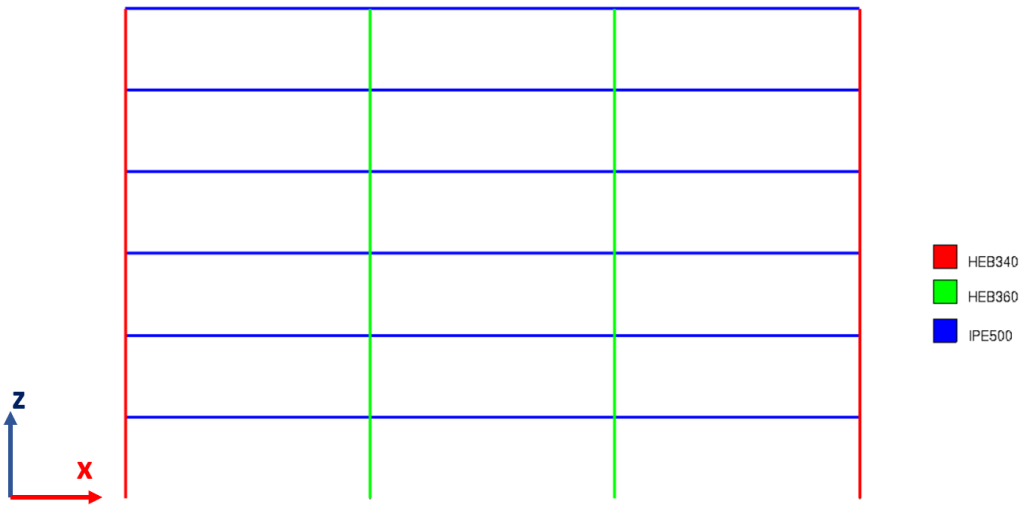

Figure 2.4: Cross-section of short facades elements.

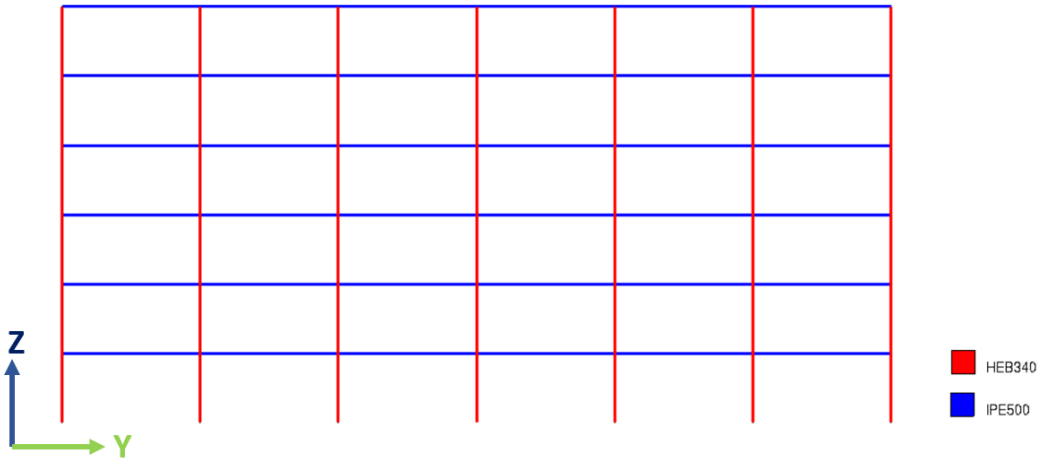

Figure 2.5: Cross-section of long facades elements.

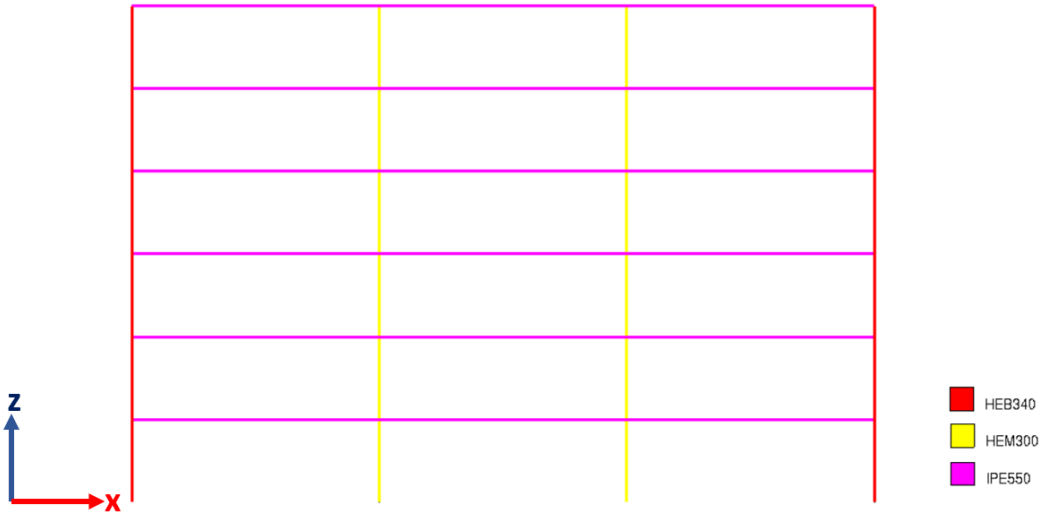

Figure 2.6: Cross-section of short internal frame elements, without inner core.

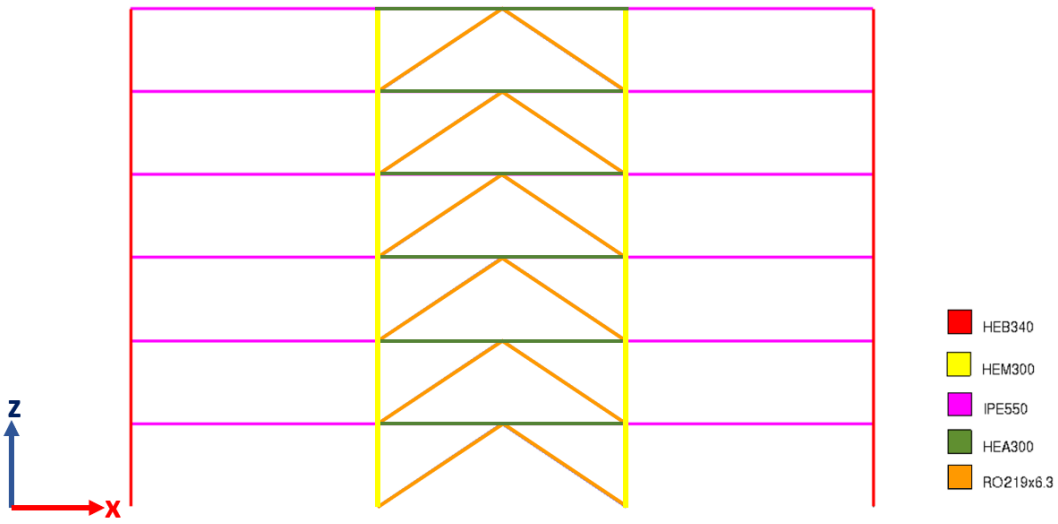

Figure 2.7: Cross-section of short internal frame elements, with inner core.

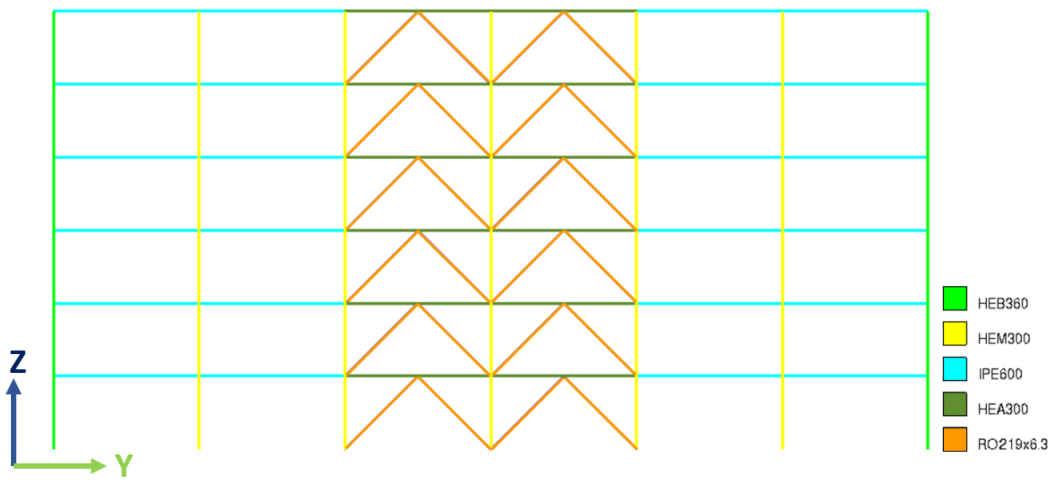

Figure 2.8: Cross-section of long internal frame elements.

For beam-column connections, there are 9 different types of connections. These are identified in Figure 2.9.

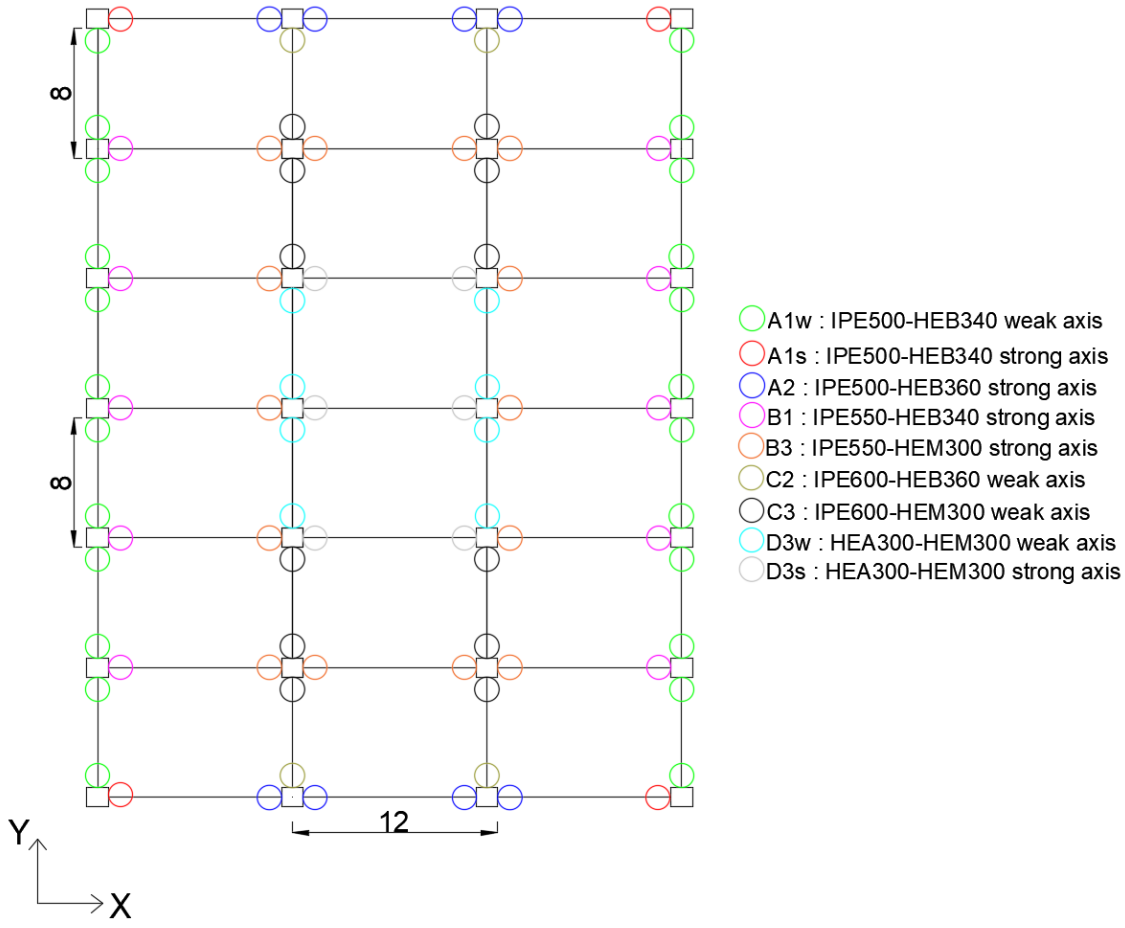

Figure 2.9: Identification of the different types of connections in the structure.

Since the column-beam connections are all hinged, a fin plate connection is used. All connection plates have a thickness of $t_p = 10$ mm, and are fillet welded with a design throat thickness of $a = 6$ mm. Concerning the bolts used, all connections except C2 and C3 have M20 10.9 bolts. The bolts of connections C2 and C3 are M24 10.9. Finally the steel grade of the fin plate is S355.
The geometric properties of the connections are given in Figure 2.10 to Figure 2.18, all the dimensions are in millimetre.

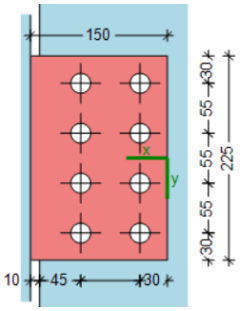

Figure 2.10: Geometric properties of the connection A1W.

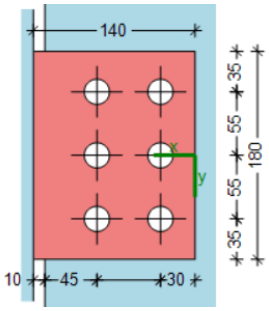

Figure 2.11: Geometric properties of the connection A1S.

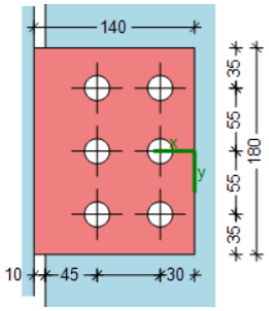

Figure 2.12: Geometric properties of the connection A2.

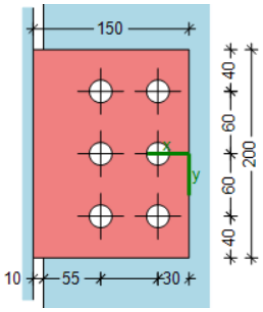

Figure 2.13: Geometric properties of the connection B1.

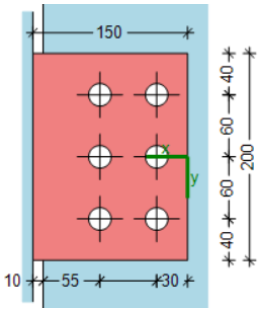

Figure 2.14: Geometric properties of the connection B3.

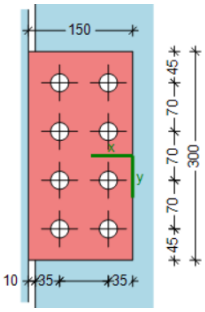

Figure 2.15: Geometric properties of the connection C2.

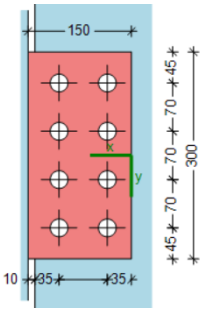

Figure 2.16: Geometric properties of the connection C3.

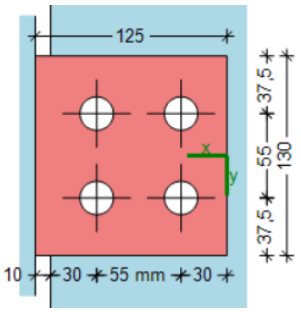

Figure 2.17: Geometric properties of the connection D3w.

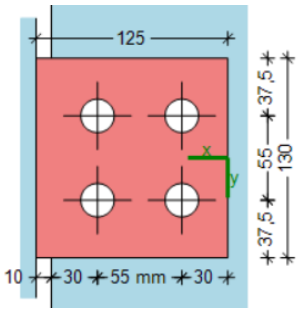

Figure 2.18: Geometric properties of the connection D3S.

3 Applied loads

In the study, five load cases are considered :

1. Permanent load (self-weight and dead load)
   The self-weight of the steel elements is automatically computed by the software. It has to be noted that the gravity constant in `Finelg` is equal to $g = 10$ m/s^2.
   The concrete slab dead load is 5 kN/m^2. On the perimeter beams, there is a facade linear load of 4 kN/m in direction of Z-axis.

2. Live Load
   We consider the function of the building as office. According to EN1991-1-1 (2002), the live load is 3 kN/m^2. Like the permanent load, the direction of this load is towards Z-axis.

3. Wind X-direction
   The direction of this load is towards X-axis and Z-axis. It is computed according to EN1991-1-4 (2005) with a reference wind pressure of 0.9 kN/m^2.

4. Snow
   These loads are computed according to EN1991-1-3 (2003). The characteristic snow load on the ground is 0.85 kN/m^2. The direction of this load is towards Z-axis.

5. Wind Y-direction
   The last load case considered is the wind towards Y-axis. Parameters are the same as the ones for wind X-direction.

4 Validation of the initial design

4.1 Linear elastic analysis of the structure

4.1.1 Modelling of global imperfections

In a first step, a first order linear elastic analysis is carried out to design the structure. Since the analysis is at first order, local imperfections are not taken into account in the analysis. They are taken into account during the verification of the elements. However, the global imperfections must be considered. According to EN1993-1-1 (2005), they are taken into account by horizontal forces applied at each floor with one direction at a time.

The horizontal imperfection force is equal to the product of the vertical force V_i applied on each floor and a coefficient ϕ, as follow,

$$H_{i,\text{imperfection}} = \phi \cdot V_i \tag{2.1}$$

where,

- i is the considered floor
- $\phi = \phi_0 \cdot \alpha_h \cdot \alpha_m$
  where,
  - $\phi_0 = \dfrac{1}{200}$
  - $\alpha_h = \dfrac{2}{\sqrt{h}} = \dfrac{2}{\sqrt{24}} = 0.6666$ because $\dfrac{2}{3} \leq \alpha_h \leq 1$, and h the building height (24 m).
  - $\alpha_m = \sqrt{0.5 \cdot \left(1 + \dfrac{1}{m}\right)}$ with m, is the number of columns in a row, including only those with a vertical load N_{Ed} greater than or equal to 50% of the average value per column in the vertical plane considered

For ease, two imperfection load cases are created per load case, one imperfection load case per direction. Moreover, formula 2.1 from EN1993-1-1 (2005) is for one frame. Since it's a 3D structure, the total imperfection force H_i is broken down into four frames for imperfection according to Y-direction and into seven frames for imperfection according to X-direction.

In each frame, the vertical forces acting in one storey level in a column are found as the difference between the normal forces in the column below the floor and the normal force in the column above the floor. Then these forces are multiplied by the coefficient ϕ, as explained in Figure 2.19 for the 4th floor.

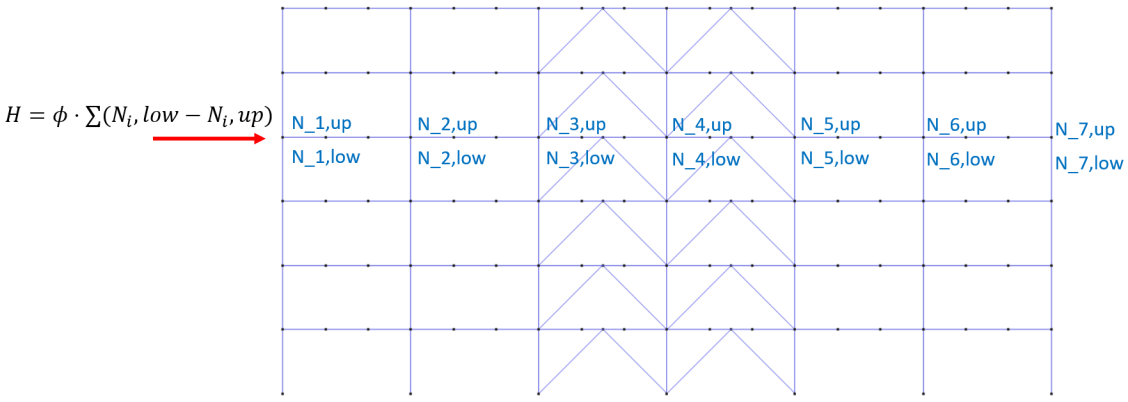

Figure 2.19: Computation of the horizontal imperfection force.

4.1.2 Modelling of loads

The transfer of the surface load from the slab to the beams is achieved by a slab of dimensions 12 m long and 2.66 m wide. Since one length is predominant over the other, the assumption of a span in one direction of the slab can be made.

In the model, the loads are therefore modelled as linear loads distributed over the secondary beams, 12 m long. A load descent is made from the slab to the secondary beam. The linear load as a function of the surface load for an internal beam is obtained by,

$$q_{linear} = \frac{q_{surface} \cdot 2.66}{2} \cdot 2$$

and for the facade beams by,

$$q_{linear} = \frac{q_{surface} \cdot 2.66}{2}$$

4.1.3 Materials law

The beams and columns of the structure follow an elastic law for this analysis. This is shown in Figure 2.20. Since an elastic law is considered, the verification of the elements is done a posteriori.

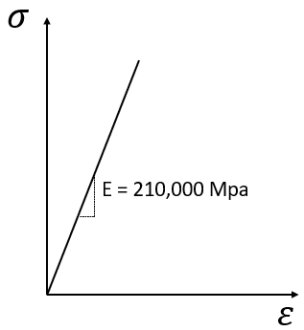

Figure 2.20: Material law considered for the beams and columns.

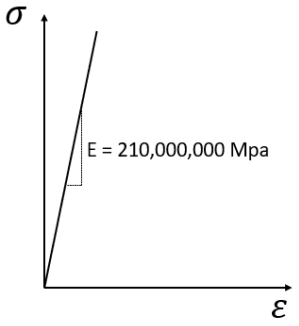

Figure 2.21: Material law considered for the diagonal rods simulating the diaphragm effect.

The material law for the rods modelling the concrete slab is also an elastic law. The great stiffness of the slab acting as a diaphragm is taken into account by allocating to the rods a very large Young's modulus, as shown in Figure 2.21.

Finally, the connections are considered infinitely stiff and ductile in the model. The strength of the joints will also be checked afterwards.

4.2 Checks at SLS

After the analysis, a first check is made. The verification at serviceability limit states is performed with the displacements obtained by the envelope (minimum and maximum) of all the load combinations. The load combinations are not detailed. However, a factor of 1 is applied to the dead load and to the predominant variable load. A ψ_0 factor is applied to the other variable loads, its value depends on the load considered : $\psi_0 = 0.7$ for the live load, $\psi_0 = 0.5$ for the snow and $\psi_0 = 0.6$ for the wind.
The limitation of vertical displacement is $L/250$, with L the beam span. All the results are given in Table 2.1.

Elements	Length [mm]	L/250 [mm]	Displacement [mm]
IPE500 short facade	12,000	48	42.8
IPE500 long facade	8,000	32	27.6
IPE550 internal beam X-dir.	12,000	48	44.2
IPE600 internal beam Y-dir.	8,000	32	26.9
HEA300 inner core beam X-dir.	12,000	48	5.3
HEA300 inner core beam Y-dir.	8,000	32	3

Table 2.1: SLS checks for displacements in Z-direction.

About the horizontal displacements, the requirement for the inter-storey drift is $h_{storey}/250$. The results are given in Table 2.2.

Elements	Height [mm]	H/250 [mm]	Displacement [mm]
HEB340	4,000	16	3.5
HEB360	4,000	16	1.96

Table 2.2: SLS checks for inter-storey drift.

As a conclusion, all the requirements at serviceability limit state are fulfilled.

4.3 Checks at ULS

In this part, the verification of the resistance of the different elements is made. As for SLS, the internal forces are coming from the diagram envelope. For the load combinations at ULS, a coefficient of 1.35 is applied to the permanent load and 1.5 on the dominant variable load while a factor of $1.5 \cdot \psi_0$ is applied to the other variable loads. Values of ψ_0 are the same than for SLS combination.
The internal force diagrams that were used for the design are presented in appendix A.

As a first step, the check of the columns is made, then the beams and the bracings are studied, to finish with the verification of the joints.

4.3.1 Columns

The first check performed is the one about the resistance of the columns. Due to the fact that beam-column connections are hinged, these ones are principally subjected to an axial force. There is also a small bending moment, but it is negligible in comparison to the internal axial force. The internal forces in the most critical sections are given in Table 2.3. Therefore, the check of the columns is based only on the internal axial forces, and the buckling instability are verified. All the sections are of class 1, it means that a plastic verification can be done. The verification of the columns is carried out in Table 2.4.

Columns	N_{Ed} [kN]	$M_{y,Ed}$ [kN.m]	$M_{z,Ed}$ [kN.m]	$T_{y,Ed}$ [kN]	$T_{z,Ed}$ [kN]
Long facade	-3780	16.01	0.12	0.23	20.94
Short facade	-3921	0.5	23.72	35.8	0.25
Internal	-6993	0.24	2.35	0.38	0

Table 2.3: Internal forces in the most critical section.

Columns	Cross section	N_{Ed} [kN]	$N_{Pl,Rd}$ [kN]	$N_{b,Rd}$ [kN]	Work ratio
Long facade	HEB340	-3,780.2	6,066.95	4,414.58	0.86
Short facade	HEB360	-3,930.6	6,411.3	4,651.59	0.84
Internal	HEM300	-6,993.3	10,760.05	8,099.3	0.87

Table 2.4: Verification of the columns, based on the internal axial force.

As shown in Table 2.4 all work ratios are below unity. The design of the columns is therefore ensured.

4.3.2 Beams

There are three different types of beams in the structure

1. the beams around the inner core, which represent all the beams in the structure except the beam of the bracing and the bracing elements,
2. the beam of the bracing,
3. the bracing.

Beams around the inner core
Firstly, the internal beams of the structure are verified, this does not include the beams of the bracing and the bracings. Contrary to columns, beams are mainly subjected to bending moment, so they will be checked on the basis of the resistant bending moment. The lateral instability of the beam will not be taken into account, since the slab restrains the transverse displacements of the beams. The internal forces are presented in Table 2.5. All beams are class 1, so a plastic verification can be performed. The verification of the beams is presented in Table 2.6.

Beams	N_{Ed} [kN]	$M_{y,Ed}$ [kN.m]	$M_{z,Ed}$ [kN.m]	$T_{y,Ed}$ [kN]	$T_{z,Ed}$ [kN]
Short facade	-1.83	401.47	0	0	93.74
Long facade	-18.77	577.54	0	0	14.39
Internal X-direction	-10.2	590.11	0	0	105
Internal Y-direction	-40.3	1060.11	0	0	9

Table 2.5: Internal forces in the most critical section of the different beams.

Beams	Cross section	$M_{y,Ed}$ [kN.m]	$M_{y,Pl,Rd}$ [kN.m]	Work ratio
Short facade	IPE500	401.47	778.87	0.52
Long facade	IPE500	577.54	778.87	0.74
Internal X-direction	IPE550	590.11	989.38	0.60
Internal Y-direction	IPE600	1062.33	1246.76	0.87

Table 2.6: Verification of the beams, based on the bending moment.

Contrary to the columns, the work ratios are not very close to the unit (except for the internal beams in Y-direction). The beams cannot be optimised with respect to bending moment, otherwise the displacements would have exceeded the permitted limit. Therefore the beams are designed to the SLS and not to the ULS except the internal beams in Y-direction which are designed at ULS.

Beams of the bracing

The beams of the bracing are different from the other beams because they are subjected to high bending moment and axial force. The design must therefore take into account the M-N interaction. In addition, the cross-section of the beams is class 3. A plastic verification cannot be performed and an elastic verification is made. The internal forces are presented in the Table 2.7. The elastic verification of the element taking into account the bending moment and the compression force is given in Table 2.8.

Beam	N_{Ed} [kN]	$M_{y,Ed}$ [kN.m]	$M_{z,Ed}$ [kN.m]	$T_{y,Ed}$ [kN]	$T_{z,Ed}$ [kN]
Beams of the bracing	-419.4	87.93	0	0	72.23

Table 2.7: Internal forces in the most critical section.

Axis	Cross-section	Axial contribution	Bending contribution	Work ratio
Strong axis	HEA300	0.14	0.21	0.35
Weak axis	HEA300	0.64	0.16	0.8

Table 2.8: Verification of the beams, based on axial force and the bending moment.

Since the work ratio is lower than one, the resistance of the internal core beams are verified.

Inverted V-bracing

As the diagonals are hinged at the extremities, they are only subject to normal force. It is therefore checked for axial forces and resistance to buckling. The cross-section of the bracings is class 1, so a plastic check can be performed. Since the length of the bracings in the two directions is not the same, the short bracing (Y-direction) and the long one (X-direction) are distinguished. The internal forces are presented in Table 2.9. The verification of the elements face to buckling is performed in Table 2.10.

Bracing	N_{Ed} [kN]	$M_{y,Ed}$ [kN.m]	$M_{z,Ed}$ [kN.m]	$T_{y,Ed}$ [kN]	$T_{z,Ed}$ [kN]
Long	-584.7	2.41	0	0	0
Short	-638.2	1.26	0	0	0

Table 2.9: Internal forces in the most critical section of the bracings.

Bracing	Cross section	N_{Ed} [kN]	$N_{Pl,Rd}$ [Kn]	$N_{b,Rd}$ [kN]	Work ratio
Long	RO219x6.3	-584.7	1494.5	675.45	0.87
Short	RO209x6.3	-683.2	1494.5	920.07	0.74

Table 2.10: Check of the bracings against buckling.

As before, the work ratios are all less than unit. Therefore the strength and the stability of the bracings are verified.

4.3.3 Joints

The last check carried out is the strength of the joints. There are 9 different types of joints, as already shown in Figure 2.9. Their shear resistance are computed with the software `COP`.

The joints are mainly subjected to a shear force, the normal force being relatively small and therefore negligible, the joints are designed on the basis of shear. For simplicity and as the design of the reference structure is not the main objective of this work, the shear force and shear strength of the joints are presented in Table 2.11. As before, the shear force comes from the envelope diagrams.

Connections	V_{Ed} [kN]	V_{Rd} [kN]
A1w	223	255.1
A1s	134	170.3
A2	134	170.3
B1	197	230
B3	197	230
C2	400	443.6
C3	400	443.6
D3w	70	102.6
D3s	120	122

Table 2.11: Shear resistance of the joints.

In order to meet the strength requirements, the thickness of the fin plate of the B1 and B3 connection has been increased by 2 mm and is now equals to $t_p = 12$ mm. This increase in plate thickness increases the weld throat thickness to $a = 7$ mm. Finally, the fin plate height for connection D3s has been increased by 10 mm.

The shear strengths of the connections are all greater than the applied force, so strength is assured.

5 Comparison with the preliminary design

After checking the design of the structure with `Finelg`, it appears that there are some differences with the design done by the FELDMAN+WEYNAND office.

Firstly, there is a difference in the design of the columns under axial load. The comparison of the work ratio between the two designs is presented in table 2.12.

Elements	WR from RSTAB	WR from FINELG
HEB340	0.95	0.86
HEB360	0.98	0.84
HEM300	0.95	0.87

Table 2.12: Comparison of the work ratio (WR) obtained by the design with the two models.

The difference comes from the fact that FELDMAN+WEYNAND being a German office, their standard recommends to use $\gamma_{M1} = 1.1$, whereas in Belgium, the code indicates $\gamma_{M1} = 1.0$. If we look closely, the difference between the work ratios is more or less 10%, which corresponds to the difference in value between the γ_{M1}.
For information, the design was also done with a $\gamma_{M1} = 1.1$, and the work ratios obtained with the two softwares then are the same.

A small difference in horizontal stiffness was also found between both model. This can be seen in the internal forces of the inner core, which is reflected in a difference in the work ratio of the core elements. But as the difference is relatively small, it is neglected.

Moreover the strength of some connections were very close to the applied force in the design made by FELDMAN+WEYNAND office. Due to the fact that, in the `Finelg` model, the internal forces differ by a few kN with the `Rstab` model, and since the initial resistance was very close to the applied shear force, some connections had to be modified slightly with the `Finelg` design.

In conclusion, differences between the two models exist but they are relatively small and the `Finelg` model can be validated.

6 Conclusion

In this first part, the reference structure was presented. The different beams and columns elements as well as the connections have been detailed. The applied loads have also been explained.

A first model was created using the `Finelg` software. Based on a linear elastic analysis, the internal forces in the structure have been established. This made it possible to verify the design of the reference structure.

Thanks to the verification of the design, the `Finelg` model could be validated. Although some differences in results were found, these were so small that they could be neglected.

In summary, now that the model of the structure has been verified, it can be used in the rest of this master thesis to study the scenario of the loss of the column.

3 Nonlinear analysis of the structure

1 Introduction

In this part, the nonlinear model is discussed.

Firstly, the nonlinear calculation software is presented. The modelling and discretisation of the nonlinear model is also explained.

Then, the differences between the parameters of the linear elastic analysis and those of the nonlinear analysis are established. Some new parameters have to be taken into account.

Finally, several comparisons between the linear and nonlinear model are made in order to validate the nonlinear model.

The aim of this part is therefore to set up the nonlinear model.

2 Description of the numerical model

As previously mentioned, the structure was modelled in `Finelg` software. It is a finite element software that allows to perform first order linear analysis, instability analysis, as well as nonlinear analysis. The non-linearity can be material (linear elastic perfectly plastic law, bi-linear law,...) or geometrical (local imperfections of the elements).

The structure was discretised in the software with elements of type 86 with a length of 1 metre. Each node is associated with 6 degrees of freedom, 3 in translation along the 3 directions X, Y and Z and 3 in rotation along the 3 axes of rotation around X, Y and Z.
This type of element makes it possible to take into account a 7th degree of freedom at each node, representing the warping. But, considering the hypothesis of the slab preventing instabilities like warping, the 7th degree of freedom is not used.

The fibre modelling the beam in the software is taken at the neutral axis of the beams. This means, at the connections, the forces are transferred between the neutral axis of the different elements.

The section used are type 91, which corresponds to a double tee section with equal flanges. The torsion theory considered by the software for this section is the Vlassov theory. A representation of the section is shown in Figure 3.1.

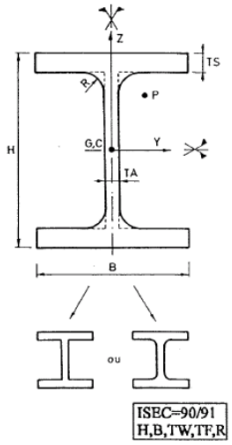

Figure 3.1: Representation of the section 91 in `Finelg`, (Greish and ULiege, 2003).

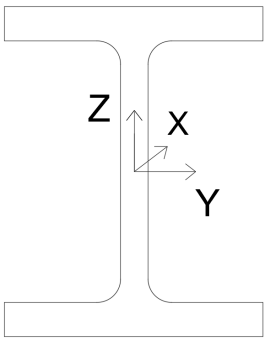

Figure 3.2: Representation of the local axes.

The parameters that must be entered into the software are the section height h, the section width b, the web thickness t_w, the flange thickness t_f and the fillet radius r. All these geometric values are taken from the Arcelor Mittal catalogue (ArcelorMittal, 2018). All the static properties of the section are calculated by the software a posteriori.

For each beam element, a local axis system is established. In the model, the local x-axis corresponds to the longitudinal axis of the beam, the local y-axis corresponds to the horizontal cross-sectional axis and the local z-axis corresponds to the global Z-axis, i.e. the vertical axis directed upwards. The local axes of the section are shown in Figure 3.2.

On a beam element, 4 integration points are present. These are not equally spaced along the length of the element. The Gaussian integration method is used. A representation of the distribution of the integration point over one element is given in Figure 3.3.

Concerning the integration points in the section, 13 columns of 3 integration points are present on each flange. On the web of the section, there are three columns of 7 integration points each. Finally, one integration point is present at each fillet radius. The distribution of integration points is given according to Figure 3.4, with the value used highlighted in red.

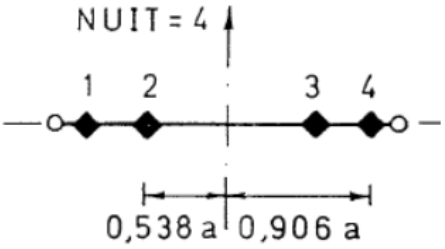

Figure 3.3: Representation of the integration point along the element (X-direction) (Greish and ULiege, 2003).

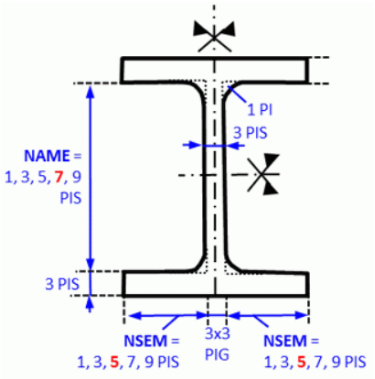

Figure 3.4: Representation of the integration point over the section (Greish and ULiege, 2003).

3 Differences with the linear analysis

Compared to a linear elastic analysis, several new parameters have to be considered when a nonlinear analysis is conducted. This part aims to describe these new parameters taken into account.

3.1 Material laws

Contrary to linear elastic analysis, which considered a linear elastic material law, nonlinear analysis considers an elastic perfectly plastic material law. This law is presented in Figure 3.5.

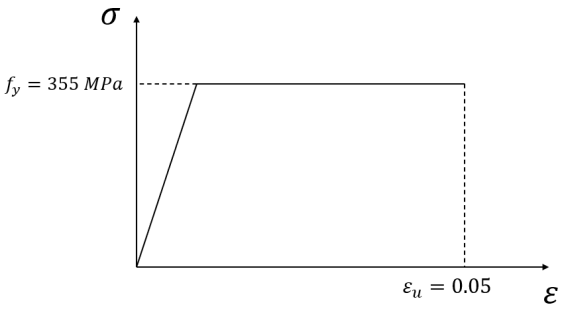

Figure 3.5: Steel law considered for the nonlinear analysis.

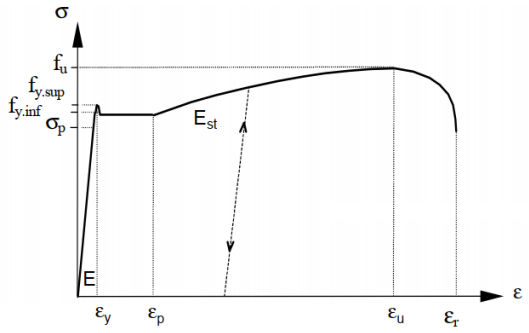

Figure 3.6: Real steel law behaviour, (Jaspart, 2015).

If we compare this law with the real law of steel, shown in Figure 3.6, it can be seen that the model law is safer than the real one. In the model, once the elastic limit f_y is reached, the stress cannot go any further and the deformation becomes infinite. The difference with the real material law is that the modelled law does not take into account the strain hardening of the steel. In the elastic-perfectly plastic law, the material is assumed to deform infinitely. But, in practice, the deformation of the element is finite. This limit is taken into account by the ultimate deformation ε_u. The chosen value of this parameter is 0.05.

3.2 Imperfections

As previously mentioned, two types of geometric imperfections are to be taken into account, the global imperfections relative to the whole structure and the local imperfections relative to each element.

The global imperfections are the same as in the linear analysis, they are detailed in part 4.1.1 of section 2.

Whereas the local imperfection was taken into account by the buckling curves in the verification of the elastic analysis, it is now taken explicitly in the analysis.
For that, a critical analysis is performed in order to know the shape of the deformed structure when a buckling instability appears in a column. This critical analysis can be done with the `Finelg` software. The method used to perform this analysis is not detailed in this work. Knowing the mode, an amplification factor of 4/1000 (where 4 is the height of the column) is applied on all the displacements of the structure. This factor corresponds to the deformation taken by the element at the exit of the rolling mill, taken as L/1000. Multiplying all displacements by 4/1000 gives a local deformation of L/1000 at the most critical element

After that, residual stresses are applied on the elements susceptible to buckle, in order to take into account all the local imperfection. In `Finelg`, there are pre-established schemes of residual stresses. The one used in the model, which corresponds to residual stresses in rolled profiles, is presented in Figure 3.7.

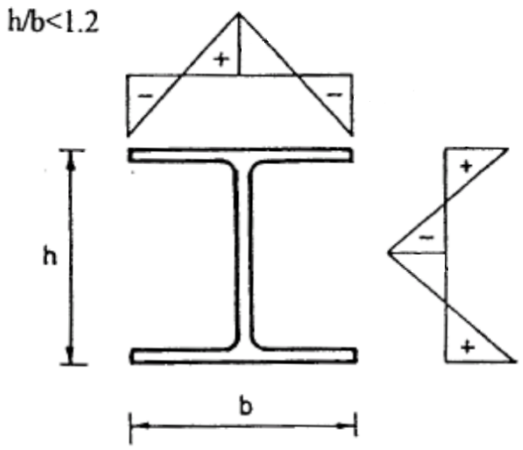

Figure 3.7: Scheme of residual stresses, (Greish and ULiege, 2003).

By combining the local deformation and the residual stresses at the exit of the rolling mill, the local imperfection is explicitly taken into account. For practical reasons, it was not possible to apply this local imperfection to all elements of the structure. However, having carried out a critical analysis, the critical column could be identified and the local imperfection applied to it. It was chosen to apply the local imperfection to a column because it is the element most likely to have instability first.

3.3 Lateral torsional instability restrain

As mentioned previously, the lateral torsional instability of beams is prevented by the slab. But the slab is not modelled explicitly, so the beams are free to move. To overcome this problem, the torsional inertia I_t is increased fictitiously in the software. The torsional buckling of a beam is an instability created by a rotation of the beam around its longitudinal axis with a lateral displacement. By fictitiously increasing the torsional inertia of the beam, it will not rotate and therefore the torsional buckling will not occur.

Several simulations were carried out to determine the minimum multiplier to be applied to avoid the occurrence of the torsional instability. The lowest multiplier found was a coefficient that multiplies the torsional inertia by 100.

3.4 Loads sequence modelling

The application of loads in a nonlinear analysis is different from the linear analysis. In a nonlinear analysis, loads are applied in increments. Several methods are available to apply the load. In this case, the imposed load step method is chosen. This consists of applying a fixed load increment $d\lambda$ at each step. The principle of the method is shown at Figure 3.8.

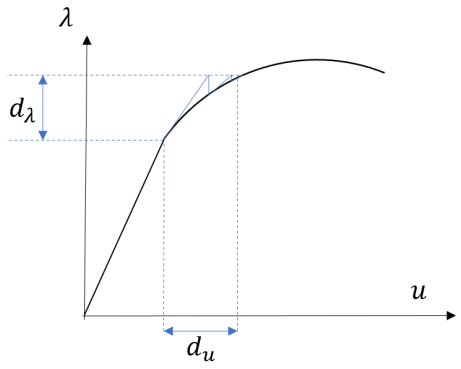

Figure 3.8: Imposed load step method.

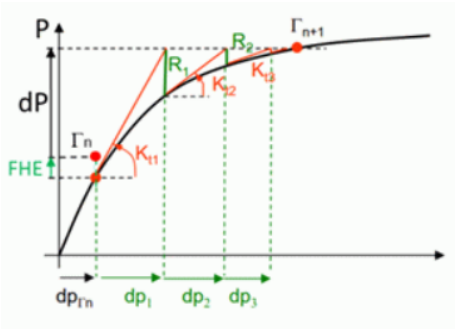

Figure 3.9: Iterative method, (Greish and ULiege, 2003)

Within each step $d\lambda$, iterations must be performed in order to find a new equilibrium in the structure after the application of the load increment $d\lambda$. For that, there are also several possible methods. In this case, the Newton-Raphson method is used. This iterative method is sketched in Figure 3.9.

4 Validation of the results of the nonlinear model

In order to validate the nonlinear model for research, some comparisons are made between the nonlinear and the linear analysis. Because it is not the topic of this master thesis, the detailed calculations are not shown, but only the different steps of analysis, their purpose and the conclusion.

A total of 4 cases were analysed :

1. The same vertical loads as in the linear analysis are applied in the nonlinear model, both without imperfections, in order to compare the vertical displacements. The difference between the two is almost zero.

2. The same vertical and horizontal loads as in the linear analysis are applied in the nonlinear model, both with imperfections, to compare the vertical and the horizontal displacements. The difference between the two is on average 1 mm, which is negligible.

3. Vertical loads are applied progressively and imperfections (global and local) are taken into account, in the nonlinear model. The aim is to compare the compressive load in the column for which buckling occurs, with the one computed analytically. All the beams have a behaviour infinitely elastic in order to promote the occurrence of a column buckling. For this case, the difference is remarkable with the value calculates with the codes. But the difference comes from the consideration of the non linearities. In fact, the equation which calculates the buckling resistance given in the Eurocodes is safer than the reality. So, having an axial force higher than the one given by the code is not surprising.

4. The last case concerns the yielding of the elements. For that, the nonlinear model is run a first time, it gives the bending moment for which the IPE600 beams yield. The value coming from the nonlinear model is compared with the plastic bending moment obtained analytically. The model is run a second time but this time with the beams IPE600 having an infinitely elastic law, in order to have the yielding of an other element. The method is repeated till all the values of yielding of the elements are checked.

All these checks gave results close to the results obtained with the linear elastic analysis. The nonlinear model may therefore be considered as being valid.

5 Conclusions

This short but essential part set the basis for the rest of this work : a numerical tool for nonlinear analysis.

Firstly, the `Finelg` calculation software was presented, followed by an explanation of the modelling and discretisation of the structure.

Then, the new parameters to be taken into account during the nonlinear analysis were explained.

Finally, the comparison of the results obtained with the nonlinear model with those of the linear model made it possible to validate the nonlinear model.

This model will therefore serve as a basic tool for the study of the column loss scenario developed in the next part.

4 Study of the column loss scenario

1 Introduction

This part of the work studies the scenario of the loss of a column of the reference structure and its robustness.

Firstly, the definition of the scenario is explained. The load combination taken into account as well as the modelling of the column loss are explained.

Next, the application of the indirect tying method is considered. It will give a first approach to the robustness of the structure.

Afterwards, a nonlinear analysis is performed using `Finelg` software. Two types of material laws are studied. The analysis is followed by a strength check of the structure.

Subsequently, a more precise study of the joints under membrane forces will be made. Ways to improve the tensile strength of these joints will also be studied.

Finally, a new analytical method to ensure the robustness of the structure is explained and applied.

In this section three methods for ensuring the robustness of the structure are studied, which allow comparisons and critical analysis.

2 Definition of the scenario

2.1 Load combinations

The scenario of the loss of a column is an exceptional scenario. According to EN1990 (2002), the combination of loads to be used is the following,

$$E_d = \sum_{j\geq 1} G_{k,j}" + "A_d" + "(\psi_{1,1} \text{ or } \psi_{2,1}) \cdot Q_{k,1}" + "\sum_{i>1} \psi_{2,i} \cdot Q_{k,i} \tag{4.1}$$

Since there is no fire or impact the term A_d for accidental action is zero. Moreover, the value of $\psi_{2,1}$ for climatic action is also zero according to EN1990-ANB:2021 (2013). The value of $\psi_{2,1}$ for the live load is equal to 0.3 for offices.
All in all, the load combination for the loss of a column for the case under consideration is

$$E_d = 1 \cdot \text{ Dead load } + 0.3 \cdot \text{ Live load}$$

Since the exceptional loading is quite simple, the linear applied load can be detailed. As a reminder, the load only acts on the IPE500 front beams and on the IPE550 and IPE600

internal beams.
The internal beams (without considering its self-weight) are subjected to a load of,

$$q_{inside} = (5 + 0.3 \cdot 3) \cdot \frac{8}{3} = 15.73 \ kN/m$$

while facade beams (without considering its self-weight) are subjected to a load of,

$$q_{facade} = (5 + 0.3 \cdot 3) \cdot \frac{8}{6} + 4 = 11.86 \ kN/m$$

2.2 Column loss location

The scenario studied is the one where the ground floor column n°6 is lost, see Figure 4.1. There are several reasons for this choice. The first, about the position on the height, is that a column lost on the ground floor will have a bigger impact than a column lost at the top of the structure. The redistributed forces will be more important. The second reason concerns the position of the column in the horizontal plane. Four possibilities could be studied :

1. a column at the corner of the structure, (columns 1; 4; 25; 28, Figure 4.1). If this column was studied, the results would not be conclusive. In fact, since the column is located at the corner, there is no rigidity on both side in the two directions. The loss of the column would lead to the ruin of the building. In general, corner columns should be sized as key elements.

2. a column in the front (columns 2-3; 5; 8; 9; 12; 13; 16; 17; 20; 21 ; 24; 26-27, Figure 4.1). This scenario is a little less damaging than the previous one. Depending on the column chosen, in one direction the column would have had stiffness on both sides of the DAP, but in the other direction there would have been stiffness only on one side.

3. a column in the inner core (columns 10-11; 14-15; 18-19, Figure 4.1). If this scenario was considered, the loss of the column would result in the loss of the bracing. However, following the loss of a column, large tensile forces appear in the beams of the structure. Since the structure's connections are all hinged, it is necessary to have an efficient bracing system to ensure that the horizontal forces are taken up. Therefore, the loss of one of the central inner core columns should totally be prevented.

4. an internal column (columns 6-7; 22-23, Figure 4.1). By studying these columns, the robustness of the structure is more likely to be ensured. Indeed, the IAP provides rigidity on both sides in both directions. The structure is therefore more likely to take up the redistributed forces and is therefore more likely to be able to resist the loss of the column.

All possibilities would be interesting to study. In this master thesis, only case 4 is analysed in detail because it corresponds to the best possibility of finding an alternative load path.
So, it is therefore the scenario of the loss of the internal column n°6 at the level of the ground floor that is envisaged.

As a result, the DAP of the short frame is showed in Figure 4.2 and in plane it is represented in the Figure 4.3.

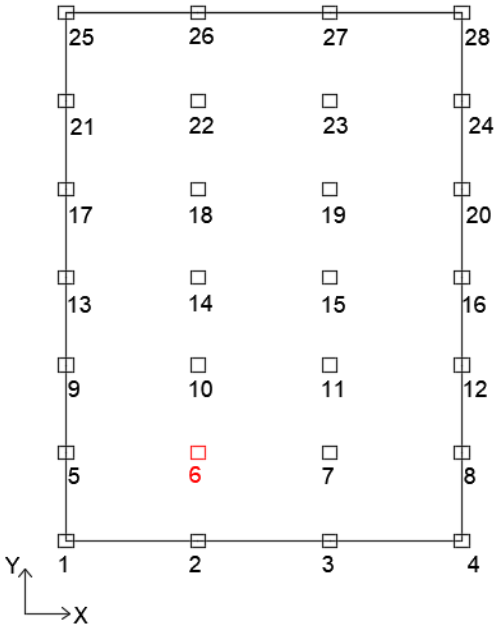

Figure 4.1: Plan view of the column considered.

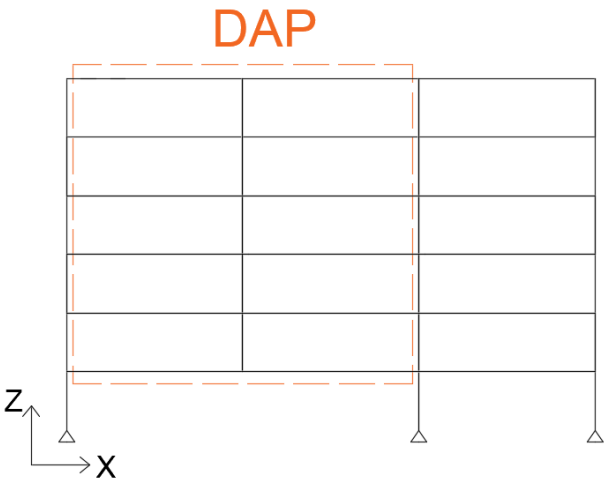

Figure 4.2: Representation of the DAP in the short frame.

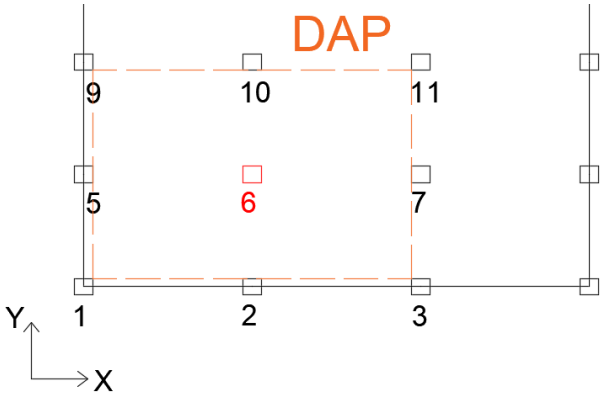

Figure 4.3: Representation of the DAP in plane.

2.3 Simulation of the column loss

In the numerical model, the column is not removed instantaneously, as this would lead to problems of numerical instabilities. The procedure followed to model the column loss in FINELG is as follows,

1. First, the structure is analysed under the combination of accidental loads, with all its columns present. The column to be removed in the next step, column n°6 at ground level, is subject to internal forces $[M_0,N_0,V_0]$ as shown in Figure 4.4 in the X-direction frame.

2. After that, the column will be removed and, at the upper intersection between the removed column and the beams, the internal forces $[M_0,N_0,V_0]$ is applied, as shown in Figure 4.5. Physically the column will no longer be there, but from a static point of view it will be present by the application of the external forces $[M_0,N_0,V_0]$.

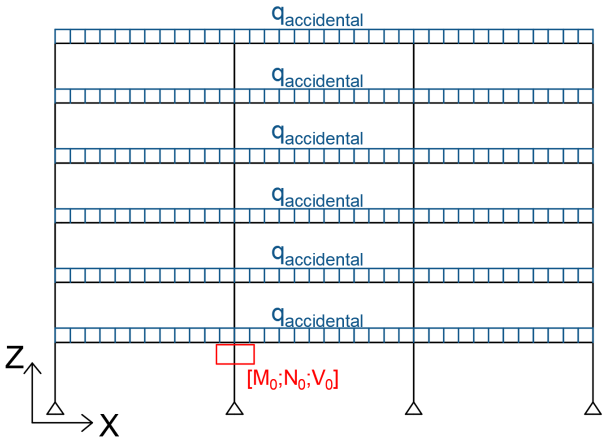

Figure 4.4: Initial configuration before the removal of the column.

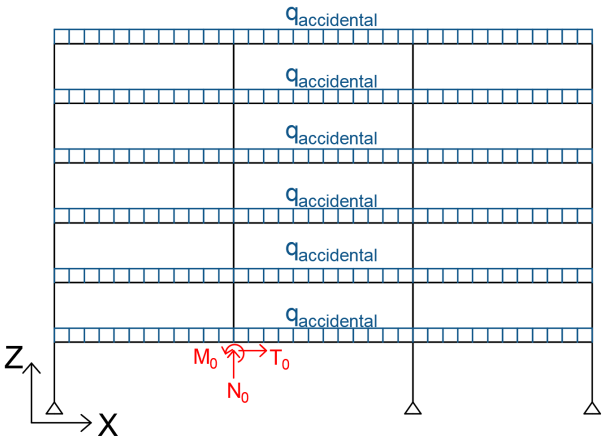

Figure 4.5: Removed column with internal forces applied.

3. Finally, to simulate the loss of the column, while the $[M_0,N_0,V_0]$ forces are applied, opposite forces are applied $[\lambda \cdot M_0,\ \lambda \cdot N_0,\ \lambda \cdot V_0]$, as shown in Figure 4.6. The removal of the column will be done gradually starting from $\lambda = 0$ to $\lambda = 1$ in steps of $d\lambda = 0.05$.

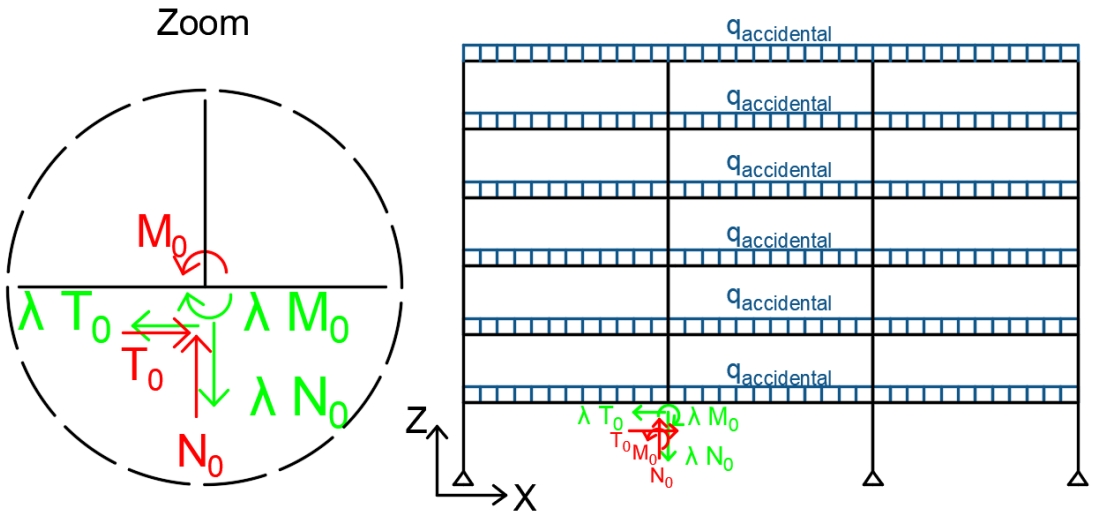

Figure 4.6: Simulation of column loss.

At the beginning, when $\lambda = 0$, the situation is as shown in Figure 4.5. The resultant of the force is

$$N_{result} = N_0 - \lambda \cdot N_0 = N_0 \tag{4.2}$$

This means that the column is still here.

When $\lambda = 1$, it means that the column is completely removed. The resultant of the force is

$$N_{result} = N_0 - \lambda \cdot N_0 = 0 \tag{4.3}$$

About the loading sequence, it follows the same principle as explained in the section 3.4. First, the accidental load combination is applied by imposed load steps of $d\lambda = 0.5$. In this sequence, the column has been removed but internal forces are applied to simulate the presence of the column, we are in the situation of Figure 4.5. The load is increased until it reaches the application of one time the accidental combination on the structure.

Once the accidental load combination has been applied, the column begins to be removed, this is the second sequence. Also through the imposed loading method, λ is increased gradually from 0 to 1 by steps of $d\lambda = 0.05$. We are in the case of the Figure 4.6. Once the column is completely removed, the program stops and returns the different results.

The load increment is higher when the accidental load combination is applied than when the column is removed because in the first case it is known that the structure is still in the linear range since the structure was originally designed for a higher load combination.

When considering the column loss scenario and in order to respect the assumption of a slab infinitely rigid in its plane, the slab model had to be adapted.

The connecting rods converging on the lost column have been removed for all storeys. Indeed, following the loss of the column, large vertical displacements occur. Since the connecting rods are very rigid, the displacement would put them in tension, which would have pulled on the indirectly affected part. But in reality, this is not the case: the column will slide through the slab, as there is no composite action. This is why these rods are removed.
The new slab model is shown in Figure 4.7.

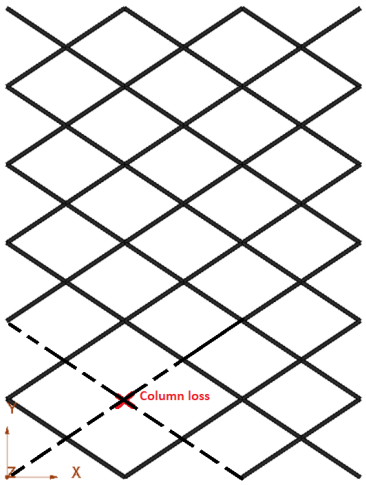

Figure 4.7: Modelling of the slab taking account the scenario of the loss of a column, with removed rods in dashed lines.

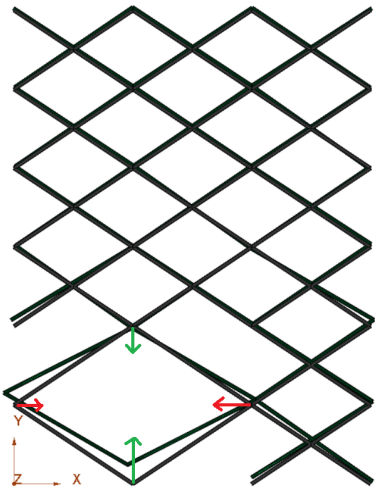

Figure 4.8: Deformed shape of the slab when the column is completely lost.

But after running the model, it appears that, when the column is completely lost, the modelled slab get deformed, see Figure 4.8. The tensile force along Y (green in Figure 4.8) is higher than the tensile force along X (red in Figure 4.8), which caused the deformation of the rhombus, and thus the deformation of the slab, which violated the assumption of an infinitely rigid slab. If the rhombus is deformed, it is because the whole of the bottom left corner is not at all rigid, unlike the top right corner which is very rigid due to the presence of the slab beyond the directly affected part.

To overcome this problem, infinitely rigid triangular plates are used to simulate the slab in the model. For this purpose, the sides of the rhombus will be closed externally by connecting rods of the same properties as the others rods.

The new model of the slab taking into account the improvements is shown in Figure 4.9.

Since during the loss of the column important membrane forces appear, a quick study is made to choose the axial stiffness of the connecting rod modelling the slab.

So far the connecting rod modelling the slab had an area of $A_{Slab} = 0.1$ m^2 and a Young's modulus of $E_{slab} = 2.1 \cdot 10^8$ MPa. In order to know if the connecting rod is stiff enough, three new simulations taking into account the scenario of the loss of the column were done by giving a different area to the connecting rod modelling the slab ($A_{slab} = 1$; 0.01; 0.001 m^2) and by keeping the Young's modulus constant.

The results are compared on the basis of the maximum displacement along X-direction and Y-direction of the DAP. The resulting displacements of the four analyses are presented in Table 4.1.

	A = 1 m^2	A = 0.1 m^2	A = 0.01 m^2	A = 0.001 m^2
Displacements X-direction	1.11	1.12	1.22	1.94
Displacements Y-direction	1.32	1.35	1.5	3.26

Table 4.1: Horizontal displacements of the DAP according to the area of the rods modelling the slab, in [mm].

Looking at the displacements of the DAP as a function of the area of the connecting rod, it can be seen that the larger the area the smaller the displacements. This is logical since the larger the area, the more rigid the slab and therefore the smaller the displacements. We can also see that for a cross-sectional area of 1 m^2 and 0.1 m^2, the difference in displacements between the two is almost zero. The choice to model the slab by a 0.1 m^2 connecting rods is thus relevant since above this value, the displacements are practically constant.

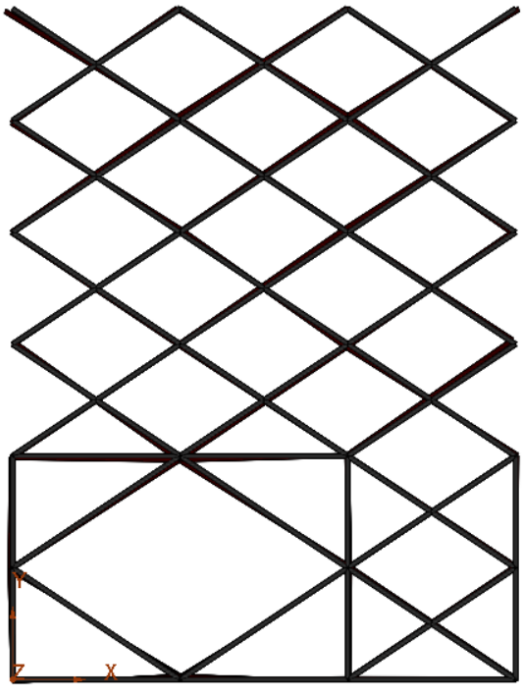

Figure 4.9: New slab modelling.

3 Application of the EN1991-1-7 tying method

3.1 Presentation of the method

The first method applied to give robustness to the reference structure is the tying method. Eurocode EN1991-1-7 (2006) states that a minimum level of resistance, following an exceptional event, can be provided to a structure by installing horizontal and vertical ties. Horizontal ties allow the horizontal elements to be fixed to the vertical elements so that the structure forms a whole. The vertical ties ensure that the forces are redistributed to the foundations by an alternative path following an exceptional event.

The need to consider ties depend on the consequence class of the structure. If the structure is of lower class 2, only horizontal ties are required. If the structure is of upper class 2, then vertical ties are required, in addition to horizontal ones. The reference structure studied is upper class 2 since it is an office building with more than 4 floors and less than 15.

The code states that "*horizontal ties should be provided around the perimeter of each floor and roof level and internally in two right angle directions to tie the column and wall elements securely to the structure of the building.*" EN1991-1-7 (2006). By ensuring the transfer of forces through these horizontal ties, the horizontal elements are attached to the vertical elements, thus the structure forms a whole with continuity.

Horizontal ties can be of different types; either laminated beams, the steel bars in the reinforced concrete slab or steel sheets for a composite structure.

Furthermore, in order to ensure that these horizontal elements have sufficient strength, the code allows the calculation of a tensile force that the ties must resist. It should be noted that the connections of the ties, as they transmit the tensile force, must also be checked.

Regarding vertical ties, it is stated in the Eurocode that *"each column and wall should be tied continuously from the foundations to the roof level"*(EN1991-1-7, 2006) in order to provide an alternative path for forces that may appeared during an exceptional event.

The verification of vertical ties is different from horizontal ties. In fact, the Eurocode states that "*In the case of framed buildings (e.g. steel or reinforced concrete structures) the columns and walls carrying vertical actions should be capable of resisting an accidental design tensile force equal to the largest design vertical permanent and variable load reaction applied to the column from any one storey*" (EN1991-1-7, 2006).
In other words, the vertical ties must resist a tensile force equivalent to the difference in axial force in a column on either side of a floor.

The tying method is simple and quick to apply. It does not require calculation of the redistribution of forces in the structure, nor its behaviour under the exceptional event.

However, this method is known to have some inaccuracies. Indeed, the tying method is an indirect method, it is only respecting calculation rules and no scenario is considered. It does not take into account the ductility of the connections and ties, it is based on very simple equations, the background of the equations used to obtain the force is not clear, the position of the ties in the structure is not clear either.

First, the value of the tensile force will be computed by the tying method. After, the tying resistance of the different members and the connections will be checked. Finally a conclusion will be made about the method.

3.2 Derivation of the tying forces

3.2.1 Horizontal ties

The tensile force that the structural elements must resist varies depending on whether it is an internal or external tie. The tying forces are calculated by :

$$\text{Internal tie} : T_i = \min(0.8 \cdot (g_k + \psi \cdot q_k) \cdot s \cdot L \ ; \ 75 \ kN) \tag{4.4}$$

$$\text{External tie} : T_e = \min(0.4 \cdot (g_k + \psi \cdot q_k) \cdot s \cdot L \ ; \ 75 \ kN) \tag{4.5}$$

where,

- s is the span between two ties
- L is the length of the tie
- ψ is the partial factor of the accidental load combination
- g_k is the permanent characteristic surface load applied on the floor
- q_k is the variable characteristic surface load applied on the floor

Given the configuration of the structure, in this case there are 4 different types of ties:

1. An internal tie according to X-direction, $T_{I,X}$
2. An internal tie according to Y-direction, $T_{I,Y}$
3. An external tie according to X-direction, $T_{E,X}$
4. An external tie according to Y-direction, $T_{E,Y}$

The different types of ties are shown in Figure 4.10 for a half floor as the structure is symmetrical.

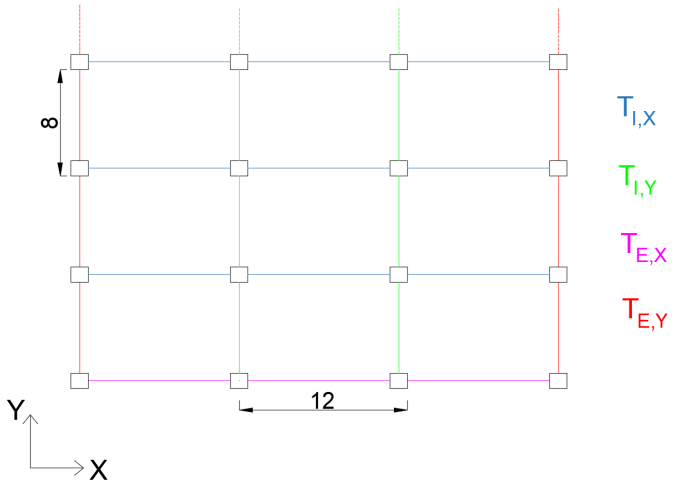

Figure 4.10: Positions of the horizontal ties in the structure.

The tensile force to be resisted by the ties can therefore be calculated using equations 4.4 and 4.5. The result is shown in Table 4.2.

Ties	g_k [kN/m^2]	q_k [kN/m^2]	ψ	s [m]	L [m]	T$_i$[kN]
$T_{I,X}$	5	3	0.3	8	12	453.12
$T_{I,Y}$	5	3	0.3	12	8	453.12
$T_{E,X}$	5	3	0.3	8	12	226.56
$T_{E,Y}$	5	3	0.3	12	8	226.56

Table 4.2: Value of the tying force in the ties.

It should be noted that the tying method considers a surface loading that can be sustained by the tie. However, some ties are subjected to punctual forces or linear loading. But these are not taken into account because the method does not allow it. It is therefore only the surface loading that is considered.

3.2.2 Vertical ties

The tensile force that the vertical ties must resist is the difference in normal force in the column on either side of the floor. In other words, since the applied load is the same for the entire floor area and for all floors, the tensile force is equal to the force taken up by the column at one floor. However, a distinction is made between internal columns and facade columns.

This vertical tensile force can be easily computed. As mentioned before, the accidental load combination is considered. This one is equal to

$$E_d = 1 \cdot \text{Dead load} + 0.3 \cdot \text{Live load} = 1 \cdot 5 + 0.3 \cdot 3 = 5.9 \ kN/m^2 \tag{4.6}$$

The inner column sustains the surface load applied to an area 8 m wide and 12 m long. The resultant of this surface load is

$$N_{comb,acc,in} = 5.9 \cdot 12 \cdot 8 = 566.4 \ kN \tag{4.7}$$

to this must be added the self-weight of the structural elements,

$$\begin{aligned} N_{SW,in} &= 8[m] \cdot q_{Sw,IPE600}[kN/m] + 3 \cdot 12[m] \cdot q_{Sw,IPE550}[kN/m] + 4[m] \cdot q_{Sw,HEM300}[kN/m] \\ &= 8 \cdot 1.22 + 3 \cdot 12 \cdot 1.06 + 4 \cdot 2.38 \\ &= 57.44 \ kN \end{aligned} \tag{4.8}$$

The force applied at each floor, for an internal column, is therefore $P_{floor,in} = 623.84 \ kN$.

For the facade columns, they sustain a surface load of an area of 4 m wide and 12 m long. The resultant of this surface load is the half of the one for an inner column, i.e. $N_{comb,acc,fac} = 566.4/2 = 283.2 \ kN$.
To this, the self-weight of the elements has to be add. It represents a force of

$$\begin{aligned} N_{SW,in} &= 4[m] \cdot q_{Sw,IPE600}[kN/m] + 2 \cdot 12[m] \cdot q_{Sw,IPE550}[kN/m] + 4[m] \cdot q_{Sw,HEM300}[kN/m] \\ &= 4 \cdot 1.22 + 2 \cdot 12 \cdot 1.06 + 4 \cdot 2.38 \\ &= 39.84 \ kN \end{aligned} \tag{4.9}$$

And the vertical force acting on each floor of the facade column is $P_{floor,fac} = 323.04 \ kN$

3.3 Evaluation of the tying resistance of the structural elements

3.3.1 Beams

First, the tying resistance of the horizontal ties is checked.
As already mentioned, there are 4 different beam sections to consider. Since the sections are class 1 and class 3, the tensile strength is calculated as follows,

$$N_{Pl,Rd} = A \cdot f_y \tag{4.10}$$

The tensile resistance of the beams is shown in Table 4.3.

Beams	A [mm^2]	N$_{Pl,Rd}$ [kN]
IPE500	11550	4,100.25
IPE550	13440	4,771.2
IPE600	15600	5,532.0
HEA300	11250	3,993.7

Table 4.3: Tensile resistance of the beams.

It should be noted that the tensile strength is the strength of the entire section, without taking into account the joint holes. The strength taking into account the holes is considered in the tensile strength of the connections in the next part.

After calculating the different tensile resistance of the beams, this is compared with the tensile force obtained by the tying method, in Table 4.4.

Ties	Beams	Tying force T_{Ed} [kN]	$N_{Pl,Rd}$ [kN]	Check ?
$T_{I,X}$	IPE550	453.12	4,771.2	Yes
	HEA300	453.12	3,993.7	Yes
$T_{I,Y}$	IPE600	453.12	5,532.0	Yes
	HEA300	453.12	3,993.7	Yes
$T_{E,X}$	IPE500	264.96	4,100.2	Yes
$T_{E,Y}$	IPE500	252.16	4,100.2	Yes

Table 4.4: Comparison between the applied tying force and the tensile resistance of the beams.

The resistance is verified as all tensile forces are lower than the strength of the beams.

3.3.2 Joints

As previously mentioned, the joints have been design based on the shear forces at ULS in a classical way, i.e. for the initial structure with all its column. The connection is a fin plate one.

The tensile strength of the connection is computed by the component method. This method consists in identifying the components of the connection that are active under the considered force, here the tensile force, and then calculating the strength of each component. Finally, the

strength of the connection corresponds to the strength of the weakest component.

In total, there are eight components activated in tension,

- Bolts in shear
- Fin plate in bearing
- Fin plate in tension (gross section)
- Fin plate in tension (net section)
- Beam web in bearing
- Beam web in tension (gross section)
- Beam web in tension (net section)
- Supporting member in bending

The tensile resistance is computed according to the European Recommendations for the Design of Simple Joints in Steel Structures (Jaspart et al., 2009). The detailed calculation is provide in appendix from B to J and the resistance of each joint associated with the weakest component is given in Table 4.5. As mentioned in the appendix, the ductility criteria are well respected.

Ties	Joints	Tying force T_{Ed} [kN]	N_u [kN]	Weakest components	Check ?
$T_{E,Y}$	A1w	252.16	407.04	Supporting member in bending	Yes
$T_{E,X}$	A1s	264.96	437.36	Fin plate in bearing	Yes
$T_{E,X}$	A2	264.96	437.36	Fin plate in bearing	Yes
$T_{I,X}$	B1	453.12	514.67	Fin plate in bearing	Yes
$T_{I,X}$	B3	453.12	514.67	Fin plate in bearing	Yes
$T_{I,Y}$	C2	453.12	433.03	Supporting member in bending	No
$T_{I,Y}$	C3	453.12	785.78	Fin plate in tension	Yes
$T_{I,Y}$	D3w	453.12	247.83	Beam web in bearing	No
$T_{I,X}$	D3s	453.12	291.64	Beam web in bearing	No

Table 4.5: Tying resistance of the connections.

According to Table 4.5 the resistance of the joints is ensured for 6 of them. C2, D3w and D3S connections do not have sufficient strength.

The tensile force is not far from the resistance, by making some slight modifications to the fin plate, it is possible to find a connection configuration that can withstand the tensile force. To achieve this, the following changes need to be made

- For the C2 connection, an increase in plate height of 30 mm results in an ultimate tensile resistance of $N_u = 459.7\ kN$.
- For connection D3w and D3s, by adding a row of bolts and increasing the height of the plate by 60 mm, the resistance becomes $N_u = 483.9\ kN$.

As a result of these modifications, the resistance of all connections is assured.

3.3.3 Columns

As shown above, the tensile force that an internal vertical tie must withstand is $P_{floor,in} = 623.84\ kN$ whereas for a vertical tie located in facade, the force is $P_{floor,fac} = 323.04\ kN$.

The vertical ties are trivially verified since the columns have been designed for a much higher compressive force. The plastic axial resistance $N_{Pl,Rd}$ of the columns has been calculated in Table 2.4.

However, even if the tensile resistance of the columns is verified, the splicing connections could be a problem. But since in this work they are not considered, the resistance of the splicing joints is not evaluated.

3.4 Robustness assessment

It was shown that the structure resists the tying force obtained by the tying method. This would mean that the structure is robust. Furthermore, by using the tying method, it is ensured that all elements of the structure are connected to each other. This allows the structure to form a whole.

However, as explained above, the tying method does not consider any failure scenario. The question arises as to which exceptional events the structure is robust to.

Moreover, the method is not very precise since it considers only one formula that applies to all structures regardless of their configuration. Some of the terms in the equation such as the 0.8 factor are not justified.

No ductility is taken into consideration when applying this method. However, it is known that the ductility of the structure must be brought in when studying its robustness. The rotation of the beam is not considered either. What is the maximum allowed rotation of the connection, the code does not mention it.

It is also necessary to know if during the exceptional event the beam will only be subjected to a tensile force. Perhaps there will also be a bending moment applied to the beam. In this case, due to the M-N interaction, the tensile strength of the beam will be reduced.

The result of the analysis with the tying method should therefore be taken with caution. With hindsight, we realise that there are a number of uncertainties with this method.

3.5 Conclusions

Through the application of the tying method, the tensile force, that can be developed in the beams following an exceptional event, could be easily calculated. By comparing the membrane forces with the strength of the ties, it was shown that the beams have sufficient strength. After that, the tensile strength of the connections was studied. It was shown that this was also verified with slight modifications. Finally, it has been shown that for columns without splicing joints, the resistance of them is trivially ensured.

Therefore, having designed the structure with classical load combinations at ultimate limit states, as a design office does, the tying method showed that the structure possessed a sufficient level of robustness.

Nevertheless, as previously stated, this method is not sufficiently accurate. The results concerning the robustness of the structure studied by the tying method must therefore be qualified by a more sophistical method.
However, this method could be used to ensure that all the elements are well connected to each other.

4 Numerical simulations of the actual structural response in case of column loss

4.1 Introduction

In this second part, the structure will be numerically analysed taking into account the scenario of the loss of the column. The results of this analysis will be compared to the results obtained by the tying method. This will show whether the tying method is a reliable approach when the loss of a column is considered.

Firstly, the structure will be analysed with a linear elastic material law. Then an elastic perfectly plastic material law will be used for all elements, except those modelling the slab. This approach will allow to highlight the consideration of the plasticity of the elements and to compare the benefit or not of using such a law. Finally, the results will be analysed.

4.2 Analysis with an elastic law

The first numerical analysis performed is a nonlinear analysis with a linear elastic material law. The modelling of the column loss is the same as explained in part 2.3.

The purpose of starting with an analysis with an elastic law is firstly to have a first approach of the behaviour of the structure under the scenario of the column loss and, secondly, to make a comparison with the results obtained by the tying method.

A diagram relating the multiplier of unloading λ of the column to the vertical displacement u at the point where the lost column is attached is shown in Figure 4.11. Two behaviours can be observed in this curve. The first one, the vertical line merging with the y-axis, is the sequence of loading of the structure with the accidental load combination when all columns are present. The second behaviour of the curve, with an exponential trend, is the vertical displacement when the column is being removed. When the column is completely removed, $\lambda = 1$, the bottom of the DAP moves by 426 mm.

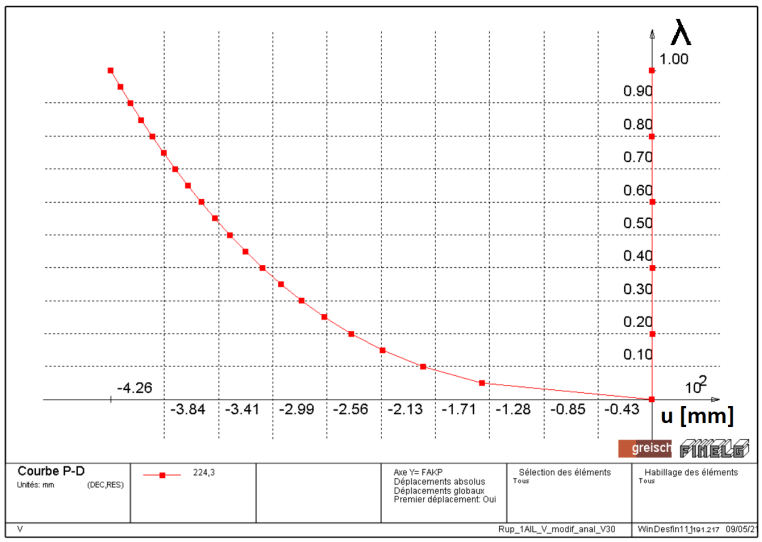

Figure 4.11: $\lambda - u$ curve for an analysis with a linear elastic law, displacement in [mm].

This curve is different from the one shown in Figure 1.10 in section 1 part 3.2. Indeed, in this curve, there is no linear phase when the column starts to be removed. This is due to the presence of the hinged connections. Since they are as such, hinges already exist at the ends of the beams and rotation is already allowed when the column starts to be removed. So we go directly from a phase 1 (normal loading of the structure), to a phase 3 (development of the catenary actions).

Looking at the structure as a whole, only the DAP of the structure is affected by the loss of the column. After the column was completely removed, significant catenary actions appeared in the directly affected part. But outside this area, in the IAP, the tensile forces in the steel structure are very small compared to those in the DAP. In fact, by reaction, the tensile forces will be taken up by the slab where a horizontal compression ring around the area affected by the column lost will develop. The large difference between the tensile forces in the DAP and in the IAP can be seen in Figure 4.12 and 4.14. As the DAP is mainly affected by the loss of the column, it is on this part that the study will mainly focus.

For the IPE550 beams, the tensile forces are presented in Figure 4.12 and the internal bending moment is presented in Figure 4.13. For the IPE600 beams, the internal tensile forces are shown in Figure 4.14 and the internal bending moment in Figure 4.15.

It should be noted that according to these figures, the tensile force decreases along a same beam. In reality this is not the case, it is because `Finelg` shows the results along the global axes. If the results were shown along the local axis of the beam, the tensile force would have been constant. It is therefore an error in the presentation of the results by the software.

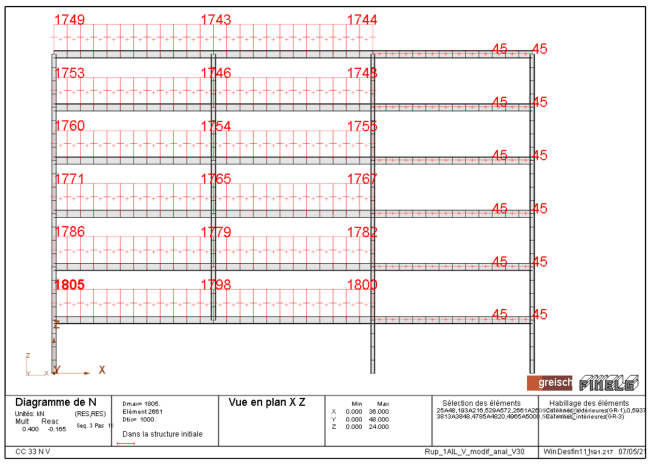

Figure 4.12: Internal axial forces ([kN]) in the IPE550 beams, when the column is completely removed.

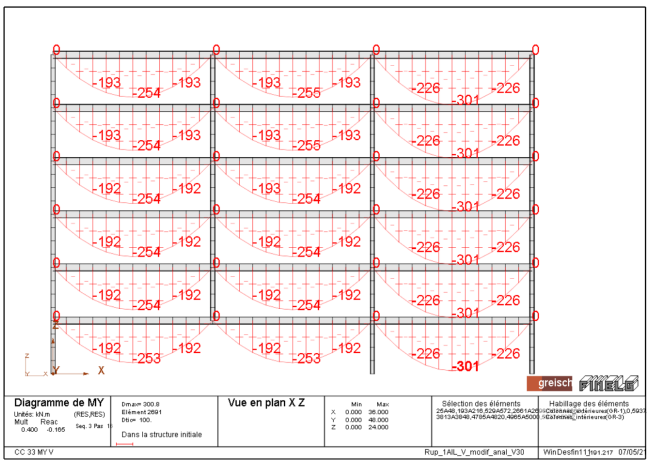

Figure 4.13: Internal bending moment ([kN.m]) in the IPE550 beams, when the column is completely removed.

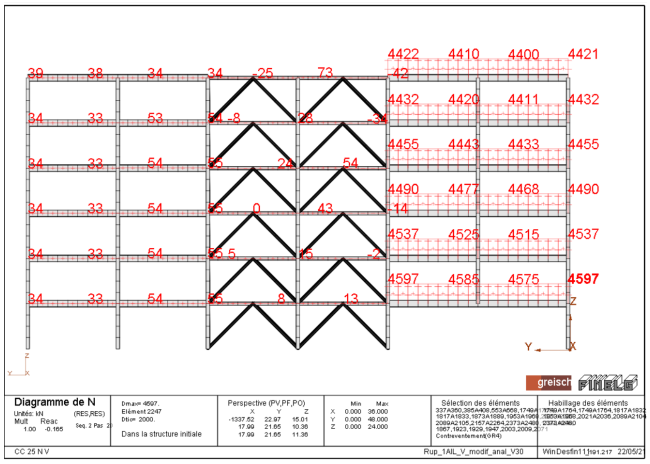

Figure 4.14: Internal axial forces ([kN]) in the IPE600 beams, when the column is completely removed.

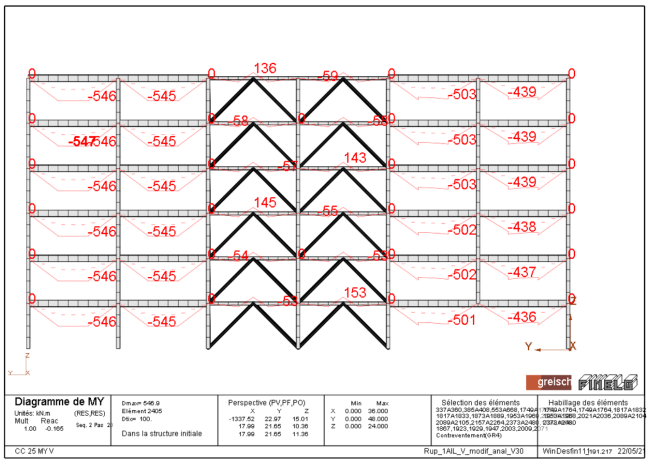

Figure 4.15: Internal bending moment ([kN.m]) in the IPE600 beams, when the column is completely removed.

A first observation can already be made at this stage. In the DAP, the tensile forces obtained by the numerical model are much higher than those obtained by the tying method. On the contrary, the tensile forces in the IPA are smaller with the numerical model than with the tying method.
The tensile forces obtained by the two methods are presented in Table 4.6.

Beams (Ties)	Tying method	Numerical approach DAP	Numerical approach IAP
IPE550 ($T_{I,X}$)	453.12	1805	45
IPE600 ($T_{I,Y}$)	453.12	4598	54

Table 4.6: Tying forces obtained by the tying method and by the numerical approach with an elastic law, in [kN].

Another observation that can be made is that the forces in both directions of the DAP are not the same, contrary to the tying method. This is due to the difference in stiffness between the

two perpendicular beams. Indeed, the IPE600 will take more internal forces as it has a bigger cross-section than the IPE550.
Another factor causing this phenomenon is the length of the beams. The IPE550 beam is 12 m long while the IPE600 beam is 8 m long. The latter is shorter and therefore attracts greater forces.
These two factors together make the IPE600 beams take more load than the IPE550 ones.

If the results over the height of the building are analysed, it can be seen that the tensile forces are not constant over the height of the structure. The forces are higher at the bottom and decrease for the upper floors. This is due to the stiffness of the IAP. In the lowest floors, the horizontal displacements of the IAP are zero, but with increasing height, the displacements increase due to a global movement of the structure. The structure at the top is therefore less stiff and does not attract as much force as the first floor.

4.3 Analysis with an elastic-perfectly plastic law

After performing a nonlinear analysis with an elastic material law, an analysis taking into account an elastic perfectly plastic material law is performed in order to get as close as possible to reality. All the elements are characterised by this law, except the elements modelling the slab, which remain elastic.

The λ-u curve obtained by the plastic analysis is given in Figure 4.16. As in the case of the previous analysis, a distinction is made between two behaviours, one related to the loading of the structure under accidental combination with all the columns and the other to the progressive removal of the column. When the column is completely removed, the displacement at the bottom of the DAP is 451 mm.

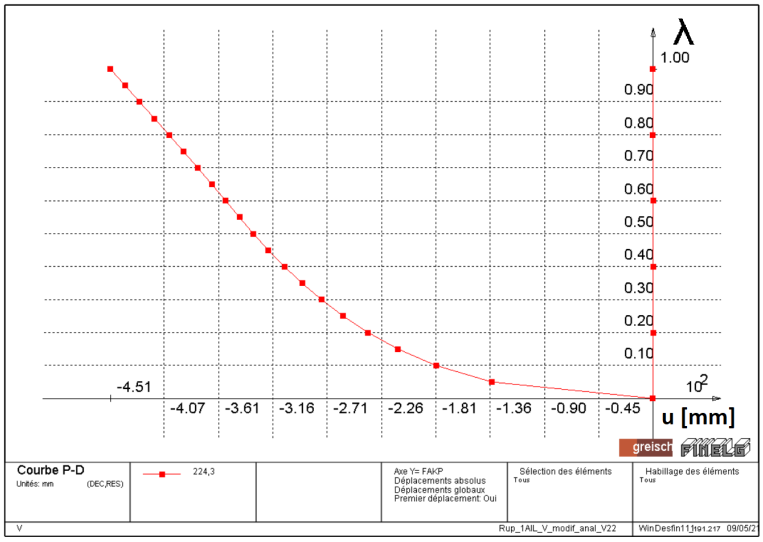

Figure 4.16: $\lambda - u$ curve for an analysis with an elastic perfectly plastic law, displacements in [mm].

About the tensile forces in the structure, the same conclusion as for the elastic analysis is made. Only the DAP is affected by the loss of the column. The rest of the structure is not affected by the exceptional event, the tensile forces are very low.
This difference between the tensile forces can be seen in Figure 4.17 and 4.19.

Concerning the internal forces in the DAP, the tensile forces for the IPE550 beams are presented in Figure 4.17 and the bending moment in Figure 4.18. For the IPE600 beams, the tensile forces are shown in Figure 4.19 and the bending moment in Figure 4.20.

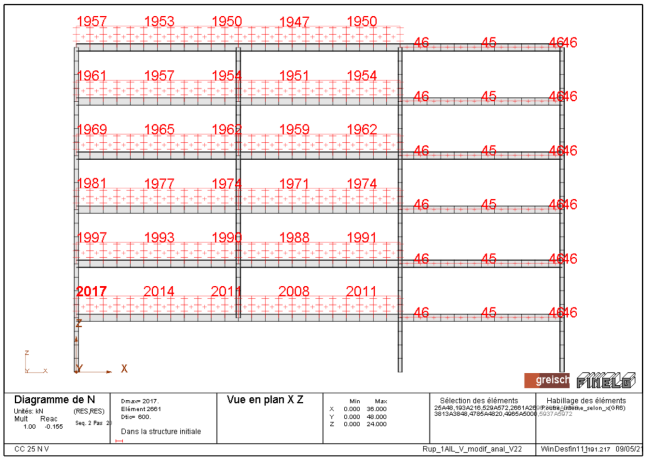

Figure 4.17: Internal axial forces ([kN]) in the IPE550 beams, when the column is completely removed.

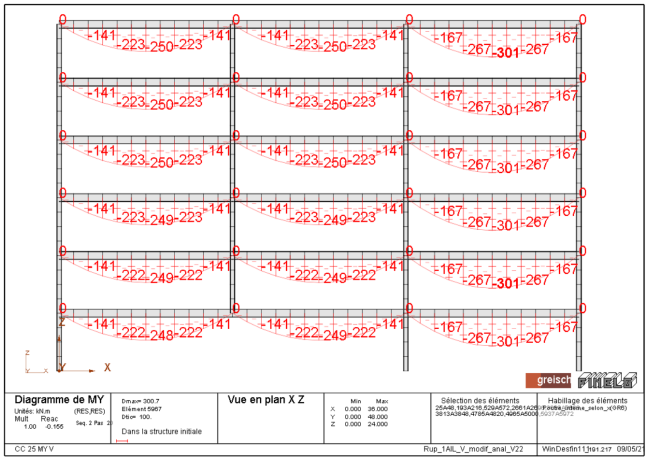

Figure 4.18: Internal bending moment ([kN.m]) in the IPE550 beams, when the column is completely removed.

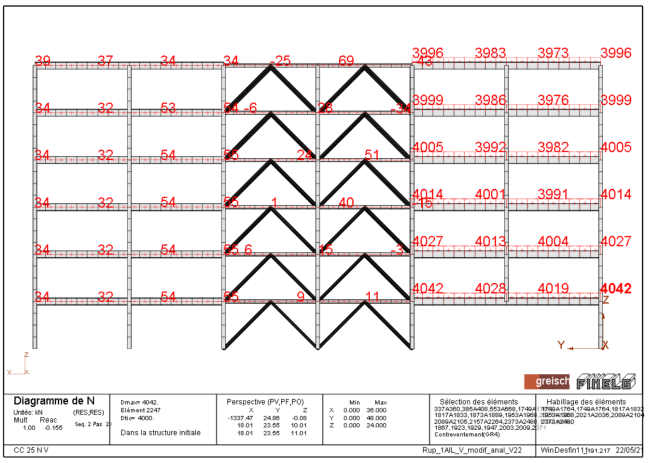

Figure 4.19: Internal axial forces ([kN]) in the IPE600 beams, when the column is completely removed.

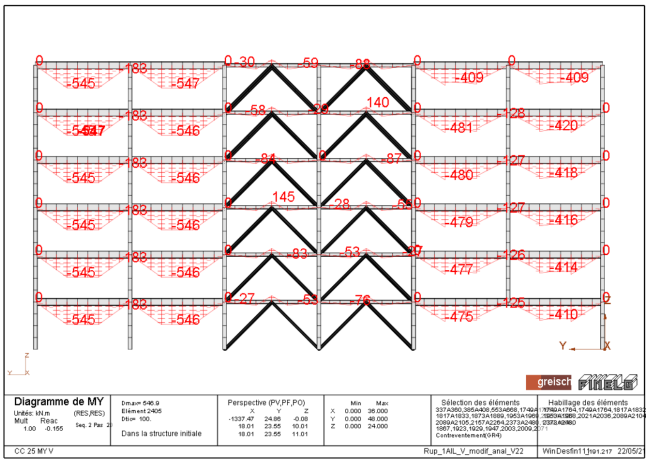

Figure 4.20: Internal bending moment ([kN.m]) in the IPE600 beams, when the column is completely removed.

Once again, the tensile forces in the DAP obtained numerically are greater than those obtained by the tying method. For the IAP it is the opposite, the tensile forces of the tying method are higher than the numerical ones. Table 4.7 shows the tensile forces obtained from the two methods.

Beams (Ties)	Tying method	Numerical approach DAP	Numerical approach IAP
IPE550 ($T_{I,X}$)	453.12	2017	45
IPE600 ($T_{I,Y}$)	453.12	4042	54

Table 4.7: Tying forces obtained by the tying method and by the numerical approach.

Concerning the distribution of forces over the height of the building, the same observation can be made as for the analysis with the elastic material law. The tensile forces are greater in the lower floors than in the upper floors. Again, this is caused by the overall displacements of the structure.

4.4 Analysis of the results

In the previous two sections, the results of the elastic or plastic analyses were compared with the results given by the tying method. In this section, both elastic and plastic analyses will be compared with each other.

First, the λ-u curves are compared with each other in Figure 4.21.

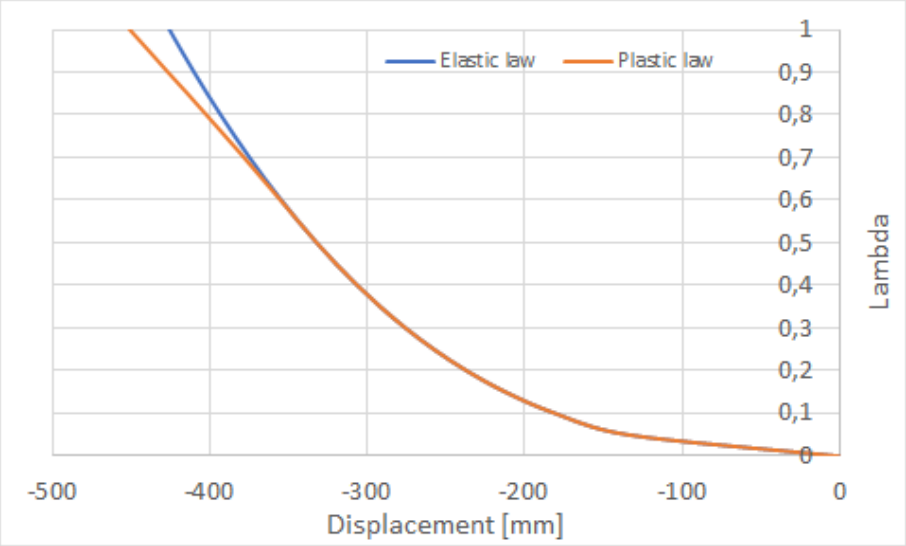

Figure 4.21: Comparison of lambda-u curves for a elastic law and a plastic law.

The two curves merge until $\lambda = 0.6$. From this point, the curve from the plastic law analysis deviates from the curve obtained with an elastic analysis. After this point, for a same value of λ, the displacement is higher with the analysis with a plastic law. This means that there is a loss of stiffness in the structure, which leads to larger displacements.

The difference between the two analyses is the material law considered. Unlike the elastic analysis, when a nonlinear plastic analysis is carried out, yielding of some fibres in section may occur.

The `Finelg` software allows to see if yielding appears in the structure. Figure 4.22 shows the yielding in the short frame, consisting of IPE550 beams and Figure 4.23 shows the yielding in the large frame consisting of IPE600 beams, both when $\lambda = 0.55$. Since no part is coloured blue, all fibres are still in the elastic range and there is no yielding. Figure 4.24 shows the yielding in the short frame, consisting of IPE550 beams and Figure 4.25 shows the yielding in the large frame consisting of IPE600 beams, both when $\lambda = 0.6$. Here, some fibres have yielded in the IPE600 beams, highlighted by the orange rectangle, so the structure has lost stiffness. It is this yielding that causes the difference between the curves in Figure 4.21.

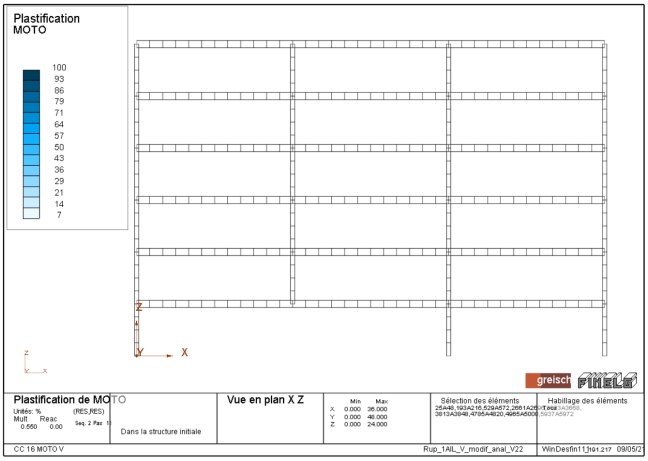

Figure 4.22: Yielding of IPE550 beams in the short frame for $\lambda = 0.55$.

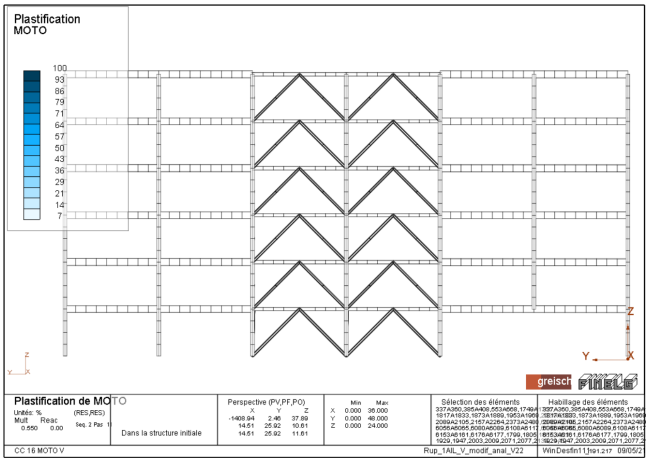

Figure 4.23: Yielding of IPE600 beams in the long frame for $\lambda = 0.55$.

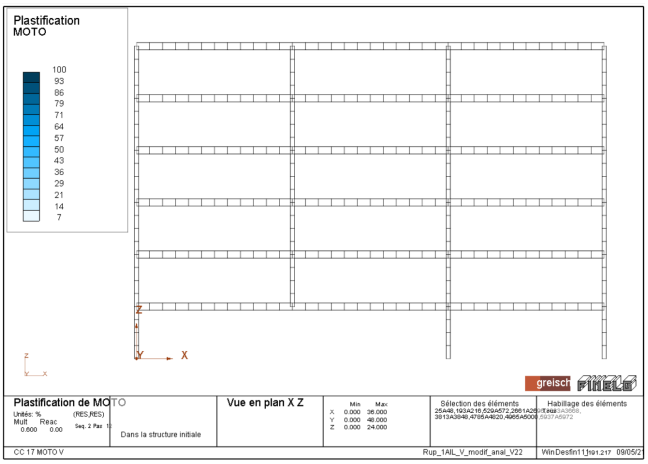

Figure 4.24: Yielding of IPE550 beams in the short frame for $\lambda = 0.60$.

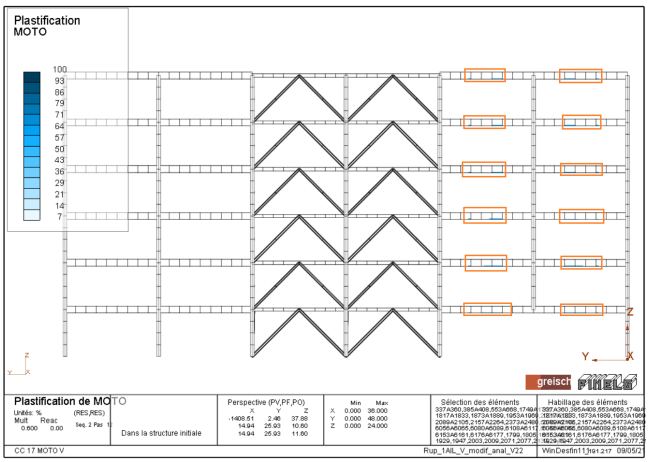

Figure 4.25: Yielding of IPE600 beams in the long frame for $\lambda = 0.60$.

The higher the λ, the higher the yielding in the cross-section of the IPE600 beams. In contrast, IPE550 beams never yield when the column is removed. Figure 4.26 shows the yielding of the short frame when the column is completely removed, nothing is blue so everything is still in the elastic domain. While Figure 4.27 shows the yielding of the IPE600, it is coloured blue, which means that some fibres are yielded. The fibres are yielded in tension, under positive moment, the fibres at the bottom of the section are in tension while the one above are in compression. And due to the tensile force caused by the loss of the column, the fibres at the bottom of the section yield.

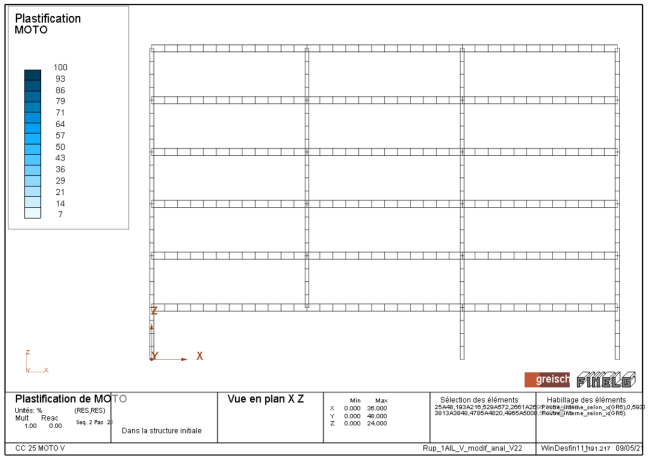

Figure 4.26: Yielding of IPE550 beams in the short frame for $\lambda = 1$.

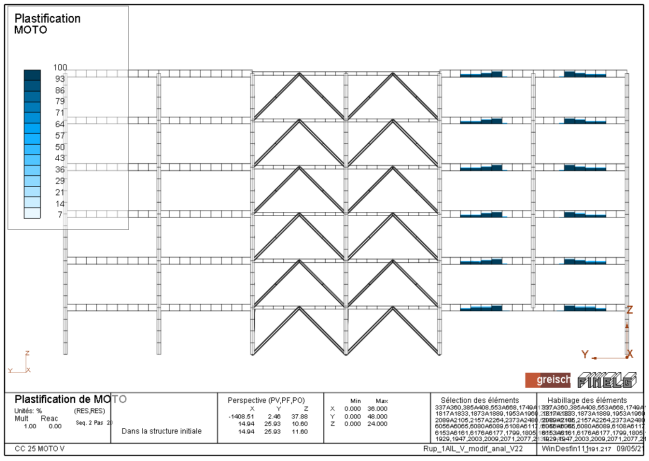

Figure 4.27: Yielding of IPE600 beams in the long frame for $\lambda = 1$.

The yielding of the IPE600 beams is also the reason for the different distribution of internal forces between the two frames, depending on whether an elastic or plastic analysis is considered. The tensile forces in the two frames according to the two analyses are presented in Table 4.8.

Beams	Linear elastic analysis	Elastic perfectly plastic analysis
IPE550 (short frame)	1805 kN	2014 kN
IPE600 (long frame)	4598 kN	4042 kN

Table 4.8: Comparison of the tying forces between the linear analysis and the plastic one.

As some of the fibres of the IPE600 beams yield, the beams become less rigid and therefore attract less force. However, the force due to the loss of the column must still be supported. The IPE550 beams will take up the part of the force that the IPE600 beams cannot take up due to its yielding. Therefore, the tensile forces obtained by the plastic analysis in the IPE600 beams are lower than the tensile forces obtained with the elastic analysis. Consequently, the tensile forces obtained with the plastic analysis for the IPE550 beams are higher than those obtained with the elastic analysis.

Since the model with the plastic material law is the one that comes closest to reality, the internal forces obtained with this analysis will be compared to the resistance of the different elements in the next section.

4.5 Evaluation of the resistance of the structure

After analysing the structure, the resistance of the structure is studied based on the plastic analysis, as said before.
Since the beams are subjected to an axial force and a bending moment, the strength check is based on the $M_{Pl,Rd} - N_{Pl,Rd}$ diagram envelope calculated from EN1993-1-1 (2005).
The plastic resistance of the elements is provided in Table 4.9.

Beams	A [mm^2]	f_y [N/mm^2]	$N_{Pl,Rd}$ [kN]	w$_{pl,y}$ [mm^3]	$M_{y,Pl,Rd}$ [kN.m]
IPE500	11,550	355	4,100.25	2,194· 10^3	778.87
IPE550	13,440	355	4,771.2	2,787· 10^3	989.4
IPE600	15,600	355	5,538.0	3,512 · 10^3	1,246.8

Table 4.9: Plastic axial resistance of the beams.

First, the resistance of the beams is studied. Contrary to the tying method where the beams were subjected only to tensile force, here the beams are subjected to a tensile force and a bending moment. In order to check the resistance of the beams, the force couple $M_{y,Ed} - N_{Ed}$ will be compared to the plastic resistance envelope $M_{y,Pl,Rd} - N_{Pl,Rd}$.
The IPE550 beam is subjected to an internal axial force of $N_{Ed,550} = 2017\ kN$ and an internal bending moment of $M_{y,Ed,550} = 248.44\ kN.m$. This force couple is plotted on the M-N graph in Figure 4.28. Since the force couple is inside the envelope, the resistance of the beam is ensured. For the IPE600 beam, it is subjected to an axial internal force of $N_{Ed,600} = 4042\ kN$ and an internal bending moment of $M_{y,Ed,600} = 475.67\ kN.m$. The force couple is plotted on the M-N graph in Figure 4.29. In this case, the point is slightly outside the curve. But, the $M_{y,Pl,Rd} - N_{Pl,Rd}$ interaction curve is safe compared to the results returned by FINELG. So in this case, the strength of the beam can be considered as verified.

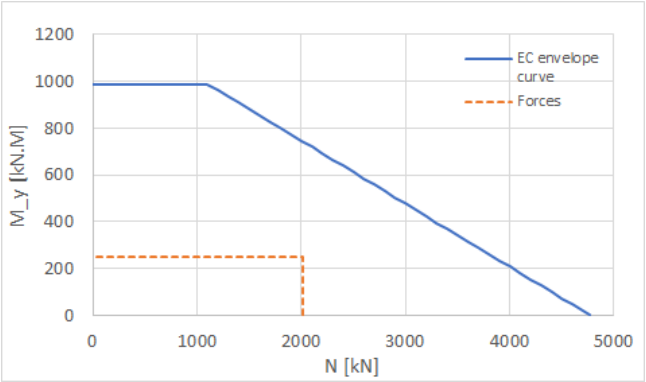

Figure 4.28: Check of the resistance for the IPE550 beam, when the column is completely removed.

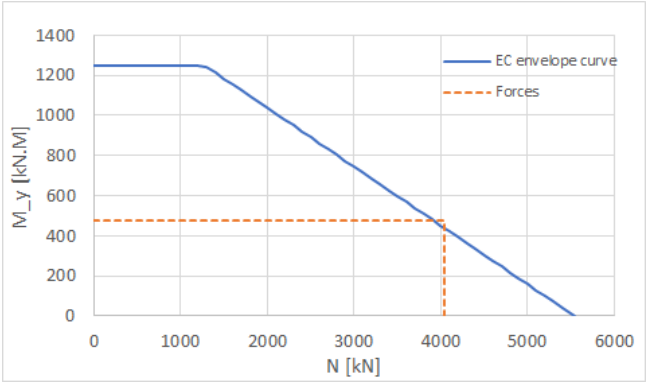

Figure 4.29: Check of the resistance for the IPE600 beam, when the column is completely removed.

Secondly, the strength of the joints is studied. As a reminder, the tensile strength of the connections has already been calculated in Table 4.5 in part 3.3.2. The internal tensile forces and joint strengths are presented in Table 4.10.

Joints	Internal forces	Resistance	Check ?
B1	2017 kN	566.13 kN	No
B3		566.13 kN	No
C2	4042 kN	473.33 kN	No
C3		864.36 kN	No

Table 4.10: Check of the resistance of the connections.

Since all internal tensile forces are greater than the strength of the connections, the resistance of the connections is not checked.

About the strength of the columns around the DAP, the resistance of the columns is assured. If this was not the case, the software would not have converged to $\lambda = 1$, since it takes into account the instability of the members.

4.6 Conclusions

This section highlighted several observations.

Firstly, the linear elastic analysis was used to show the behaviour of the DAP when the column loss scenario is considered. It was shown that the tensile forces obtained numerically are very different from those obtained by the tying method coming from the Eurocode. It was also shown that the tensile forces are not constant over the height of the building between each floor, which also differs from the tying method.

Then, by performing an analysis with an elastic perfectly plastic material law, it was shown that the yielding of the DAP influences the redistribution of the internal forces between the two perpendicular beams. In this case, the yielding of the beam leads to a decrease of the tensile force in the beam. This loss of tensile force is taken up by an increase of tensile force in the perpendicular beam, which in this case does not yield.

After carrying out the different analyses, the resistance of the structure was studied. The strength of the beams under tensile force and bending moment is verified. However, the resistance of the connections is in a first approach not ensured. A more detailed study of these connections is carried out in the following part. However, the columns have the capacity to take up the extra forces due to the loss of the column.

Finally, this part showed that with the numerical analysis, considering the scenario of the loss of the column, the structure was not robust. The connections fail under the tensile forces.

5 Ways of enhancement of the tying resistance of simple joints

5.1 Introduction

Through the numerical study of the structure, it has been shown that the strength of the structure is not assured when the scenario of the loss of a column is considered. This is because of a too low tensile strength of the connections.

In this section, the tensile forces found with the plastic analysis will be briefly recalled. Then the strength of the original connection of the reference structure is studied in detail. The connection will be optimised in order to try to find a connection configuration that can sustain the tensile forces.

In a second part, another type of hinged connection is studied, the header plate. This connection will first be designed at the ULS, and the tensile strength will then be evaluated. An optimisation of the connection will be considered.

The aim of this part is therefore to find out if there is a way to ensure the robustness of the reference structure while retaining hinged joints but optimising them.

5.2 Analysis with the original connection

As before, the strength of the joints will be compared to the membrane forces obtained by the analysis made with an elastic perfectly plastic material law. It is this material law that gives results closer to reality, compared to the elastic material law.

When the column is completely removed, the tensile forces in the short frame, consisting of the IPE550 beams, are shown in Figure 4.30. The tensile forces in the IPE600 beams of the large frame are shown in Figure 4.31. The bending moment are not recalled here, as the connections are hinged, and therefore the bending moment is zero.

Figure 4.30: Tensile forces when the column is completely removed for the short frame.

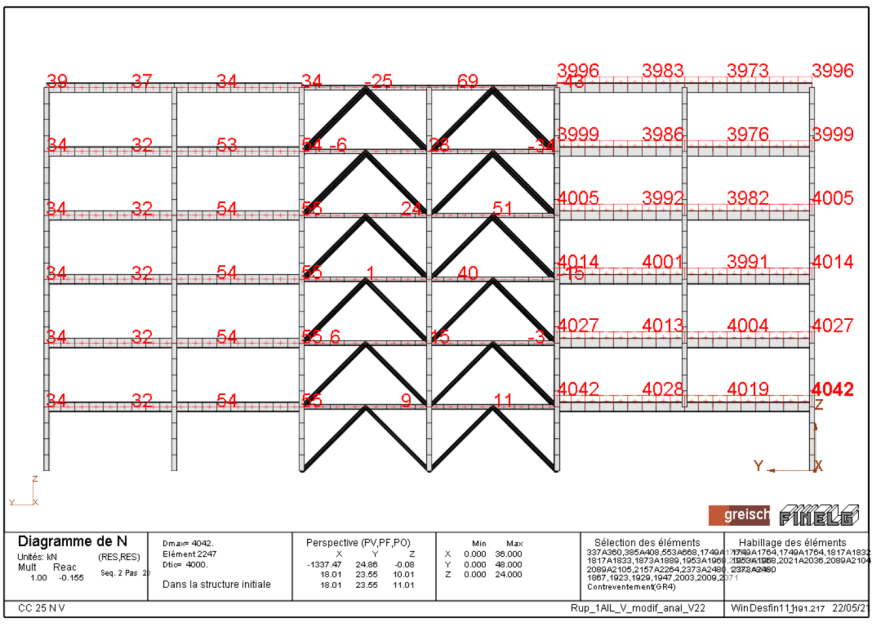

Figure 4.31: Tensile forces when the column is completely removed for the large frame.

In the following, it is the greatest tensile force that will be considered for the design. This allows for only one joint configuration for the same type, even if the tensile force decreases with the height of the structure and an optimisation could therefore be considered. This makes it easier to construct the structure on site.

5.3 Resistance of the fin plate connection

5.3.1 With the original connection design

As shown in section 4.5, the connections, designed at ultimate limit state to take up shear forces due to gravity, are not resistant to tensile forces due to the column loss. A more detailed study is carried out here to find out which components do not resist, in order to optimise them and give them sufficient strength. As a reminder, the original connections are fin plate. It consists of a plate bolted on the web of the beam and welded on the column. A representation of these connections is given in Figure 4.32.

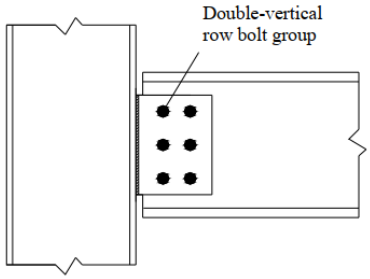

Figure 4.32: Representation of a fin plate connection (Jaspart et al., 2009).

The connections at the extremities of the IPE550 beam are first studied. For a fin plate connection in tension, eight components are activated. Table 4.11 gives the ultimate tensile resistance of each component of the original connection. As mentioned earlier, the strength of the weakest component governs the strength of the joint.

Components	Connection B1	Connection B3	Check ?
Bolts in shear	668.18	668.18	No
Fin plate in bearing	514.67	514.67	No
Fin plate in tension : gross section	890.91	890.91	No
Fin plate in tension : net section	537.22	537.22	No
Beam web in bearing	733.14	733.14	No
Beam web in tension : gross section	2,312.07	2,312.07	Yes
Beam web in tension : net section	1,787.16	1,787.16	No
Column flange in bending	>>>	>>>	Yes
Tensile resistance of the connection	**514.67**	**514.67**	**No**

Table 4.11: Ultimate tensile resistance for each component of the initial connections B1 and B3, in [kN].

From this table, we can directly see that for the same component, the ultimate tensile resistance of both connections is the same. This is logical since the connection is the same except that the cross-section of the column changes. The only component that should change between the two is the *column flange in bending*. But here, an assumption has been made, it is assumed that the plate is welded exactly in the middle of the column flange. This means that the flange is not activated in bending and therefore its resistance in tension is greater than required for both connections.

After that, it can be seen that all components, except the *beam web in tension : gross section* and the *column flange in bending*, do not have sufficient strength to support the tensile force $N_{Ed,550} = 2,017\ kN$. It is therefore necessary to modify the properties of the connections to give them a tensile resistance higher than the tensile force. The optimisation will be done in the next part.

The same approach is done for the connections at the extremities of the IPE600 beam. The ultimate tensile strength of the components is given in Table 4.12.

Components	Connection C2	Connection C3	Check ?
Bolts in shear	1,283.64	1,283.64	No
Fin plate in bearing	794.12	794.12	No
Fin plate in tension : gross section	1,336.4	1,336.4	No
Fin plate in tension : net section	785.78	785.78	No
Beam web in bearing	952.95	952.95	No
Beam web in tension : gross section	2,747.6	2,747.6	No
Beam web in tension : net section	1,972.57	1,972.57	No
Column web in bending	433.03	>>>	No
Tensile resistance of the connection	**433.03**	**785.78**	**No**

Table 4.12: Ultimate tensile resistance for each components of the initial connections C2 and C3, in [kN].

A similar conclusion can be made as for the previous connections, the same component has the same resistance for both connections except the one related to the *column web in bending*. This makes sense since the C2 and C3 connections have the same properties with the only difference being that the cross-section of the column is not the same.

The reason why the resistance of the *column web in bending* component for the C2 connection is not unlimited is that the column for this connection is located on the building facade. The plate being welded to the web of the column, this causes bending in the web which is supported by the flanges, as shown in Figure 4.33.
For connection C3, the assumption of effective transfer of the tensile force from one beam to the other, by the welds, is made. This results in the web of the column not bending and therefore the resistance of the tensile component is greater than required because this one is not activated. This case is represented in Figure 4.34.

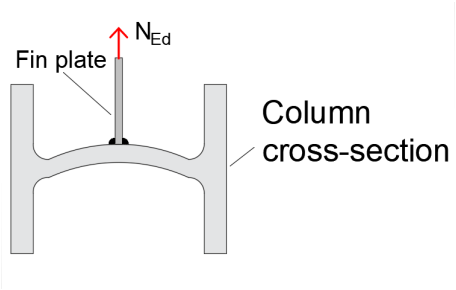

Figure 4.33: Bending of the web of the column (exaggerated deformation).

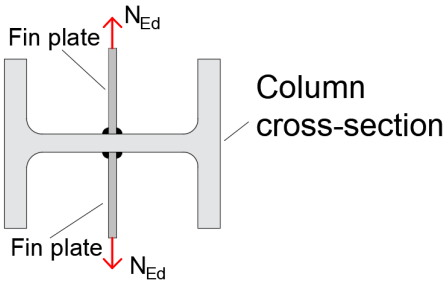

Figure 4.34: Transmission of the tensile force from one plate to the other.

Finally, as with the previous connections B1 and B3, no component, except *column web in bending* for connection C3, resists the tensile force $N_{Ed,600} = 4,042\ kN$. An optimisation of the connection is therefore carried out in the next part.

5.3.2 Optimisation of the fin plate connection

It was shown in the previous part that the properties of the connections were not sufficient to withstand the tensile force that develops following the loss of the column. In this part, the properties of the fin plate will be improved to give sufficient strength to the connections.

Firstly the connections B1 and B3 are optimised. Since the connections had the same ultimate tensile strength, they were optimised together. As a result, both connections have exactly the same properties. These are given in Table 4.13 and in Figure 4.35 for the geometry of the plate.

After optimising the plate, the ultimate tensile strength of the components is shown in Table 4.14.

Bolts	M36 10.9
Plate thickness	16 mm
Weld	10 mm

Table 4.13: Properties of the B1/B3 connection with the optimised plate.

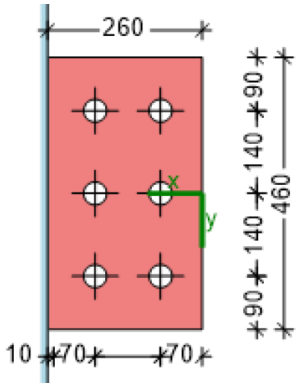

Figure 4.35: Optimised plate of the B1/B3 connection, in [mm].

Components	Connection B1	Connection B3	Check ?
Bolts in shear	2,228.18	2,228.18	Yes
Fin plate in bearing	2,302.66	2,302.66	Yes
Fin plate in tension : gross section	3,278.55	3,278.55	Yes
Fin plate in tension : net section	2,200.19	2,200.19	Yes
Beam web in bearing	1,597.47	1,597.47	No
Beam web in tension : gross section	2,312.07	2,312.07	Yes
Beam web in tension : net section	1,560.2	1,560.2	No
Column flange in bending	>>>	>>>	Yes
Tensile resistance of the connection	**1,560.2**	**1,560.2**	**No**

Table 4.14: Ultimate tensile resistance for each components after the optimisation of the plate for the connections B1 and B3, in [kN].

After optimising the fin plate, the components linked to the plate and bolts can sustain the tensile force $N_{Ed,550} = 2,017\ kN$. However, the beam components, *beam web in bearing* and *beam web in tension : net section*, still do not have sufficient strength. These components have not been optimised, as the influence of the plate properties is small for the strength of the beam components.

Even after optimising the fin plate, the connection still does not have sufficient tensile strength due to the beam components. So, in the next part, the beam of the connections B1 and B3 will be optimised, so that it can resist the tensile forces.

Afterwards, the connection C2 and C3 are optimised. As for connections B1 and B3, connections C2 and C3 are the same, except for the column which supports the beam. The result of the optimisation is shown in Table 4.15 for the plate properties and in Figure 4.36 for the geometry of the plate.

The ultimate tensile resistance of the different components, after the optimisation, is presented in Table 4.16.

Bolts	M36 10.9
Plate thickness	34 mm
Weld	20 mm

Table 4.15: Properties of the C2/C3 connection with the optimised plate.

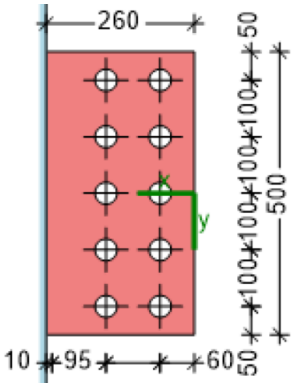

Figure 4.36: Optimised plate of the C2/C3 connection, in [mm].

Components	Connection C2	Connection C3	Check ?
Bolts in shear	3,713.64	3,713.64	No
Fin plate in bearing	5,283.9	5,283.9	Yes
Fin plate in tension : gross section	7,572.7	7,572.7	Yes
Fin plate in tension : net section	4,157.45	4,157.45	Yes
Beam web in bearing	2,043.62	2,043.62	No
Beam web in tension : gross section	2,747.56	2,747.56	No
Beam web in tension : net section	1,534.68	1,534.68	No
Column web in bending	578.95	>>>	No
Tensile resistance of the connection	**578.95**	**2,043.62**	**No**

Table 4.16: Ultimate tensile resistance for each components after the optimisation of the plate for the connections C2 and C3, in [kN].

By optimising the plate, the components linked to the plate, except the *bolts in shear* can now take the tensile force of $N_{Ed,600} = 4,042.0\ kN$. Due to constructive provisions of distance between bolts, the number of these is limited. This results in a shear strength of the bolts that is less than the applied tensile force, and the resistance of this component is not ensured.

Moreover, other components, do not yet have the necessary strength to sustain the tensile force, the *beam web in bearing*, the *beams web in tension : net section* for both connections and the *column web in bending* for the connection C2. These components are linked to the structural elements, the beam and the column. In the next part, these structural elements will be optimised in order to give them the required properties to have the necessary strength.

It should be noted that in order for the components linked to the plate to have sufficient strength, a plate thickness of 34 mm is required, as well as a weld with a throat thickness of 20 mm. The weld is quite large and not common.

In conclusion, after optimising the fin plate, the results are different from a connection to another.
For the connections B1 and B3, all the components about the plate have a sufficient resistance. But, the components linked to the beam, have not a resistance higher than the applied tensile force and the resistance is not ensured.
For the connections C2 and C3, the conclusion is the same, except that the bolts due to constructive provisions do not have the necessary strength either.
This is why in the next part, the structural elements are going to be optimised for the four connections.

5.3.3 Optimisation of the elements

In the previous part, it was shown that the only components that did not have sufficient strength were those related to the structural elements beams and columns for both connections, and the component about the bolts for the C2/C3 connection. In this section, these elements will be optimised in order to give them the necessary strength.

As the cross-sections of the DAP beams change, the internal forces in the beams are modified. In order to know the new tensile forces due to the loss of the column after the beam optimisation, a new nonlinear analysis is performed taking into account these new cross-sections. Only the final results of the optimisation are presented below, with details.

In order to verify the strength of the connections, the cross-section of the DAP beams of the short frame is changed from IPE550 to HEM1000. The cross-section beams of the long frame is also changed from IPE600 to HEM1000. The tensile forces taking into account these changes are presented in Figure 4.37 for the short frame and Figure 4.38 for the long frame.

The tensile force in the short frame is now $N_{Ed,short} = 2,280.1\ kN$ while that in the large frame is $N_{Ed,long} = 5,005.6\ kN$

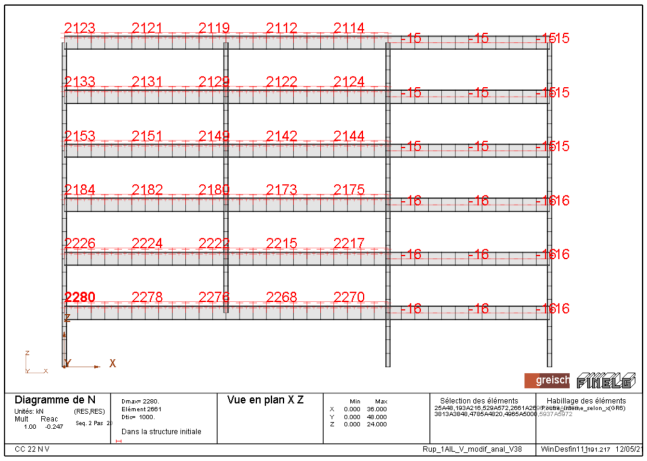

Figure 4.37: Internal tensile forces when the column is completely removed with the beam optimised.

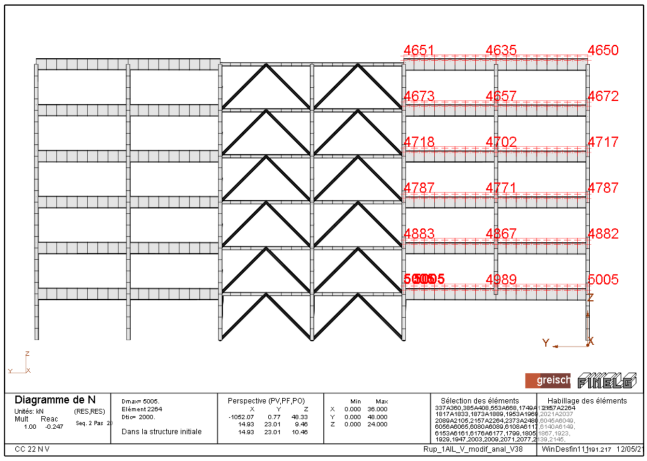

Figure 4.38: Internal tensile forces when the column is completely removed with the beam optimised.

The structural elements of connections B1 and B3 are optimised first. For these connections, only the beam needs to be modified.

To have sufficient connection strength, the cross-section of the beam was changed from IPE550 to HEB600. It is thanks to the increased thickness and height of the web that the strength can be ensured.
But, by keeping the HEB600 beam instead of the IPE550, the tensile force in the DAP of the long frame (IPE600) would be so high, that there would be no section that could take the tensile force to replace the IPE600 beam. So, to reduce the tensile force in the long frame, stiffness is brought into the small frame. Thus, the beam of the short frame is changed from an IPE550 section to a HEM1000 section.

In order to meet the ductility criteria, the connection plate had to be slightly modified. The new plate and its properties are presented in Table 4.17 and Figure 4.39.
After the optimisation, the ultimate tensile resistance of the components is presented in Table 4.18.

Bolts	M36 10.9
Plate thickness	16 mm
Weld	10 mm

Table 4.17: Properties of the B1/B3 connection with the optimised beam.

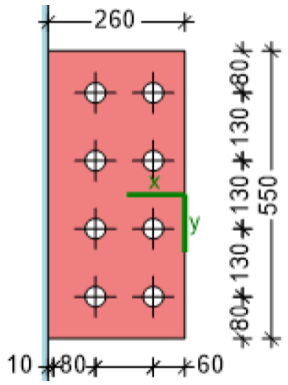

Figure 4.39: Optimised plate of the B1/B3 connection with the optimised beam, in [mm].

Components	Connection B1	Connection B3	Check ?
Bolts in shear	2,970.91	2,970.91	Yes
Fin plate in bearing	2,631.61	2,631.61	Yes
Fin plate in tension : gross section	3,920	3,920	Yes
Fin plate in tension : net section	2,527.33	2,527.33	Yes
Beam web in bearing	4,605.31	4,605.31	Yes
Beam web in tension : gross section	8,119.75	8,119.75	Yes
Beam web in tension : net section	5,994.4	5,994.4	Yes
Column flange in bending	>>>	>>>	Yes
Tensile resistance of the connection	**2,527.33**	**2,527.33**	**Yes**

Table 4.18: Ultimate tensile resistance for each components of the optimised connections B1 and B3, in [kN].

After modifying the cross-section of the beams, a connection configuration that resists the tensile force was found. The strength of the weakest component is higher than the tensile force $N_{Ed,short} = 2,280.1\ kN$, which ensures the resistance of the connection.

About the connection C2 and C3, the IPE600 beam has been optimised to have a HEM1000 section. The difference may seem large, but the optimisation was done gradually. As the cross-section increased, the tensile force became greater and greater, as the stiffness attracts the force. In addition, in order to meet the ductility criteria, a HEM1000 section is required. As mentioned before, the tensile force was such that stiffness in the short frame had to be increased in order to decrease the tensile force in the large frame.
About the column, to verify the resistance of the component *column flange in bending*, the HEB360 column have been optimised to a HD260*229 cross-section.

The properties of the plate are given in Table 4.19 and the geometric properties in Figure 4.40. The resistance of each component after the optimisation of the elements is given in Table 4.20.

Bolts	M36 10.9
Plate thickness	26 mm
Weld	15 mm

Table 4.19: Properties of the C2/C3 connection with the optimised beam.

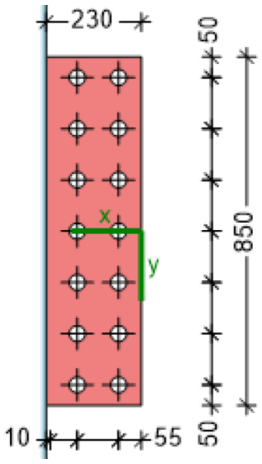

Figure 4.40: Optimised plate of the C2/C3 connection with the optimised beam, in [mm].

Components	Connection C2	Connection C3	Check ?
Bolts in shear	5,199.1	5,199.1	Yes
Fin plate in bearing	5,185.46	5,185.46	Yes
Fin plate in tension : gross section	9,844.55	9,844.55	Yes
Fin plate in tension : net section	6,014.44	6,014.44	Yes
Beam web in bearing	6,548.18	6,548.18	Yes
Beam web in tension : gross section	8,119.75	8,119.75	Yes
Beam web in tension : net section	5,009.36	5,009.36	Yes
Column web in bending	6,262.4	>>>	Yes
Tensile resistance of the connection	**5,009.36**	**5,009.36**	**Yes**

Table 4.20: Ultimate tensile resistance for each components of the optimised connections C2 and C3, in [kN].

Also for these connections, after modifying the cross-section of the beams of both connections and the column of connection C2, a configuration that can sustain the tensile force was found. As the resistance of the weakest component is higher than the value of the tensile force $N_{Ed,long} = 5,005.6\ kN$, the strength of the connection is checked.

In conclusion, in order for the connections to withstand the tensile force, the plates and structural elements had to be modified.
But to have a connection that can withstand the tensile forces the cross-sections have been increased. As the price of the structure is mainly a function of the weight of the steel, this leads to an increase in the price of the structure. Table 4.21 compares the weight of the original and the optimised beams.

Connections	Init. beams	Weight	Opti. beams	Weight	Difference	Percentage
B1/B3	IPE550	106 kg/m	HEM1000	349 kg/m	243 kg/m	229%
C2/C3	IPE600	122 kg/m	HEM1000	349 kg/m	227 kg/m	186%

Table 4.21: Weight difference with the optimised beams for the fine plate connection.

Comparing the increase in weight of the elements, it can be seen that the weight of the beams in the DAP of the short frame is more than tripled, whereas the beams in the DAP of the long frame are almost tripled. This means that the cost will also be tripled.
Such a solution is not feasible. It is worth remembering that the event of the loss of the column may never happen during the life of the structure. So it would be excessive to triple the weight/cost of the structure for something that is unlikely to happen.

In summary, the tensile strength of the initial ULS-dimensioned connection was first investigated. It was shown that none of the tensile activated components had the necessary strength. Therefore, as a second step, the plate of the connection was optimised. It was found that the components about the plate and the bolts had sufficient strength. But the components about the structural elements, the beam and the column, did not have the necessary strength.
So a last optimisation, concerning the structural elements, was done. It was shown that to have an acceptable configuration, stiffness had to be added in one direction to decrease the tensile force in the other. The problem is that as a result of this last optimisation, the beam profiles have changed significantly, which results in an important modification of the structure.

In order to avoid this structural modification, in the next section, another type of hinged connection will be studied. This is to find out if there is another type of connection that does not require such a major change of the cross section.

5.4 DAP with header plate connection

In the previous part, a fin plate connection configuration was considered. However, in order to have a connection resistant to tensile forces, significant modifications had to be made to the reference structure, which is not acceptable.

In this part, another type of hinged connection will be studied, the header plate. The header plate is first designed at ULS to take up the shear forces when all the columns are present. Then, the tensile strength of the connection will be studied. Afterwards, an optimisation of the connection is made. Finally, an optimisation of the structural elements beams and columns is carried out.

5.4.1 Design of the header plate connection at ULS

The header plate connection consists of a plate, which is welded to the web of the beam and bolted to the column. A representation of the connection is given in Figure 4.41.

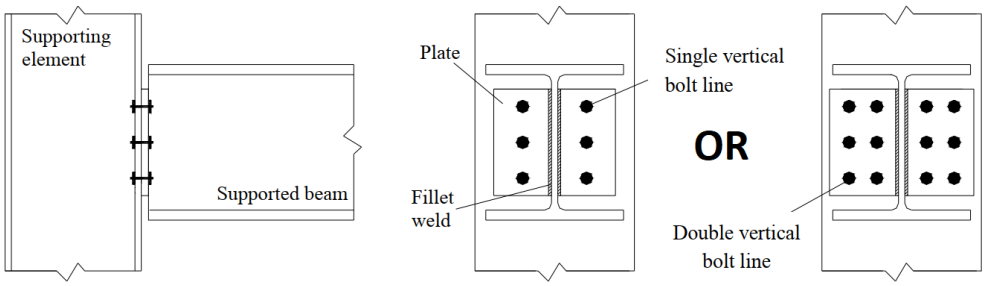

Figure 4.41: Presentation of a header plate connection (Jaspart et al., 2009).

First of all, the connection is designed to the ultimate limit states. It is therefore designed to take the forces of the analysis performed in part 4 of the section 2, where the scenario of the loss of the column is not considered. Since, in the analysis, the assumption of an infinitely resistant joint was made, with a verification a posteriori, the results of the analysis do not change. The maximum shear force to be resisted is therefore $V_{Ed,550} = 197$ kN for the connections in the short frame and $V_{Ed,600} = 400$ kN for the connections in the long frame.

The connection is designed with the COP software. The bolts for all the configurations are M20 10.9, the elastic limit stress for the plate is $f_{yp} = 355$ MPa and the weld throat is $a_w = 7$ mm for the four connections. Geometric properties are presented in Figure 4.42 and 4.43. It is good to know that the weak component in shear for the four connections is the header plate in bending, which is a ductile failure mode.

Since the shear resistance is higher than the applied shear force, as shown in table 4.22, the resistance of the connection is ensured. In addition, all the ductility criteria of the connections are verified.

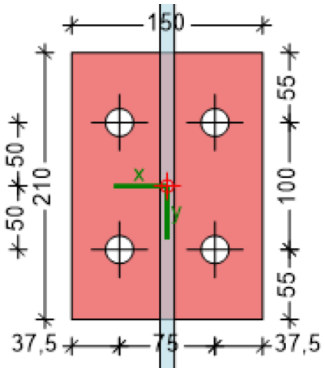

Figure 4.42: Configuration of the header plate B1/B3, thickness of the plate $t_p = 4\ mm$.

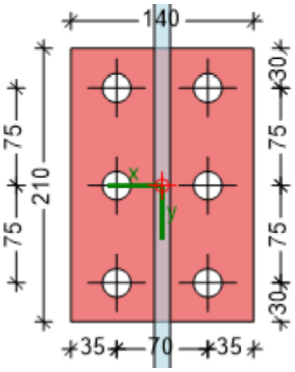

Figure 4.43: Configuration of the header plate C2/C3, thickness of the plate $t_p = 8\ mm$.

Connections	V_{Rd} [kN]	V_{Ed} [kN]
B1	261.3	197
B3	261.3	
C2	427.64	400
C3	427.64	

Table 4.22: Design of the header plate connections.

5.4.2 Resistance with the header plate connection

Now that the connections have been designed at ULS to withstand the shear forces, under conventional loading when all the columns are present, the tensile strength of the connections is studied. The exceptional scenario of column loss is considered.

The tensile strength of the connections is calculated on the basis of the European Recommendations for the Design of Simple Joints in Steel Structures (Jaspart et al., 2009), based on the component method. Only the final strength, of each component activated in tension, is given here. The detailed calculations can be found in the appendix K to N. In contrast to fin plate connection, four tensile components are activated in the header plate connection,

1. Bolts in tension
2. Header plate in bending
3. Supporting member in bending
4. Beam web in tension

The connections at the ends of the IPE550 beam are first studied. The ultimate tensile strength of each component is given in Table 4.23.

Components	B1	B3	Check ?
Bolts in tension	890.1	890.1	No
Header plate in bending	72.52	72.52	No
Column flange in bending	890.1	890.1	No
Beam web in tension	1,038.85	1,038.85	No
Tensile resistance of the connection	**72.52**	**72.52**	**No**

Table 4.23: Ultimate tensile resistance for each component of the ELU designed header plate connections B1 and B3, in [kN].

As a reminder, the tensile force in the short frame in the IPE550 beam is $N_{Ed,550} = 2,017\ kN$. The resistance of all components is lower than the tensile force, so the resistance of the connection is not ensured.

About the tensile resistance of the connections at the ends of the IPE600 beams in the long frame, the tensile resistance of each component is presented in Table 4.24.

Components	C2	C3	Check ?
Bolts in tension	1,336.36	1,336.36	No
Header plate in bending	373.22	373.22	No
Column web in bending	378.18	>>>	No
Beam web in tension	1,122.55	1,122.55	No
Tensile resistance of the connection	**373.22**	**373.22**	**No**

Table 4.24: Ultimate tensile resistance for each component of the ELU designed header plate connections C2 and C3, in [kN].

The assumption of effective transmission of forces between beams by the bolts is made. Therefore, component *column web in bending* has a resistance greater than required for the connection C3.
The force in the IPE600 beam is $N_{Ed,600} = 4,042\ kN$. All strengths are lower than the tensile force, so the resistance of the connections is not assured.

Thus, after computing the strength of each of the connections, it was shown that a connection designed at ULS to take shear force cannot sustain tensile forces coming from the loss of the column. Therefore, in the next part, the plate will be optimised in order to try to give it properties such that the connections can sustain the tensile forces.

5.4.3 Optimisation of the header plate connection

In the previous part it was shown that the connection designed at ULS could not bear the tensile force of the column loss. Therefore, in this part, an optimisation of the header plate is performed. This is done in order to find a plate configuration which ensures the resistance of the connection.

Firstly, the B1 and B3 connections are optimised. In contrast to the fin plate connection, the joints cannot be optimised together, due to ductility criteria.
After optimisation, the properties of connection B1 are given in Table 4.25 and in Figure 4.44 and those of connection B3 in Table 4.25 and in Figure 4.45.

The resistance of each component after the optimisation is given in Table 4.26.

	B1	B3
Bolts	M36 10.9	M36 10.9
Plate thickness	26 mm	21 mm
Weld	7 mm	7mm

Table 4.25: Properties of the B1 and B3 connection with the optimised header plate.

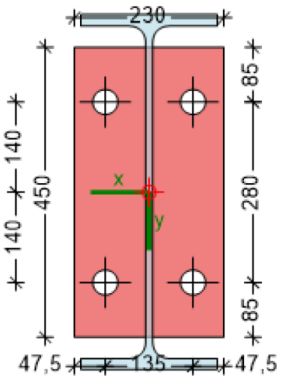

Figure 4.44: Optimised header plate of the B1 connection, in [mm].

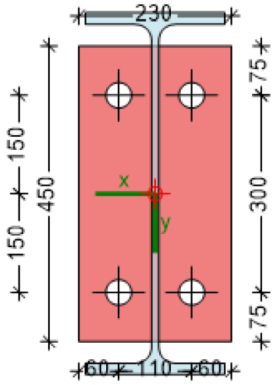

Figure 4.45: Optimised header plate of the B3 connection, in [mm]

Components	B1	B3	Check ?
Bolts in tension	2,970.9	2,970.9	Yes
Header plate in bending	2,057.23	2,123.52	Yes
Column flange in bending	2,233.6	2,970.9	Yes
Beam web in tension	2,225.05	2,225.05	Yes
Tensile resistance of the connection	**2,057.23**	**2,123.52**	**Yes**

Table 4.26: Ultimate tensile resistance for each component of the optimised header plate connections B1 and B3, in [kN].

The strength of each component is higher than the internal tensile force $N_{Ed,550} = 2,017\ kN$, so the resistance of the connection is assured.
If we look in more detail at the values of the resistance, it can be noticed that the resistance of the *bolts in tension* component is largely greater than the tensile force. This is due to compliance with the ductility criterion and not to a component strength criterion.

The difference in resistance for the *column flange in bending* component is also marking between the two connections. This is because for connection B1, the thickness of the column flange is small, so the failure mode of the component is a mode 2. Whereas for connection B3, the thickness of the column flange is large, so it is failure mode 3 that appears.

The ultimate tensile strength of C2 and C3 joints is then studied. Contrary to connections B1 and B3, the result of the optimisation of connection C2 is the same as that of connection C3. The properties of the optimised connections are given in Table 4.27 and the geometric properties in Figure 4.46.

The ultimate tensile strength of each component after header plate optimisation is given in Table 4.28.

Bolts	M36 10.9
Plate thickness	34 mm
Weld	7 mm

Table 4.27: Properties of the C2 and C3 connection with the optimised header plate.

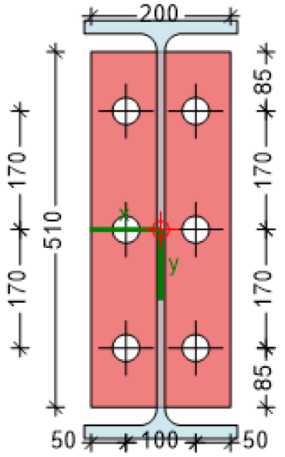

Figure 4.46: Optimised header plate of the C2 and C3 connection, in [mm].

Components	C2	C3	Check ?
Bolts in tension	4,456.4	4,456.4	Yes
Header plate in bending	4,093.27	4,093.27	Yes
Column web in bending	419.26	>>>	No
Beam web in tension	2,726.18	2,726.18	No
Tensile resistance of the connection	**419.26**	**2,726.18**	**No**

Table 4.28: Tensile resistance for each component of the optimised header plate connections C2 and C3, in [kN].

After optimisation, the *header plate in bending* and *the bolts in tension* have resistance greater than the applied tensile force $N_{Ed,600} = 4,045\ kN$. However, the structural element components, the *column web in bending* and the *beam web in tension*, do not have sufficient strength. In order to give them sufficient strength, the structural elements must be optimised. This is done in the next part.

In summary, by optimising the header plate, the ultimate tensile strength of the B1 and B3 joints could be met. However, the structural elements of connections C2 and C3 do not have sufficient strength, which leads to the failure of the connection.
In the next part, an optimisation of the beams and columns is carried out, in order to find a configuration with the necessary strength.

5.4.4 Optimisation of the elements

In the previous part, the header plate was optimised. It was shown that some components did not have the required strength. In this part, the beams and columns will be optimised, in order to give the connection sufficient strength to take the tensile force.

Since the tension activated components related to the beam of the long frame do not resist, they have been optimised. However, as the cross-sectional area of the beams increases, the internal tensile force increases as the stiffness attracts the force. In order not to have large cross-sections for the beams of the long frame, stiffness is provided in the perpendicular direction. This means that the DAP beams of the short frame were modified to a section with a higher axial stiffness. Thus, by increasing the stiffness in the short frame, the tensile force in the large frame is reduced. As a result, the strength of the connections can be assured.

For this purpose, the beam of the short frame had a cross-section of IPE550 and now has a cross-section of IPE600V. For the long frame beam, the cross-section is changed from IPE600 to HEM900.

As a result of the modification of the beam cross-sections, the internal tensile forces are also modified, and a new nonlinear analysis, with an elastic perfectly plastic material law, was therefore carried out. The tensile forces in the short frame are shown in Figure 4.47 and those in the DAP beams of the long frame in Figure 4.48.

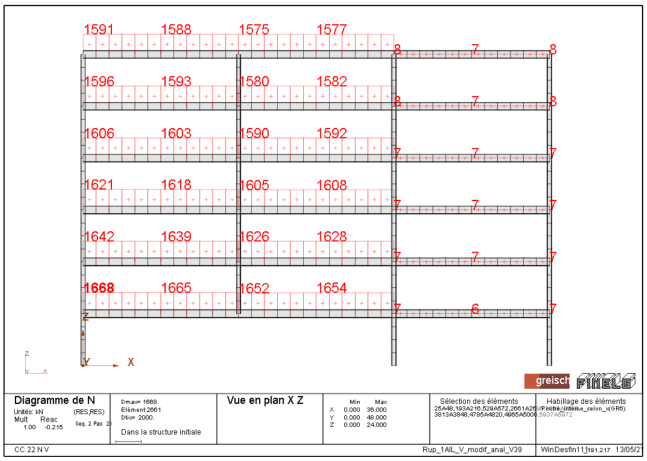

Figure 4.47: Internal tensile forces (in [kN]) when the column is completely removed with the beam optimised, for a header plate connection.

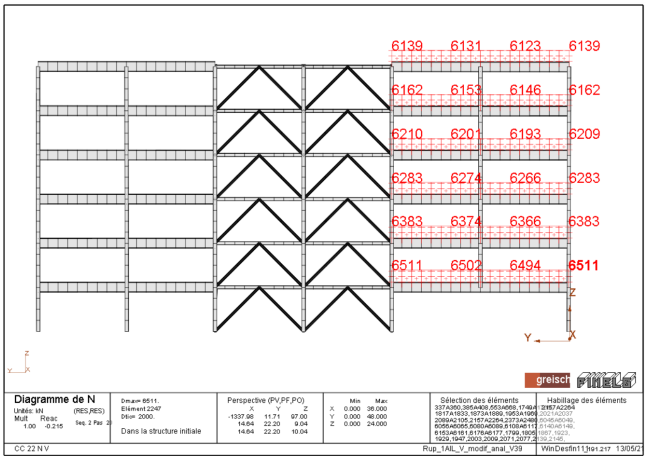

Figure 4.48: Internal tensile forces (in [kN]) when the column is completely removed with the beam optimised, for a header plate connection.

The internal tensile force in the DAP beams of the short frame is now $N_{Ed,600V} = 1,668.2\ kN$ and in the DAP beams of the long frame, it is $N_{Ed,900M} = 6,511.3\ kN$.

Since the cross-section of the DAP beams of the short frame is changed, small adjustments have to be made to the header plate. Therefore, the strength of the different components of the connections B1 and B3 at the ends of the beam is calculated, taking into account the modifications.

The result for connection B1 is shown in Table 4.29 and Figure 4.49 for the geometry. For connection B3, the properties are shown in Table 4.29 and the geometry is shown in Figure 4.50.

The ultimate strength of each component after optimisation is shown in Figure 4.30.

	B1	B3
Bolts	M36 10.9	M36 10.9
Plate thickness	18 mm	16 mm
Weld	11 mm	11 mm

Table 4.29: Properties of the B1 and B3 connections with the optimised beams.

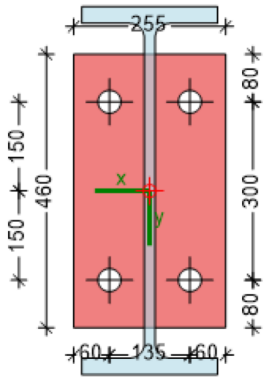

Figure 4.49: Header plate of the connection B1 with the beam optimised, in [mm].

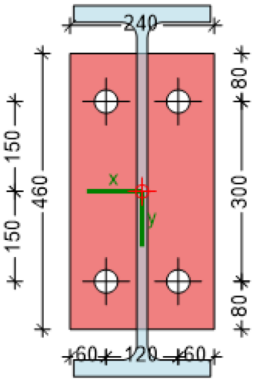

Figure 4.50: Header plate of the connection B3 with the beam optimised, in [mm].

Components	B1	B3	Check ?
Bolts in tension	2,970.9	3,268.0	Yes
Header plate in bending	1,970.85	1,952.85	Yes
Column flange in bending	2,253.1	2,970.91	Yes
Beam web in tension	3,688.4	3,688.4	Yes
Tensile resistance of the connection	**1,970.85**	**1,952.85**	**Yes**

Table 4.30: Ultimate tensile resistance for each component, with the beam optimised, for the connections B1 and B3, in [kN].

With the new nonlinear analysis, taking into account the IPE600V cross-section, the tensile force in the beams of the short frame of the DAP is $N_{Ed,600V} = 1,668.2\ kN$. The resistance of the weakest component is greater than the tensile force, so, the strength of the connection is ensured.

In order for the C2 and C3 connections to have sufficient strength, the long frame beam had to be modified from an IPE600 to a HEM900. The header plate had to be modified as the cross-section of the beam is increased, the beam is stiffer and therefore the tensile force is greater than before.
The result of the optimisation for connections C2 and C3 is shown in Table 4.31 and Figure 4.51 for the geometry.

The ultimate resistance of each component after optimisation is shown in Table 4.32.

Bolts	M36 10.9
Plate thickness	38 mm
Weld	13 mm

Table 4.31: Properties of the C2 and C3 connections with the optimised beam cross-section.

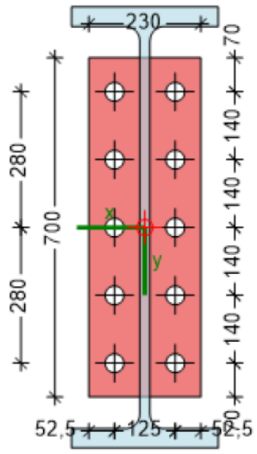

Figure 4.51: Header plate of the connections C2 and C3 with the beam optimised, in [mm].

Components	C2	C3	Check ?
Bolts in tension	7,427.27	7,427.27	Yes
Header plate in bending	6,809.37	6,809.37	Yes
Column web in bending	460.5	>>>	Yes
Beam web in tension	6,548.18	6,548.18	Yes
Tensile resistance of the connection	**460.5**	**6,548.18**	**Yes**

Table 4.32: Tensile resistance for each component, with the beam optimised, for the connection C2 and C3, in [kN].

After performing the analysis with the new beam sections, the tensile force in the beams in the DAP of the long frame is $N_{Ed,900} = 6,511.3\ kN$. Since the resistance of the weakest component, except for the *column web in bending* of the C2 connection, is greater than the tensile force, the resistance of the connection is ensured.

Even if, after optimisation of the header plate in the previous part, the strength of the *column web in bending* component was not sufficient, the column is not optimised. In fact, it is not possible, for reasons of ductility, to ensure the resistance of the plate and the column at the same time. The solution chosen is therefore to place local stiffeners at the joints.

To summarise, after optimising the header plates and beams, a joint configuration was found. However, modifications to the initial structure had to be made. Thus, the beams of the short frame were changed from an IPE550 to IPE600V cross-section. The beams of the long frame were changed from IPE600 to HEM900 cross-section.

This added weight to the structure and increased its price. A comparison between the weight of the initial and optimised beams is given in table 4.33.

Connections	Init. beams	Weight	Opti. beams	Weight	Difference	Percentage
B1/B3	IPE550	106 kg/m	IPE600V	184 kg/m	78kg/m	73.5%
C2/C3	IPE600	122 kg/m	HEM900	333 kg/m	211 kg/m	173%

Table 4.33: Weight difference with the optimised beams for the header plate connection.

The weight of the beams in the short frame is almost doubled, while the weight of the beams in the large frame is almost tripled. The increase in the weight of the structure, and therefore the price, is also significant in this case.

If we compare the increase in the weight of the sections with a header plate connection (Table 4.33) with the increase in the weight of the sections with a fin plate connection (Table 4.21), we notice that the increase is less important in the case of the connection with a header plate. This is mainly caused by the strength of the component *beam web in tension*. In the case of a fin plate connection, the web of the beam is drilled to allow the bolts to pass through. Therefore, the tensile strength of the web must be computed with a net area where the net area is the difference between the gross area and the total bolt area.
For the header plate connection, the web of the beam is welded to the plate, so the resistant area of the web is equal to the gross area.

5.5 Conclusions

The detailed study of the tensile strength of the hinged connections made it possible to highlight several points.

Firstly, it was shown that a fin plate connection, originally designed to resist the shear force at ultimate limit state, was not able to resist the tying forces caused by the column loss scenario. The tensile forces are so high that none of the tensile activated components of the connection have the required strength.

Then the optimisation of the fin plate showed that the components related to the fin plate could have sufficient strength. However, the components linked to the structural elements do not have sufficient strength. The web of the beams cannot resist the tensile forces

Finally, by optimising the beams, a connection configuration that resists tensile forces could be found. But, this implies tripling the weight of the beams, which is not economically acceptable.

The header plate connection was then studied. As with the fin plate, the tensile strength of the connection, which was designed on the basis of the shear force at ultimate limit states when all the columns are in place, is not sufficient.

After the optimisation of the plate, it was shown that for tensile forces in the short frame, a configuration could be found. However, for too high tying forces, as in the long frame, the components of the structural elements did not resist in tension.

Finally, by optimising the structural elements, a connection configuration that resists the tensile forces was found. For the header plate, the beam cross-sections are smaller than for the fin plate. This is due to the fact that for the header plate, the entire web area of the beam is considered. For the same cross section, the tensile strength of the beam web is better with a header plate than with a fin plate.

In conclusion, for the studied structure, while keeping hinged joints, it is more advantageous to design with header plate connection than fin plate connection. Even though in both cases this led to a change in the cross-sections of the beams compared to the reference structure and to a significant change in steel weight.

However, it may be possible to avoid increasing the cross-sectional area of the beams of the reference structure by using another type of connection with partial strength joint. This type of joint is studied in the next part.

6 Contribution to a new analytical robustness assessment approach

As mentioned in the previous part, since an acceptable configuration with hinged connections was not found, a solution with semi-rigid joints is considered in this part.

However, the `Finelg` software does not reflect the real behaviour of semi-rigid joints under bending moment and axial load. The use of another more powerful software should be considered. But, it has already been seen that the use of `Finelg` is time consuming. Therefore, in order not to confront the practitioner with another software, an analytical approach was proposed by the promoter of this master thesis. This gives a first approach to the robustness of the structure with semi-rigid connections by means of simple equations.

First, this model will be presented and explained. After that, the semi-rigid connections will be designed and taken into account in the model. Finally, the robustness of the structure with semi-rigid joints will be evaluated.

6.1 Presentation of the approach

Firstly, in this approach, only the beams of the DAP are studied. The rest of the structure, the IAP, is not considered. The new approach makes the hypothesis that the axial force N_{col} representing the loss of the column is divided equally between each floor. At each floor, a vertical force $P = N_{col}/n_{floors}$ is applied, where n_{floors} is the number of floors.
After that, since the properties of each storey are the same and the storey is submitted to the same vertical force P, the new model focuses on one floor, and in particular on one beam. This single beam is modelled by two diagonal rods connecting the two joints at the ends of the beam. There are springs at the extremities of each connecting rod. These represent the behaviour associated with a row of the connection. The support of the spring is fixed in translation because the assumption of an infinitely rigid slab in its plane is made.
Finally, half the force P acts at the end of this single beam.
The method thus makes it possible to find the force P for which the plastic mechanism is created.

The method assumes that the connection is a partial strength flush-end plate one, symmetrical and with two rows of bolts. In addition, both rows of bolts are in tension when the plastic hinge is created. Finally, the connection is bolted on the flange of the column.

Different parameters will be used in this model, these are presented in Table 4.34.

A representation of the modelled beam is given in Figure 4.52. Only the connecting rods have a structural role, the rectangular dashed lines are present to visualise the edge of the beam.

Parameters	Signification
N_c	Compression force in spring which represents the row in compression
$N_{Pl,c}$	Plastic axial resistance of the connection
k_c	Axial stiffness of the row in compression.
N_t	Tension force in spring which represents the row in tension
$N_{Pl,t,r1}$	Plastic axial resistance of the upper row of the connection
$N_{Pl,t,r2}$	Plastic axial resistance of the lower row of the connection
$N_{Pl,t}$	Total plastic axial tensile resistance of the connection
$S_{j,ini}$	Rotational stiffness of the connection
h_{r1}	Lever arm of the upper row of the connection
h_{r2}	Lever arm of the lower row of the connection
h_{pl}	Vertical distance between the two compression point of the beam

Table 4.34: Parameters of the new model.

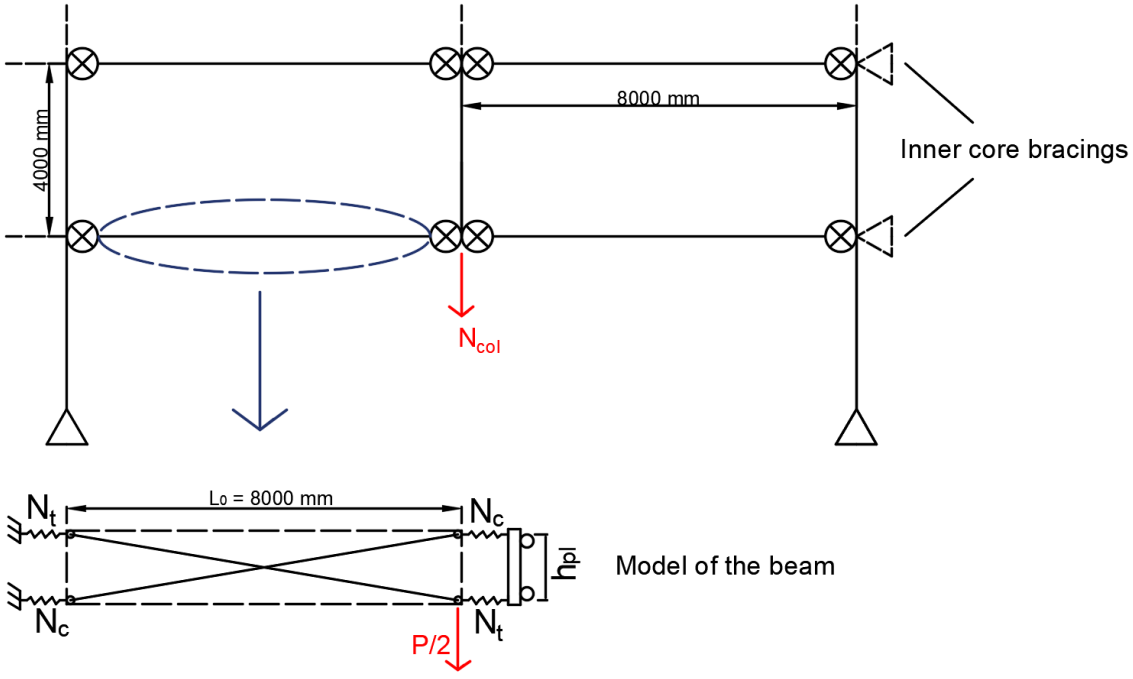

Figure 4.52: Representation of the model.

In the model representing a beam of the DAP, at each end of the connecting rod there is a spring that represents the behaviour of a row. Each row can be activated in tension or in compression.
If the row is activated in tension, a force N_t acts on the row and the row will be considered as the component activated in tension with the lowest tensile plastic resistance.
If the row is activated under compression, it is subjected to a force N_c and the row corresponds either to the *web of the column in compression* or to the *flange and the web of the beam in compression*, according to their plastic axial resistance in compression.
Here following the loss of the column, one connecting rod will be in tension and the other in compression, so the springs will be activated according to these forces.

Depending on the axial plastic resistance of the different elements, beams or bolts, yielding can occur at different locations.
In this master thesis, only one case will be studied: the one where the axial strength of the beam is the highest, followed by the row in compression and finally the row in tension. So in this case, the rows in tension yield first and these will form the plastic mechanism of the beams.

With simple static equations, it is possible to determine the vertical force for which the plastic mechanism is created. Indeed, by equalling the internal work with the external work, it comes

$$\begin{aligned} 4 \cdot M_{Pl,connections} &= P_{Pl,beams} \cdot L_0 \\ P_{Pl,beams} &= \frac{4 \cdot M_{Pl,connections}}{L_0} \end{aligned} \tag{4.11}$$

In the case where the four connections are the same and therefore have the same plastic moment.

According to the hypothesis made, it is the tensile force that causes the yielding of the joint. The plastic moment can therefore be calculated as

$$M_{pl,connection} = N_{Pl,t,r1} \cdot h_{r1} + N_{Pl,t,r2} \cdot h_{r2} \tag{4.12}$$

where h_{ri} are the effective lever arms of the connection corresponding to the row considered.

The value of $P_{Pl,beam}$ obtained is the one applied to the two beams of $L_0 = 8\ m$. When only one beam is considered, a force of $P_{Pl,beam}/2$ is applied at the extremity.

Since the spring in tension has been yielded, the tensile rod can no longer sustain additional forces. It is therefore fictitiously removed. Thus, the updated model contains only the compression rod, as shown in Figure 4.53.

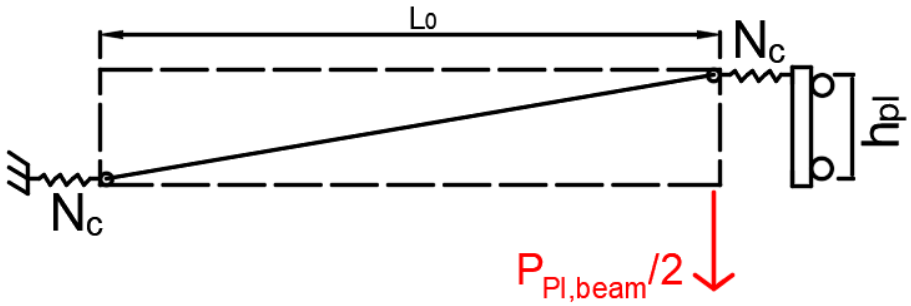

Figure 4.53: Model update without the yielded tensile rod.

However for simplicity, only one beam is shown from the beginning, but it should be noted that since the structure and loading are symmetrical on either side of the lost column, the same phenomenon takes place in the beam on the right in Figure 4.52.

Looking at the two beams of the floor as a whole, Figure 4.54, it can be seen that the connecting rods in compression are working by arch effect. And so even if the plastic mechanism caused by the $P_{Pl,beam}$ force is reached, the vertical displacements are not fully allowed since this arch has a certain resistance which has to be overcome.

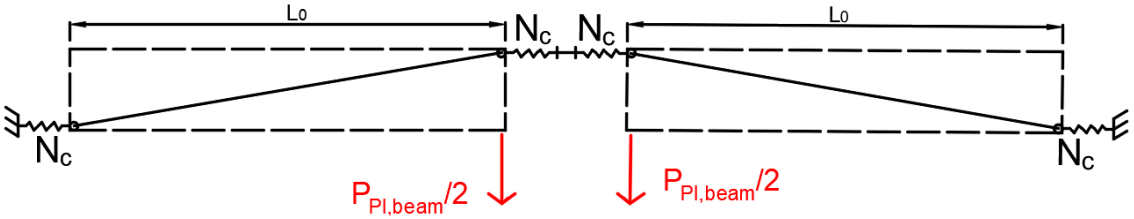

Figure 4.54: Arching effect made by the two beams.

This arch in compression is valid up to a certain value of the vertical force P higher than $P_{Pl,beam}$. If the value of P becomes too great, by reaction, the force N_c in the spring will reach $N_{Pl,c}$ which would yields the spring in compression. The connection will then has no stiffness in translation, the ends of the arch will be free to move horizontally and the arch will collapse having no resistance reserves.

Contrary to the previous development for the mechanism of the steel beams, the calculation of the additional force P_{arch}, that will yield the spring in compression, will be done at the second order because the compressive force in the springs depends on the vertical displacement of the arc.

To begin, the vertical displacement of the beam, when the beams plastic mechanism is created, at the point of application of the force is evaluated.
This displacement is decomposed into two contributions,

1. the elastic deformation of the beam submitted to the punctual force $P_{Pl,beam}$,
2. the displacement of the beam due to the rotation of the connection caused by the development of the plastic mechanism in tension.

First, the displacement of the elastic beam Δ_{beam}, subjected to the punctual force is studied. This displacement is equal to

$$\Delta_{beam} = \frac{P \cdot (2 \cdot L_0)^3}{192 \cdot E \cdot I_y} \tag{4.13}$$

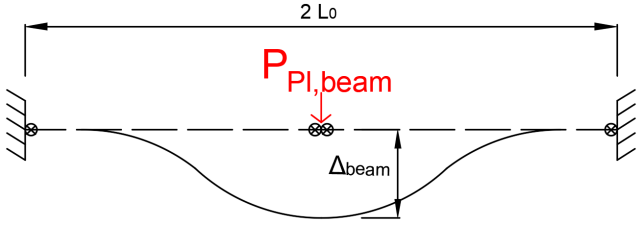

Figure 4.55: Vertical displacement of the beam.

The deflection associated with the formation of the plastic mechanism is sought. This mechanism is formed when the 4 connections (2 in each beam of $L_0 = 8\ m$) yield and thus create a plastic mechanism.

The force that create the plastic beams mechanisms has been already computed in the equation 4.11. The displacement associated with this force $P_{Pl,beams}$ is therefore

$$\Delta_{beam} = \frac{P_{Pl,beams} \cdot (2 \cdot L_0)^3}{192 \cdot E \cdot I_y} \tag{4.14}$$

This gives the first contribution to the vertical displacement.

The second contribution to the vertical displacement comes from the rotation of the joint caused by the plastic hinge, as mentioned above. A representation of this is given in Figure 4.56.

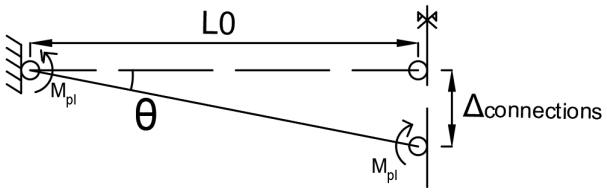

Figure 4.56: Rotation of the beam.

Since both rows of bolts were considered to be in tension when the plastic hinge develops, the rotation of the connection at yield can be obtained by means of the rotational stiffness of the joint $S_{j,ini}$,

$$M_{Pl,connections} = \theta \cdot \frac{S_{j,ini}}{\eta} \leftrightarrow \theta = \frac{M_{Pl,connections}}{\frac{S_{j,ini}}{\eta}} \tag{4.15}$$

and so, knowing the angle of rotation, the displacement of the beam can be obtained by

$$\tan(\theta) = \frac{\Delta_{connections}}{L_0} \leftrightarrow \Delta_{connections} = L_0 \cdot \tan(\theta) \tag{4.16}$$

The contribution to the vertical displacement of both parts is known, so the total vertical displacement can be expressed as

$$\Delta = \Delta_{beam} + \Delta_{connections} \tag{4.17}$$

Since, under the force $P_{Pl,beam}$, when the connection has yielded, the top of the arch moves of Δ downwards, the springs on either side of the beam will be submitted to a compressive stress. This will result in a horizontal compression of the springs and therefore a horizontal displacement $\delta_{c,el}$ of the beam ends. This displacement can be obtained by the axial stiffness of the spring under compression k_c and by the horizontal compressive force acts when the plastic hinge is developed, which is $N_{Pl,t}$ by equilibrium,

$$\delta_{c,el} = \frac{N_{Pl,t}}{k_c} \tag{4.18}$$

The horizontal and vertical projections of the length L_0 of the connecting rod will therefore be modified as a result of the compression of the springs and the vertical displacement. This results in a new length L_D. It should be noted that L_D is the result of the shortening of the springs at the extremities and not a shortening of the connecting rod.
This modified length L_D is shown in Figure 4.57.

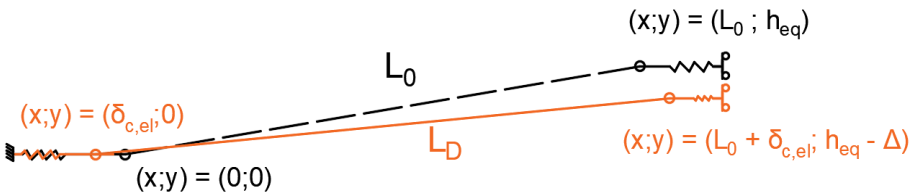

Figure 4.57: From L_0 to L_D.

It remains to find the additional force P_{arch} that will cause the row to yield in compression which allows to break the arch effect.
At this moment, the row will be compressed under a horizontal displacement of

$$\delta_{c,p} = \frac{N_{c,p}}{k_c} \tag{4.19}$$

and the connecting rod will extend of $\delta_{c,p}$ at each end, see Figure 4.58.

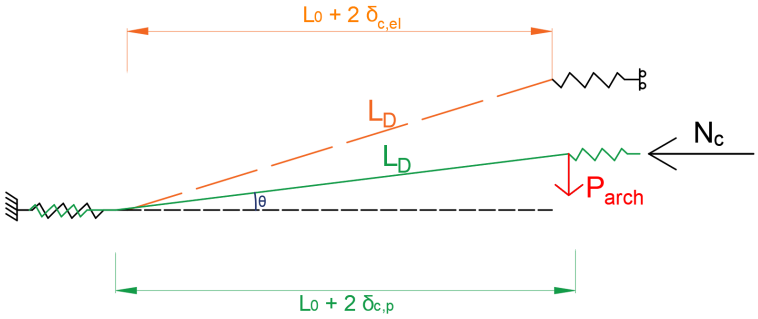

Figure 4.58: Forces act on the compression rod.

The value of the angle θ can be obtained by

$$\cos(\theta) = \frac{L_0 + 2 \cdot \delta_{c,p}}{L_D} \tag{4.20}$$

And so, knowing the angle θ, the force P_{arch} causing the row to yield in compression can be found by equilibrium,

$$\tan(\theta) = \frac{P_{arch}}{N_c} \tag{4.21}$$

where N_c is the plastic compressive resistance of the row minus the plastic tensile strength of the connection $N_{Pl,t}$, since in developing the plastic mechanism, by reaction, a compressive force of $N_{Pl,t}$ is already present in the row in compression.

The equation 4.21 thus becomes

$$\tan(\theta) = \frac{P_{arch}}{N_c} = \frac{P_{arch}}{N_{Pl,c} - N_{Pl,t}} \rightarrow P_{arch} = \tan(\theta) \cdot (N_{Pl,c} - N_{Pl,t}) \tag{4.22}$$

And so the force that creates the beams plastic mechanism and overcomes the arch effect is the sum of the two forces, i.e.

$$P = P_{Pl,beam} + P_{arch} \tag{4.23}$$

Once this force P is reached, the mechanism is perfectly developed and the membrane forces in the beams appear.

Based on the studies carried out at the same time as this master thesis, it was found that to move from the end of phase 2, where the plastic mechanism develops, to the beginning of phase 3 where the membrane forces appear, the structure must undergo large deformations, with a vertical displacement of about 1 m.
Such a deformation capacity is difficult to obtain, in this case, we will try to limit ourselves to the plastic mechanism resistance of the structure and thus not develop phase 3 to avoid these large displacements.
Moreover, once the arch effect has been overcome, its contribution is lost.

So, unlike the reference structure, where the membrane forces were directly activated after the loss of the column, here the beams plastic mechanism must first be created and then the arch effect must be overcome to finally have the development of the membrane forces.

6.2 Enhancement of the structural performance through the use of partial strength joints

6.2.1 Design of the partial strength joints at ULS

Following the study of hinged joints, it was shown that they could not ensure the robustness of the structure, they failed under the tensile force following the loss of the column. For this reason, the use of partial strength joints is being considered and more specifically the use of flush-end plate connection.

But due to technical construction constraints the partial strength joints are only installed in one direction. The connections in the other direction are the fin plate designed at ULS to take the shear forces.

The flush-end plate connection is similar to the header plate one but with a height of the plate higher than the height of the beam. Moreover, the flanges of the beam, like the web, are welded on the plate and this one is bolted on the flange of the column. A representation of a flush-end plate connection is given in Figure 4.59.

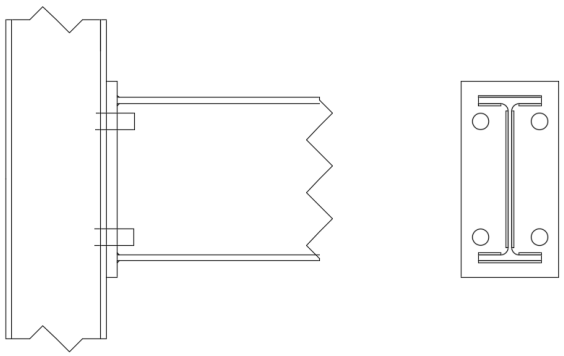

Figure 4.59: Presentation of a flush-end plate connection.

The aim of using semi-rigid joints is to delay the onset of phase 3 where tensile forces develop. Indeed, since semi-rigid joints have bending moment resistance, the force due to the loss of the column will have to be large enough to develop the plastic hinge in the joint. Phase 3 then begins, with the onset of membrane forces. So, contrary to hinged connections, this type of connection allows for a phase 2.

In the previous analyses, it was shown that the frame with the highest membrane forces is the one in the Y-direction composed of the IPE600 beams.
Moreover, for the same value of the column loss force, the bending moment at the 8 m beam ends will be lower than at the ends of the 12 m beams. Since the aim is to mobilise the bending moment resistance of the partial strength joints as much as possible, in order to delay the development of tensile forces in the beams, the flush-end plate connections will be placed at the extremities of the DAP beams of the long frame.
For the short frame, the connections remain the initial fin plate connections of the reference structure.

However, since in practice it is difficult and more costly to install flush-end plate connections on the weak axis of the column, all the columns in the structure will be rotated by 90°. This will allow the semi-rigid connection to be placed on the column flange, which is more easy.
From a static point of view in the rest of the structure, this rotation does not lead to any modification of the forces. Indeed, since all the other connections are hinged, the columns are only subjected to compression and therefore the rotation of the columns does not cause any changes.

After making this small modification, the design of the connections can be done. It has to be noted that during the design, a strong assumption is made. The connection will only be designed to take the shear force.
But, it is known that a semi-rigid connection can sustain bending moment. Nevertheless, if the design was also based on bending moment, this would result in a total modification of the structure, since the cross-section of the beams would be decreased, which would imply a new design as already done. However, not taking into account the bending moment resistance is safe for the beams, it is known that with semi-rigid connections, the forces in the beam are better distributed and their maximum value decreases.

Since the semi-rigidity of the connection is not taken into account for its design, the analysis performed previously remain valid. The shear force supported by the connection at the extremities of the IPE600 beam is $V_{Ed,600} = 400\ kN$.

The connection is designed with the software `COP`. Both connections have the same properties, they are given in the Table 4.35 and the geometry in Figure 4.60. The resistance of the connection is given in Table 4.36.

Bolts	M36 10.9
Plate thickness	13 mm
Weld	9 mm

Table 4.35: Properties of the C2/C3 connections designed at ULS.

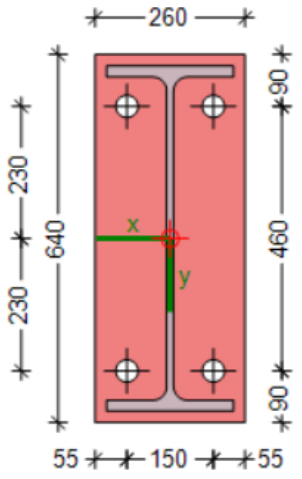

Figure 4.60: Connections C2/C3 designed at ULS.

Connections	V_{Rd} [kN]	$M_{j,Rd}$ [kN.m]	$S_{j,ini/2}$ [kN.m/rad]
C2	558.4	366	40280
C3	558.4	276.3	45890

Table 4.36: Resistance of the flush-end plate connections designed at ULS.

The new method takes into account new parameters related to the different rows of the connection. These parameters, coming from `COP`, are presented in Table 4.37.
The component with the lowest compressive strength is the *column web in compression*. About the component with the lowest plastic tensile strength it's the *end plate in bending* one.

Parameters	Value for C2	Value for C3
$N_{Pl,t,r1}$	666 kN	475.5 kN
$N_{Pl,t,r2}$	320.3 kN	475.5 kN
$N_{Pl,t}$	986.3 kN	951 kN
$N_{Pl,c}$	986.3 kN	2036 kN
k_c	2211 kN/mm	5859 kN/mm
$S_{j,ini}$	80570 kN.m/rad	91780 kN.m/rad
h_{r1}	520 mm	520 mm
h_{r2}	60.5 mm	60.5 mm
h_{pl}	581 mm	
L_0	8000 mm	

Table 4.37: Parameters to take into account in the approach.

As a reminder, semi-rigid connections are installed only in one direction. The connection at the ends of the IPE550 beams of the short frame therefore remains the initially designed connection, i.e. a fin plate connection, whose geometry is shown in Figure 2.13 and 2.14.

6.2.2 Contribution of the plastic mechanism of the steel structure

After designing the semi-rigid connections to the ULS, the new model presented in part 6.1 is applied.
While all connections were considered to be the same in the approach presentation, this is not the case with the reference structure. Connection C2 is distinguished from connection C3.
Only the beams of one storey of the DAP are studied, the model considered is shown in Figure 4.61.

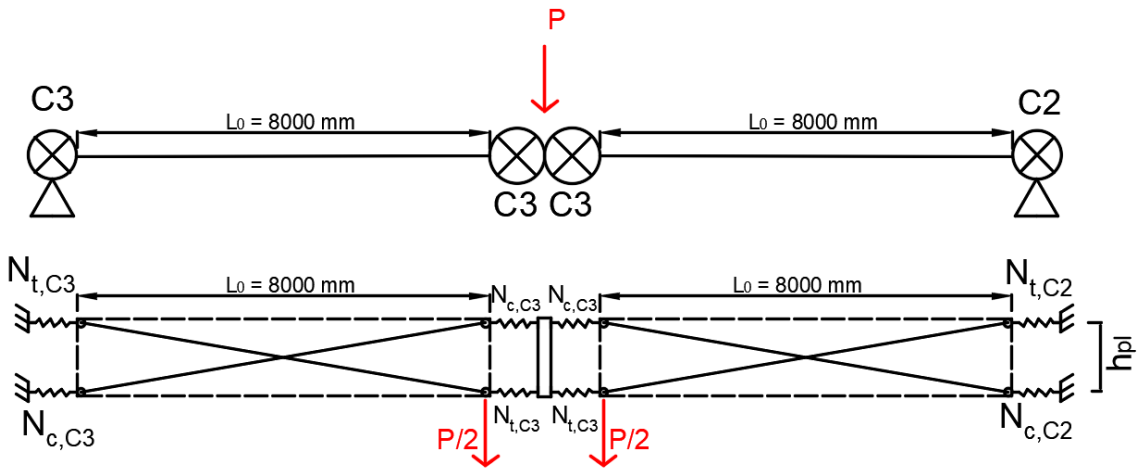

Figure 4.61: Model considered.

Firstly, the force to create the plastic beams mechanism by the yielding of the connections in tension is calculated.

The plastic moment of the connection C2 is

$$\begin{aligned} M_{Pl,connection,C2} &= N_{Pl,t,r1} \cdot h_{equ,1} + N_{Pl,t,r2} \cdot h_{equ,2} \\ &= 666 \cdot 0.52 + 320.3 \cdot 0.0605 \\ &= 366\ kN.m \end{aligned} \tag{4.24}$$

and the one for the connection C3 is

$$\begin{aligned} M_{Pl,connection,C3} &= N_{Pl,t,r1} \cdot h_{equ,1} + N_{Pl,t,r2} \cdot h_{equ,2} \\ &= 475.5 \cdot 0.52 + 475.5 \cdot 0.0605 \\ &= 276.3\ kN.m \end{aligned} \tag{4.25}$$

From this, the vertical punctual force causing the plastic beams mechanism can be deduced,

$$\begin{aligned} M_{Pl,connection,C2} + 3 \cdot M_{Pl,connection,C3} &= P_{Pl,beam} \cdot L_0 \\ 366 + 3 \cdot 276.3 &= P_{Pl,beam} \cdot 8 \\ P_{Pl,beam} &= 149.36\ kN \end{aligned} \tag{4.26}$$

Thus, this force $P_{Pl,beam}$ causes the plastic mechanism.
But as said before, vertical displacements are not yet allowed, since the effect of the arch of the connecting rods in compression must be overcome. This effect is studied in the next part.

6.2.3 Contribution of the arch effect

The vertical force that cancels the arch effect is therefore calculated. As a reminder, the vertical displacement of the beam must first be calculated to derive the vertical force.

The displacement of the beam is first computed, which is

$$\begin{aligned} \Delta_{beam} &= \frac{P_{Pl,beam} \cdot (2 \cdot L_0)^3}{192 \cdot E \cdot I_{y,IPE600}} \\ &= \frac{149360 \cdot (2 \cdot 8000)^3}{192 \cdot 21000 \cdot 92080 \cdot 10^4} \\ &= 16.47\ mm \end{aligned} \tag{4.27}$$

Then the displacement due to the rotation of the plastic hinge must be known to obtain the contribution of it on the vertical displacement.
The rotational stiffness of the connection C2 is lower than that of connection C3. However, since the two beams of length L_0 are connected to each other, it is the rotation of connection C3, which is more rigid, that will govern the vertical displacement.
The rotation of the connection is

$$\begin{aligned}\theta &= \frac{M_{Pl,connections,C3}}{S_{j,ini,C3}/2} \\ &= \frac{276.3}{91780/2} \\ &= 6.021 \cdot 10^{-3}\ rad\end{aligned} \tag{4.28}$$

And the displacement of the beam associated with this angle is

$$\tan(\theta) = \frac{\Delta_{connections}}{L_0} \leftrightarrow \Delta_{connections} = 8000 \cdot \tan(6.021 \cdot 10^{-3}) = 48.16\ mm$$

All in all, the total vertical displacement is equal to $\Delta = 16.47 + 48.16 = 64.63$ mm.

From this point, the calculations will focus on the right beam, with connection C2 at the right extremity. Indeed, it has the lowest compressive strength, once the yielding is reached, the horizontal displacement will be free, which will result in the loss of the arch contribution.

The updated length L_D of the rod subjected to Δ displacement and whose end springs have been elastically compressed by $\delta_{c,el}$, is

$$\begin{aligned}L_D &= \sqrt{(L_0 + \delta_{c,el})^2 + (h_{eq} - \Delta)^2} \\ &= \sqrt{(8000 + 0.6084)^2 + (581 - 64.63)^2} \\ &= 8017.25\ mm\end{aligned} \tag{4.29}$$

where,

$$\begin{aligned}\delta_{c,el} &= \frac{N_{pl,t}}{k_{c,C2}} + \frac{N_{pl,t}}{k_{c,C3}} \\ &= \frac{986.3}{2211} + \frac{951}{5859} \\ &= 0.6084\ mm\end{aligned} \tag{4.30}$$

To cancel the arch effect, the row in compression of the connection C2 must yield, which corresponds to a horizontal displacement $\delta_{c,p,C2}$ of

$$\begin{aligned}\delta_{c,p,C2} &= \frac{N_{Pl,c,C2}}{k_{c,C2}} \\ &= \frac{986.3}{2211} \\ &= 0.446\ mm\end{aligned} \tag{4.31}$$

The C3 connection on the left also compresses by

$$\begin{aligned}\delta_{c,p,C3} &= \frac{N_{Pl,c,C2}}{k_{c,C3}} \\ &= \frac{986.3}{5859} \\ &= 0.1683\ mm\end{aligned} \tag{4.32}$$

As a result of this displacement, the angle between the rod and the horizontal is

$$\begin{aligned}\cos(\theta) &= \frac{L_0 + \delta_{c,p,C2} + \delta_{c,p,C3}}{L_D} \\ &= \frac{8000 + 0.446 + 0.1683}{8017.25} \\ &= 0.997 \rightarrow \theta = 0.0646\ rad\end{aligned} \tag{4.33}$$

Then, the vertical force P_{arch} which yields the row in compression and which cancels the arch effect is calculated. This one is,

$$\begin{aligned}P_{arch}/2 &= N_c \cdot \tan(\theta) \\ &= (N_{Pl,c} - \cdot N_{Pl,t}) \cdot \tan(\theta) \\ &= (986.3 - 986.3) \cdot \tan(0.0646) \\ &= 0\ kN\end{aligned}$$

This contribution of the arch effect is null. It is logical since when the plastic hinge is created, the row in compression yields also. But it will be shown in part 6.2.7 how to take the contribution of the arc effect into account by making a small modification to the connection.

6.2.4 Contribution of the slab

Since the gravitational forces are transmitted to the beams through the slab, the latter must also form a plastic mechanism so that the forces are transferred to the beams.

Until now, the slab has not been considered. In a first step, the slab will be designed at ULS to take the "classical load". Then the plastic mechanism of the slab submitted to the punctual force of the column loss will be studied. This would allow to quantify the contribution of the slab to the resistance of the floor.

The concrete slab is 0.2 m thick. The class of concrete used is C30/37. The design of the slab at ULS is done in Appendix O.
To withstand the load combinations at ULS, a reinforcement with $\phi 10$ bars placed every 200 mm is required. The reinforcement is the same at the top and bottom of the section and in both directions of the slab. Finally, the plastic resistance of a 1 m slab width is $M_{Rd,Pl,slab} = 26.9\ kN.m/m$. It has to be noted that the failure mode is a ductile one. Indeed, the bending moment resistance corresponds to the yielding of the reinforcement. This is verified in the Appendix.

In the following, only the piece of the slab in the DAP is studied. This extended slab has a length of 24 m and a width of 16 m, since the column is lost. The support conditions of the slab are such that two sides, the sides in facade, are free to rotate, but restrained in displacement. While the other two sides are embedded, due to the continuity of the slab beyond the DAP.

Firstly, it is investigated whether the slab is capable of resisting the scenario of the column loss and whether it can transmit the loads to the supports.
For this purpose, in a first time, a 1 m wide and 16 m long section of slab is studied under the accidental load of 5.9 kN/m^2. The bending diagram is presented in Figure 4.62.

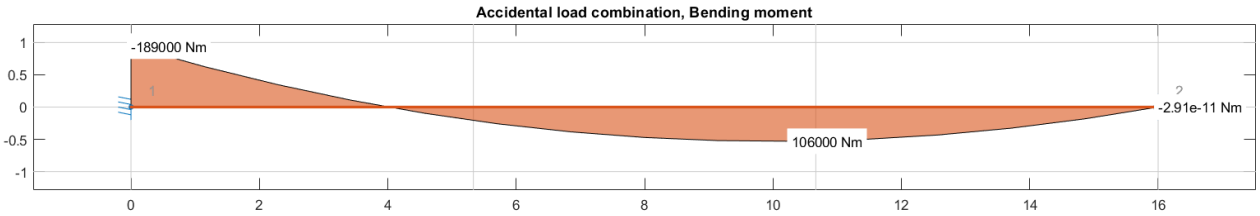

Figure 4.62: Bending moment of the 1 m width slab.

The maximum bending moment is $M_{Ed,slab} = 189\ kN.m$ which is much higher than the resistance of the slab $M_{Rd,Pl,slab} = 26.9\ kN.m/m$. Thus, the slab is not resistant and cannot transmit the external loads to its supports.

Therefore, since it is known that the slab will be brought to failure, the value of the vertical punctual force, representing the loss of the column, that causes the plastic mechanism of the slab will be calculated.
By doing this, a contribution to the resistance of the floor of the DAP will be found and it can be added to the contribution of the plastic beams mechanism and the arch effect.

However, it should be noted that the addition of the three contributions cannot be done in all cases. Indeed, the vertical displacements must be small enough for the slab to retain the plastic moment along its lines of plasticity. If the vertical displacements are too large, the ductility conditions would no longer be met and the slab would not be able to retain the plastic moment, so in this case the contribution of the slab would be zero.
Here, the vertical displacements are small, as the arch effect of the connecting rods in compression, explained earlier, restricts the vertical displacement. Furthermore, the resistant bending moment is a ductile mode since it has been shown that it is governed by the yielding of the reinforcement.
So by developing the plastic mechanism, the slab can maintain the plastic moment along these yielded lines since ductility is assured.

The load capacity of the slab submitted to a punctual force representing the loss of the column is studied trough the Johanssen method where two patterns of failure are studied.
Based on the properties of the slab, by equalling the external work with the internal work, the vertical force which creates the plastic mechanism can be deduced.

The first pattern presented is similar to a pyramid ruin, it is presented in Figure 4.63.

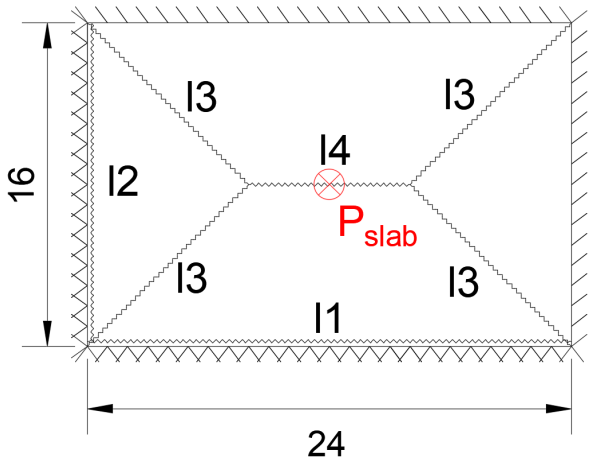

Figure 4.63: Pyramid failure pattern.

In general, the external work represents the applied force multiplied by the displacement of the slab in the continuity of the force.
In this case, assuming a maximum displacement δ_0 in line with the applied force, the work of the external forces is

$$W = P_{slab} \cdot \delta_0 \tag{4.34}$$

The work of the internal forces is the product of the plastic moment M_{Pl} by the length of the yield lines l and the rotation of it θ,

$$U = M_{Pl}\ [kN.m/m] \cdot l_{lines}\ [m] \cdot \theta\ [rad] \tag{4.35}$$

The contribution of all yield lines must be taken into account.

In this case, the internal work is the sum of the dissipation of internal energy in the seven yield lines. Since the reinforcement is the same at the top and bottom of the section, there is no distinction between positive and negative plastic moment. As a reminder, the plastic bending moment is $M_{Rd,Pl,Slab} = 26.9\ kN.m/m$.
The internal work is

$$\begin{aligned} U &= \underbrace{M_{Pl} \cdot 24 \cdot \frac{\delta_0}{8}}_{l1} + \underbrace{M_{Pl} \cdot 16 \cdot \frac{\delta_0}{8}}_{l2} + 4 \cdot \underbrace{M_{Pl} \cdot \sqrt{8^2 + 8^2} \cdot \frac{\delta_0}{8}}_{l3} + \underbrace{M_{Pl} \cdot 8 \cdot \frac{\delta_0}{8}}_{l4} \\ &= 313.56 \cdot \delta_0\ kN.m \end{aligned} \tag{4.36}$$

By equalling the work of the external forces with that of the internal forces, the vertical force causing the plastic mechanism of the slab can be found. It is

$$P_{slab,pyramid} = 313.56\ kN \tag{4.37}$$

The second failure scheme studied is that of the cone. It is shown in Figure 4.64.

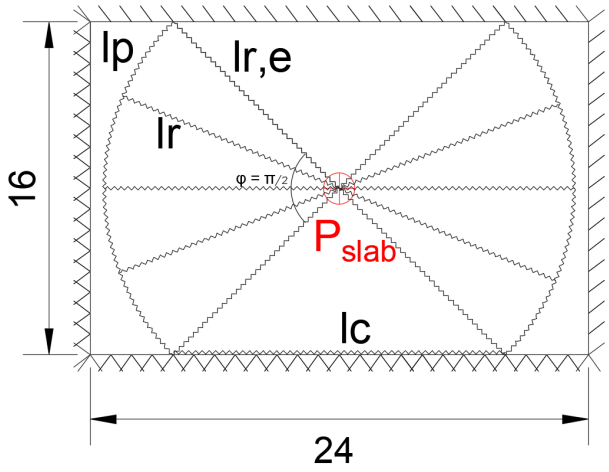

Figure 4.64: Cone failure pattern.

While in the previous failure mechanism there were a finite number of yield lines, here there are an infinite number of lines within the two disc portions.

Assuming also a maximum displacement of δ_0, the external work is equal to the one before, i.e. $W = \delta_0 \cdot P_{slab}$.

The work of the internal forces is a little more complicated than that of the first pattern. There are three distinct contributions,

1. the contribution of the infinite radius (l_r & $l_{r,e}$) inside the two disc portions

$$\begin{aligned} U_{disc} &= \underbrace{\int_{-\varphi/2}^{\varphi/2} M_{Pl} \cdot \delta_0 \cdot d_\varphi}_{lr} + \underbrace{2 \cdot \delta_0 \cdot M_p \cdot 2 \cdot \cot\left(\frac{\varphi}{2}\right)}_{l_{r,e}} \\ &= M_{Pl} \cdot \delta_0 \cdot \left(2\varphi + 4 \cdot \cot\left(\frac{\varphi}{2}\right)\right) \end{aligned} \tag{4.38}$$

2. the contribution of the perimeter l_p of the two discs

$$\begin{aligned} U_{perimeter} &= 2 \cdot \int_{-\varphi/2}^{\varphi/2} M_{Pl} \cdot r \cdot \frac{\delta_0}{r} d\varphi \\ &= 2 \cdot \varphi \cdot M_{Pl} \cdot \delta_0 \end{aligned} \tag{4.39}$$

3. the contribution of the embedded slab l_c at the support

$$\begin{aligned} U_{support} &= M_{Pl} \cdot 2 \cdot r \cdot \cos\left(\frac{\varphi}{2}\right) \cdot \frac{\delta_0}{r \cdot \sin\left(\frac{\varphi}{2}\right)} \\ &= M_{Pl} \cdot 2 \cdot \cot\left(\frac{\varphi}{2}\right) \cdot \delta_0 \end{aligned} \tag{4.40}$$

The total internal work is therefore

$$U = M_{Pl} \cdot \delta_0 \cdot \left(2\varphi + 4 \cdot \cot\left(\frac{\varphi}{2}\right)\right) + 2 \cdot \varphi \cdot M_{Pl} \cdot \delta_0 + M_{Pl} \cdot 2 \cdot \cot\left(\frac{\varphi}{2}\right) \cdot \delta_0 \tag{4.41}$$

The angle minimising the force causing the mechanism to appear is $\varphi = 90°$, so this value will be used.

The force causing the cone failure mechanism of the slab is found by equalling the internal work with the external work,

$$\begin{aligned} P_{slab,cone} &= M_{Pl} \cdot (\pi + 4) + \pi \cdot M_{Pl} + M_{Pl} \cdot 2 \\ &= 330.41 \ kN \end{aligned} \tag{4.42}$$

Now that the force causing the two types of failure mechanism has been calculated, the conclusion is that it is the pyramid-shaped mechanism that will appear since the force causing it is smaller than the force causing the cone failure mechanism.

Thus the slab can sustain a punctual force of $P_{slab} = 313.56 \ kN$ before developing its plastic mechanism.

6.2.5 Contribution of the short frame

So far, the main focus has been on the long frame with partial strength connections and on the slab. But the short frame could also contribute to the resistance of the floor. As a reminder, the beam of the DAP of the short frame is IPE550 and the connection at the ends are hinged.

To assess this contribution, a model developed by Demonceau et al. (2013) is used. Under the vertical force P, the beams of the floor will move vertically, as shown in Figure 4.65.

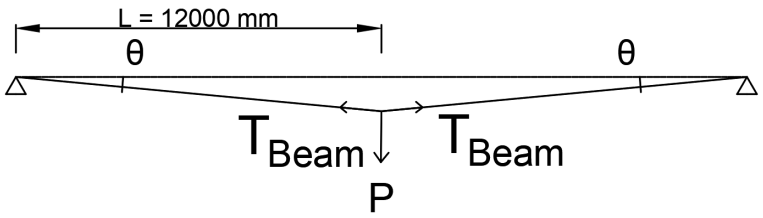

Figure 4.65: Beam under the vertical force P.

Writing the vertical equilibrium of the structure, it comes

$$P = 2 \cdot T_{beam} \cdot \sin(\theta) \tag{4.43}$$

The elongation of the beam can be obtained by

$$\Delta L = L - L_0 = T_{beam} \cdot \frac{L_0}{E \cdot A_{IPE550}} \tag{4.44}$$

where L_0 is the initial length and $L = L_0/\cos(\theta)$ the extended length.

It was previously shown that when the plastic mechanism of the beams of the long frame is created, a vertical displacement $\Delta = 62.69\ mm$ appears.
Since the two perpendicular frames are linked, the short frame also moves vertically by Δ. So it is possible to find the rotation angle θ associated with this displacement,

$$\theta = \arctan\left(\frac{64.63}{12000}\right) = 5.38 \cdot 10^{-3}\ rad \tag{4.45}$$

The tensile force in the beam can be obtain with the equation 4.44,

$$\begin{aligned} T_{beam} &= \frac{1-\cos(\theta)}{\cos(\theta)} \cdot E \cdot A_{IPE550} \\ &= \frac{1-\cos(5.38 \cdot 10^{-3})}{\cos(5.38 \cdot 10^{-3})} \cdot 210000 \cdot 13440 \\ &= 40,937.7\ N \end{aligned} \tag{4.46}$$

and the force P that can be sustain by the beams is

$$\begin{aligned} P &= 2 \cdot 40,934.7 \cdot \sin(5.38 \cdot 10^{-3}) \\ &= 440.9\ N \end{aligned} \tag{4.47}$$

Compared to the other contributions, this one is very low. This is due to the small vertical displacement which means that the tensile forces cannot be fully developed, resulting in a very low vertical force.

6.2.6 Robustness assessment

So far the resistance of the different contributions has been calculated. As a reminder, four contributions to the resistance of the floor are to be taken into account,

1. the contribution coming from the steel beams mechanism. The resistance is $P_{Pl,beam} = 149.36\ kN$
2. the contribution coming from the arch effect. The resistance is $P_{arch} = 0\ kN$

3. the contribution of the concrete slab. The resistance is $P_{slab} = 313.56\ kN$

4. the contribution of the short frame, but it's negligible face to the others.

Summing up these three contributions, the total resistance of the floor submit to the column loss is $P = 462.92\ kN$.

The value of the vertical force representing the loss of the column has already been calculated in part 3.2.2. Since an inner column is considered, the vertical force acting on the floor is $P_{floor,in} = 623.84\ kN$.

But, when the value of the force applied is compared to the resistance of the floor, it can be seen that the force of the column loss is greater than the resistance. Since the behaviour of all floors is the same, the structure is not able to resist the column loss and therefore it is not robust.

But, by modifying the structural properties, it may be possible to ensure the robustness of the structure. This is studied in the next part.

6.2.7 Optimisation of the structure

In order to ensure the robustness of the structure, it is necessary to optimise it. In order to increase the resistance of the floor, several possibilities can be considered:

1. increase the properties of the connections to delay the plastic mechanism of the beam.

2. improve the component *column web in compression* to increase the contribution of the arch effect.

3. install flush-end plate connection at the ends of the short frame beams to have a contribution of the plastic beams mechanism.

4. improve the properties of the slab to delay the plastic mechanism of it.

The first possibility studied is to improve the strength of the component *column web in compression*, for the connection C2. One way to do this is to stiffen the column locally so that this component is not activated under the tensile force in the beam.

Following this modification, the value of the parameters of the C2 connection are changed, they are presented in Table 4.38, the component considered is the *beam flange and web in compression*. The parameters of connection C3 are unchanged and remain the same as in Table 4.37.

Parameters	Value
$N_{Pl,t}$	1117.8 kN
$N_{Pl,t,r1}$	666 kN
$N_{Pl,t,r2}$	451.8 kN
$N_{pl,c}$	2146 kN
k_c	∞
$S_{j,ini}$	96260 kN.m/rad

Table 4.38: New parameters of the connection C2.

Since the tensile properties of the C2 joint are changed, the plastic moment is also changed. It comes,

$$\begin{aligned} M_{Pl,connections,C2} &= 666 \cdot 0.52 + 451.8 \cdot 0.0605 \\ &= 373.63\ kN.m \end{aligned} \tag{4.48}$$

And therefore the force $P_{Pl,beams}$ causing the plastic mechanism of the beams is also modified, it is

$$\begin{aligned} M_{Pl,connection,C2}+3 \cdot M_{Pl,connection,C3} &= P_{Pl,beam} \cdot L_0 \\ 373.63+3 \cdot 276.3 &= P_{Pl,beam} \cdot 8 \\ P_{Pl,beam} &= 150.31\ kN \end{aligned} \tag{4.49}$$

The vertical displacement of the beam Δ_{beam} is also modified since the force $P_{Pl,beams}$ that causes the beams plastic mechanism is increased,

$$\begin{aligned} \Delta_{beam} &= \frac{P_{Pl,beam} \cdot (2 \cdot L_0)^3}{192 \cdot E \cdot I_y} \\ &= \frac{150310 \cdot (2 \cdot 8000)^3}{192 \cdot 21000 \cdot 92080 \cdot 10^4} \\ &= 16.59\ mm \end{aligned} \tag{4.50}$$

The rotational stiffness of the C2 connection, following its optimisation, is greater than that of the C3 connection. It is therefore the C2 connection that governs the vertical displacement due to the rotation of the connection. The rotation θ is

$$\begin{aligned} \theta &= \frac{M_{Pl,connections,C2}}{\frac{S_{j,ini,C2}}{2}} \\ &= \frac{373.6}{\frac{96260}{2}} \\ &= 7.77 \cdot 10^{-3}\ rad \end{aligned} \tag{4.51}$$

This causes the beam to move vertically by

$$\Delta_{connection} = 8000 \cdot \tan(3.88 \cdot 10^{-3}) = 62.16\ mm \tag{4.52}$$

Then the total vertical displacement is $\Delta = 16.59 + 62.16 = 78.75\ mm$.

However, the shortening of the springs in compression under the effect of the vertical force $P_{Pl,beams}$ is modified since this force is changed.
The $\delta_{c,el,C2}$ shortening for the connection C2 is equal to zero because the stiffness is infinite, while the shortening for the connection C3 is equal to

$$\begin{aligned} \delta_{c,el,C3} &= \frac{N_{pl,t,C3}}{k_{c,C3}} \\ &= \frac{951}{5859} \\ &= 0.162\ mm \end{aligned} \tag{4.53}$$

thus,

$$\begin{aligned} L_D &= \sqrt{(L_0 + \delta_{c,el})^2 + (h_{eq} - \Delta)^2} \\ &= 8015.91\ mm \end{aligned} \tag{4.54}$$

When the compressive spring of the connection C2 yields, the shortening of the C3 spring is

$$\begin{aligned} \delta_{c,p,C3} &= \frac{N_{c,p,C2}}{k_{c,C3}} \\ &= 0.19\ mm \end{aligned} \tag{4.55}$$

So, the angle θ between the horizontal and the connecting rod in compression is

$$\begin{aligned} \cos(\theta) &= \frac{L_0 + 2 \cdot \delta_{c,p}}{L_D} \\ &= 0.998 \rightarrow \theta = 0.0626\ rad \end{aligned} \tag{4.56}$$

and therefore the force that causes the arch effect to break is

$$\begin{aligned} P_{arch}/2 &= (N_{Pl,c,C2} - N_{Pl,t,C2}) \cdot \tan(\theta) \\ &= (2146 - 1117.8) \cdot \tan(0.064) \\ &= 64.48\ kN \rightarrow P_{arch} = 128.97\ kN \end{aligned} \tag{4.57}$$

And the contribution of the arc effect is more important than before.

However, by summing the 3 contributions (beam mechanism, arch effect and slab), the resistance of the floor is $P = 150.31 + 128.97 + 313.56 = 592.84\ kN$, which is always less than the applied force representing the loss of the column $P_{floor,in} = 623.84\ kN$. So the optimisation of the structure must continue.

Another simple and inexpensive solution would be to improve the properties of the slab.
Previously, the slab was designed with $\phi 10/200$ reinforcement in both perpendicular directions. In order to increase the resistance of the slab in bending, the reinforcement is increased to $\phi 12/200$.

The detailed calculations of this optimisation is not given, but the same equations as in Appendix O are used to calculate the bending moment resistance of the slab. The optimised bending moment resistance is $M_{Pl,Rd} = 38.52\ kN.m$.
This bending moment corresponds to a yielding of the reinforcement and is therefore ductile. Indeed, when the reinforcement yields, the compressive stress in the concrete is $\sigma_c = 13.6$ Mpa which is lower than $f_{cd} = 17$ Mpa.

Increasing the bending resistance of the slab does not change the yield pattern that may occur. It is therefore possible to calculate the P_{slab} force for which the pyramid-shaped plasticity pattern appears. Starting from the equation giving the internal work (equation 4.36), it gives

$$\begin{aligned} U &= \underbrace{M_{Pl} \cdot 24 \cdot \frac{\delta_0}{8}}_{l1} + \underbrace{M_{Pl} \cdot 16 \cdot \frac{\delta_0}{8}}_{l2} + 4 \cdot \underbrace{M_{Pl} \cdot \sqrt{8^2 + 8^2} \cdot \frac{\delta_0}{8}}_{l3} + \underbrace{M_{Pl} \cdot 8 \cdot \frac{\delta_0}{8}}_{l4} \\ &= 449.02\ kN.m \end{aligned} \tag{4.58}$$

The contribution of the plastic beams mechanism and the arch effect is unchanged following the slab optimisation.

So the sum of the three contributions gives a resistance of

$$P = 150.31 + 128.97 + 449.02 = 728.35\ kN \tag{4.59}$$

and then since the force representing the column loss ($P_{floor,in} = 623.84$ kN) is lower than the sum of the three contributions ($P_{Resistant} = 728.35$ kN), the structure is considered to be able to resist the column loss scenario and is therefore qualified as robust.

6.3 Conclusion

Through this approach a method quite different from the previous ones has been studied.

Firstly, in contrast to the reference structure consisting of hinged connections, partial strength connections are used at the extremities of the DAP beams of the long frame.

These semi-resistant connections due to their moment resistance delay the onset of membrane forces. By means of a simple modelling of the beam by two rods and taking into account the connections, the contribution of this resistance has been evaluated.

In addition to the plastic mechanism to be developed, it was shown that another phenomenon had to be overcome before large displacements could occur, the effect of the arch formed by the connecting rods in compression. But considering the reference structure, this contribution is zero.

Finally it was shown that the slab made a contribution to the strength. By developing a plastic mechanism, given sufficient ductility, the slab can maintain the plastic moment along its yield lines.

For the short frame, whose beams are connected to the columns by means of hinged connections, it has been shown that the contribution of the short frame to the resistance is negligible compared to the contributions coming from the large frame.

By comparing the force of the column loss with the force required to cause large displacements, it was shown that the applied force was greater than the resisting force.
Thus the robustness of the structure was not ensured, the structure has to be optimised.

For this purpose, several possibilities exist, in this work, it was chosen to improve the properties connection of the facade column. Indeed, the contribution of the arch effect of the reference structure is quite small. By locally stiffening the column at the connections, the contribution could be increased. But this was not enough, so the reinforced concrete slab was also optimised by increasing the diameter of the reinforcement. As a result of these improvements, the robustness of the structure is ensured.

5 Critical analyses of the different approaches

1 Introduction

The aim of this section is to provide a critical analysis of the three methods used to ensure the robustness of the steel structure studied. These methods have been studied throughout this master thesis.

The critical analysis will be presented in the order of the methods studied, starting with the prescriptive tying method, moving on to the numerical approach and ending with the new analytical approach.

Finally, the three methods will be compared together.

At the end, the practitioner will have an overview of the advantages and disadvantages of the different methods that exist to ensure the robustness of a steel structure following the loss of a column.

2 Tying method

Several conclusions could be drawn by studying the tying method.

The first one is that in comparison with the membrane forces obtained by the numerical analysis, the tensile forces obtained by the tying method are largely underestimated.
Therefore, by respecting the Eurocode recommendations, the structure could not be robust under the scenario of the loss of a column. By following the Eurocode, the practitioner thinks that he can ensure the robustness of the structure when he cannot.
It is therefore necessary to revise the calculation of the tensile force or establish different tensile forces depending on the exceptional event.

Secondly, the tying method requires to provide horizontal ties throughout the structure at each floor. This means that some elements may have to be designed again so that the tensile force obtained by the tying method is lower than the resistance of these elements.
However, with the numerical method we have seen that, considering the loss of the column, there are only significant forces in the directly affected part of the structure. It is therefore not necessary to look at the rest of the structure, although the Eurocode tells us to do so with the tying method.
Here again, a scenario should be taken into account to be able to study the elements concerned and therefore not optimise the elements at the other end of the structure which would not be

affected by the exceptional event.

Another disadvantage of the method is that it does not mention any aspects of ductility and rotational capacity of the connections. This is a problem because in order to activate the tensile forces in phase 3, the structure has to deform. But for the structure to deform, it needs ductility and sufficient capacity for rotation at the connections.
This need for ductility must be covered in the Eurocode. For example the use of class 1 or class 2 sections could be mentioned. Another way to ensure this ductility could be to set a limit on the yield strength of the steel f_y.

The background of the equations to obtain the tensile force in the horizontal ties is not clear. It has been seen that the beam is not only subjected to surface loads. By the descent of loads, punctual loads act on some beams. However, the Eurocode requires that only surface loads are taken into account when calculating the tensile force.
The origin of the coefficients is not clear either in the equation, where does the 0.8 come from for example, why take a minimum value of 75, where does it come from ?

Another aspect about the verification of ties is that only the tensile force is taken into account. In our case, in addition to the tensile force, the horizontal tie was also subjected to a bending moment. This one is not taken into account in the check of the strength of the tie, so the resistance is overestimated since in the presence of a bending moment, the axial strength decreases due to the M-N interaction.

Regarding connections between beams and columns, no distinction is made between a hinged, partial strength or full strength connection. However, it has been shown that when using partial strength or full strength connections, the tensile forces were lower in the DAP than if hinged connections were considered.

The advantage of the method is that it is simple and quick to implement. It also requires the installation of vertical and horizontal ties so that the structure forms a whole.
But in contrast, when the scenario of the loss of a column is considered, the robustness of the structure is not ensured.

3 Numerical approach

Concerning the numerical method, different observations could be highlighted.

Indeed, the numerical approach takes many parameters close to reality into consideration. For example, material and geometric non-linearities are explicitly taken into account in the analysis, which is as close to reality as possible.

The numerical model makes it possible to observe the redistribution of forces in the structure by means of an alternative path. These forces can also be known and thus the verification of the strength of the structure can be conducted.
Then, all column loss scenarios can be applied once the model is built, whatever the floor and whatever the column.

On the other hand, the method has one major disadvantage, the execution time. Firstly, it takes some time to obtain a valid model. Indeed, in the case of this study, the structure first had to be modelled in the analysis software used at the University of Liege.

Then, the model had to be validated on the basis of the design carried out by the design office Feldman + Weynand.
After that, the nonlinear model had to be created and validated by making comparisons for a similar loading with the results of the linear model.
Only at this point, the scenario of column loss could be considered. After a first nonlinear analysis, the model had to be slightly modified.
After that the results of the nonlinear analysis could be used.
Moreover, it should be noted that the duration of the nonlinear calculation is not negligible, for this model the calculation time varied between 12 and 15 minutes depending on the parameters and the computer. During this time, the tensile forces of the tying method have the time to be calculated.

Practitioners cannot afford to use a numerical analysis for small structures, as it would be too much time consuming. On the other hand, it is entirely possible and cost-effective to use this approach for larger structures.

The last point to consider is that the `Finelg` software does not take into account the behaviour of connections subjected to axial force and bending moment. In this case the numerical model could not be used to study the robustness of a structure with rigid or semi-rigid connections. This represents a significant disadvantage as the use of semi-rigid connections could ensure the robustness of the structure.

4 New analytical approach

The new analytical approach is a method that was developed in the context of this master thesis. The hindsight on this method is therefore not as great as for the two others.

First of all, this method is rather limited to the type of connection considered, as it only takes into account semi-resistant or resistant connections. A structure with hinged connections cannot therefore be studied with this new approach.

Then, depending on the plastic resistance of the different elements of the beam and the connections, several yielding schemes can be considered. In this master thesis only one scheme is considered (first yielding of the row in tension, then the row in compression and finally the beam itself). It is therefore not known how the system would react if another yielding scheme was considered.

After that, the study of this method stopped at the end of phase 2 before the large displacements appear. The appearance of these membrane forces, following the vertical displacement, requires too much deformation of the system, of the order of 1 m of vertical displacement at the point of the column loss. The structure does not have this level of ductility and therefore it is necessary to avoid going beyond the end of phase 2.

Moreover, the contribution of the slab to the resistance is not systematically taken into account, the hypothesis of small displacements must be respected as mentioned previously. We have seen that the contribution of this slab was not negligible, so this one have to be studied.

Regarding the application of this method, it is simpler and faster than the numerical approach but more complicated than the tying method. On the other hand, it is more successful than the tying method, since on the one hand the equations are better mastered and on the other

hand the ductility of the connections is considered.
Unfortunately, for the reasons already mentioned, this new method could not be compared with the numerical approach.

5 Conclusions

Through the critical analysis of the different methods used in this master thesis to ensure the robustness of the steel structure, the advantages and disadvantages of these methods have been highlighted.

The tying method cannot guarantee the robustness of the studied steel structure, the tensile forces are much lower than those that will actually occur. The practitioner, by respecting the application of this method, will think that he is ensuring the robustness of the structure when he is not.

The numerical method allows to take into account real phenomena in the structure and to have a regard of its real behaviour under column loss. On the other hand, the method has its limitations, such as the type of connections used in the structure and the consequent implementation time of this method.

Finally the new approach allows to study the robustness of a structure with partial strength connections. By means of a relatively simple model, several contributions of the floor elements to the resistance can be calculated. However, this method does not allow to highlight the membrane forces that develop in the structure.

In conclusion, depending on the structure under consideration one or the other method should be used. However, the actual tying method should not be used to ensure the robustness of a structure.

6 Conclusions of the research

1 Conclusion

Throughout this master thesis, the robustness of a reference steel structure designed by the office FELDMAN+WEYNAND was studied.
The different methods used to ensure the robustness of the structure under the exceptional event of the loss of a column have all brought different conclusions.

As a reminder, the lost column considered is an inside column of the structure that is not included in the inner core.

To start, the prescriptive method of the Eurocode EN1991-1-7 (2006) was used. It was shown that the structure was robust as the ties resisted the tensile force given by the method. But by comparing the tensile forces obtained with the tying method and the membrane forces obtained with the numerical approach, it was shown that the tying method gives much lower forces. As a result, the tying method, in the case of a column loss scenario, cannot ensure the robustness of the structure.
Moreover, as already mentioned, the tying method does not take into account any aspect of ductility, which is of primary importance when considering the robustness of a structure.

After that, a substantial part of the work was the analysis and study of the robustness of the reference structure by a numerical approach, using `Finelg` software, where the alternative path method was used. Many observations could be made.

Firstly, regarding the analysis, it has been shown that the result when considering an elastic or plastic material law is not the same. When a plastic material law is considered, yielding occurs in one direction of the structure. This causes a decrease in internal forces, as the beams yield, which are taken up in the perpendicular direction.
In the DAP there is therefore a redistribution of forces between the orthogonal frames.

Secondly, with regard to the resistance of the structure to the scenario of column losses, it was shown that the weakness of the structure was in the connections. The beams and columns have sufficient resistance to sustain the loss of the column, but the ultimate tensile strength of the connections is not sufficient.
A further study of these connections was carried out where it was shown that the connections of the reference structure had to be optimised. After the optimisation of the reference connection, the fin plate one, it was concluded that to ensure the resistance of the structure, the connections and structural elements had to be optimised.
But by increasing the size of the cross-section, the weight and therefore the cost of the structure was also increased. As this solution was not feasible, another type of hinged joint was investigated, the header plate.

The purpose of this change of connections was to see if by keeping a hinged connection, it was possible to ensure the robustness of the structure.
The conclusion of the study with these connections is similar to the previous one. In order to ensure robustness, the connection must be modified and the cross-section of the beams in the DAP must be increased. This increase is however less important than the previous one but still consequent on the final weight of the structure.

So in both cases the reference structure had to be modified. The main reason why the cross section of the profiles had to be increased was because of the component "*beam web in tension*". As the thickness of the web was quite low and the net height was also low, the tensile strength of the beam was too low to sustain the tensile forces coming from the loss of the column.

The main conclusion of the numerical study was that it was not possible to ensure the robustness of the reference structure, even by optimising the connections. A modification of the structural elements of the DAP must take place.

Following this conclusion, another type of connection, a partial strength one, was considered, the flush-end plate connection. This type of connection is installed at the ends of the frame beams with the smallest spans. The connections of the other frame remain the original ones. This semi-rigid connection has the particularity of being able to bear the bending moment. Thanks to this, the appearance of membrane forces in the beams is delayed.

By means of a new simple approach, it was shown that to resist the column loss, four contributions could be considered, the contribution of the plastic beams mechanism, the contribution from the arch effect, the contribution from the slab and the contribution of the short frame.
However, the slab contribution can only be considered if small displacements occur and the contribution coming from the short frame is negligible.

The addition of the four contributions to the resistance showed that the structure designed at ULS to sustain the classical loads, with semi-rigid joints in one direction, was not robust. But by optimising the connection, by locally stiffening the column, and by optimising the slab, by increasing the radius of the reinforcement, it was shown that the robustness of the structure was ensured.
Studies in parallel with this work have also shown that between the end of phase 2 and the beginning of phase 3, the structure deforms largely, with a vertical displacement of 1 m at the lost column. Such a displacement is not feasible for ductility reasons, so it is necessary to avoid going beyond the end of phase 2 with this approach.

In summary, this master thesis has shown that the method prescribed by the Eurocode does not ensure the robustness of the structure when the loss of an internal column is considered.
Moreover, the robustness of the structure in its original configuration, with hinged connections, designed at ULS, is not ensured when it loses a column.
Finally, by using semi-rigid connections and slightly modifying the properties of the connections and the slab, it was shown that the structure is robust under the column loss scenario.
However, it should be noted that the beam spans used are quite large. In general, in steel construction, a beam has a maximum span of 6 to 7 m.

2 Perspectives

In the coming years, the tying method prescribed by the Eurocode must be modified.
This approach, as it is present in the code, is too insecure and does not provide sufficient resistance to the structure in case of column loss.
The case of application of the method should be clarified and it should take into account ductility aspects.

Then, in order to increase the possibility of studying the structures numerically, the behaviour of semi-rigid connections should be taken into account in the `Finelg` software.

About the innovative method, some simplifying assumptions have been made, such as a very rigid slab in plane that prevents horizontal displacements. This approach could also be extended to full strength connections to cover other types of configuration.

Furthermore, this work only focused on the loss of one internal column. The study of the loss of other columns could be considered in order to ensure the robustness of the structure under all column loss scenarios. In addition, the load combination considered is the lowest possible, since the combination considers a ψ_2 coefficient lower than ψ_1. The conclusion would therefore be modified is this coefficient is applied to the combination.

Bibliography

ArcelorMittal (2018). *Programme de vente : profilés et aciers marchands.* Arcelor mittal.

Demonceau, J.-F. and Dewals, B. (2020). Natural and technological risks in civil engineering. *Part dedicated to the robustness of the structures,University of Liège, Belgium.*

Demonceau, J.-F., Huvelle, C., Comeliau, L., Van Hoang, L., Jaspart, J.-P., Fang, C., Izzuddin, B. A., Elghazouli, A. Y., Nethercot, D. A., Haremza, C., Santiago, A., da Silva, L. S., Zhao, B., Taillefer, N., Dhima, D., Gens, F., , and Obiala, R. (2013). Robustness of car park against localised fire (Robustfire). *Grant Agreement Number RFSR-CT-2008-00036, Final report, EUR, European Commission.*

EN1990 (2002). Eurocode - basis of structural design. *European Committee for Standardization, Brussels,Belgium.*

EN1990-ANB:2021 (2013). Eurocode - bases de calcul des structures - annexe nationale. *European Committee for Standardization, Brussels,Belgium.*

EN1991-1-1 (2002). Eurocode 1 - action on structure - part 1-1 : General action - densities, self-weight, imposed loads for buildings. *European Committee for Standardization, Brussels,Belgium.*

EN1991-1-3 (2003). Eurocode 1 - action on structure - part 1-3 : General action - snow loads. *European Committee for Standardization, Brussels,Belgium.*

EN1991-1-4 (2005). Eurocode 1 - action on structure - part 1-4 : General action - wind actions. *European Committee for Standardization, Brussels,Belgium.*

EN1991-1-7 (2006). Eurocode 1 - action on structure - part 1-7 : General action - accidental actions. *European Committee for Standardization, Brussels,Belgium.*

EN1993-1-1 (2005). Eurocode 3 : Design of steel structures - part 1-1: General rules and rules for building. *European Committee for Standardization, Brussels,Belgium.*

Gemoets, K. (2020). *Contribution to the implementation of robustness in European design recommendations for steel and composite structures.* Master's thesis, Univerisity of Liège, Belgium.

Greish and ULiege (2003). Nonlinear finite element analysis program. In *Finelg user's manual*, page 8.86. Liège, Belgium.

Hjeir, F. (2015). *Robustness of steel structures further to a column loss : identification of the structural requirements through parametrical studies.* Master's thesis, Univerisity of Liège, Belgium.

Huvelle, C., Hoang, V.-L., Jaspart, J.-P., and Demonceau, J.-F. (2015). Complete analytical procedure to assess the response of a frame submitted to a column loss.

Jacques, M. (2019). *Robustness of steel frames further to a column loss: development of analytical methods for practitioners.* Master's thesis, Univerisity of Liège, Belgium.

Jaspart, J., Demonceau, J., Renkin, S., and Guillaume, M. (2009). European recommendations for the design of simple joints in steel structures. *ECCS - european Convention for Constructional Steelwork*.

Jaspart, J.-P. (2015). *Cours de calcul d'éléments métalliques*, pages 1–6.

Kulik, S. (2014). *Robustness of steel structures further to a column loss : consideration of couplings in a 3D structure*. Master's thesis, Univerisity of Liège, Belgium.

List of Figures

A Appendix : Internal forces for the design at ULS

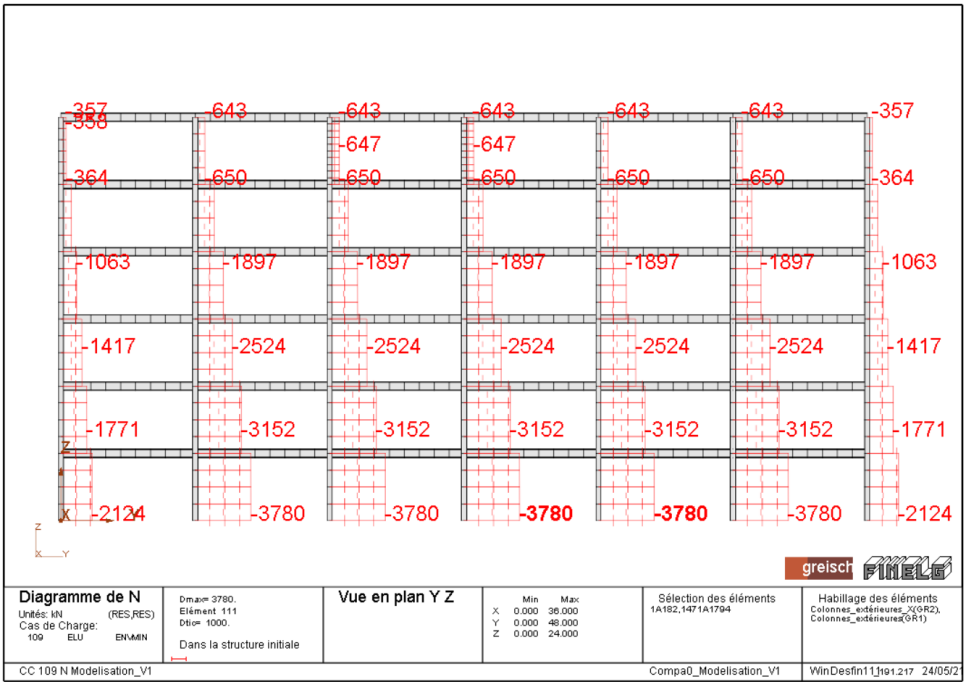

Figure A.1: Axial forces in the HEB340 columns (envelope diagram at ULS).

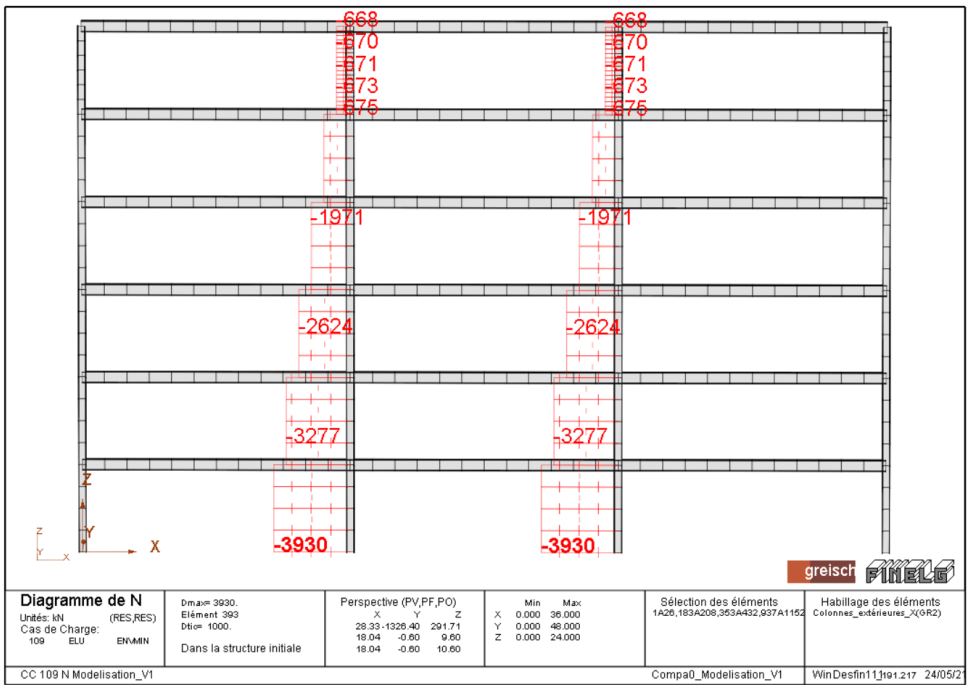

Figure A.2: Axial forces in the HEB360 columns (envelope diagram at ULS).

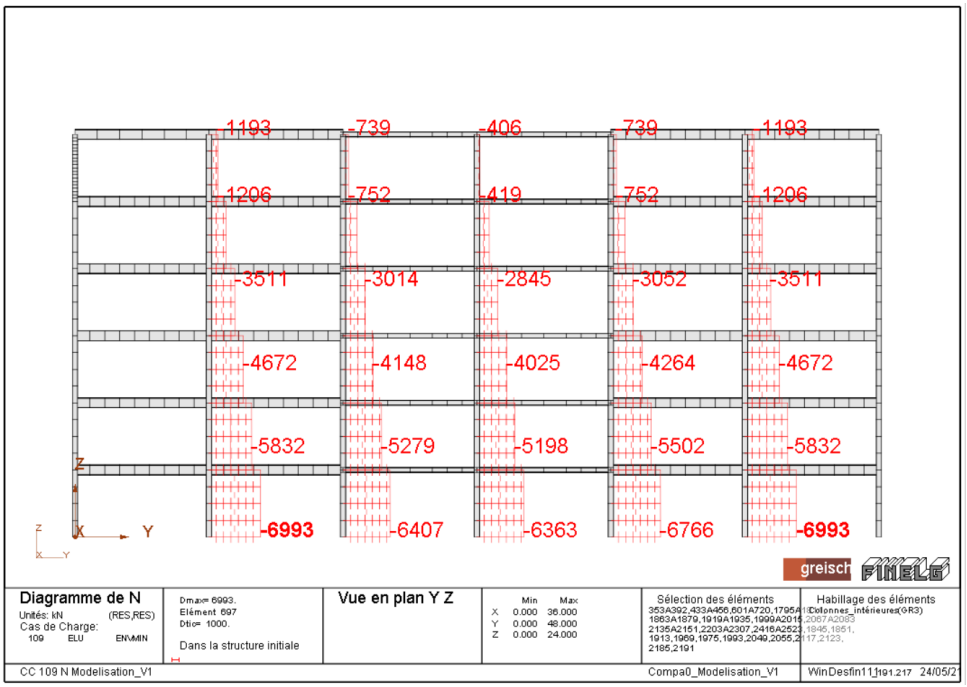

Figure A.3: Axial forces in the HEM300 columns (envelope diagram at ULS).

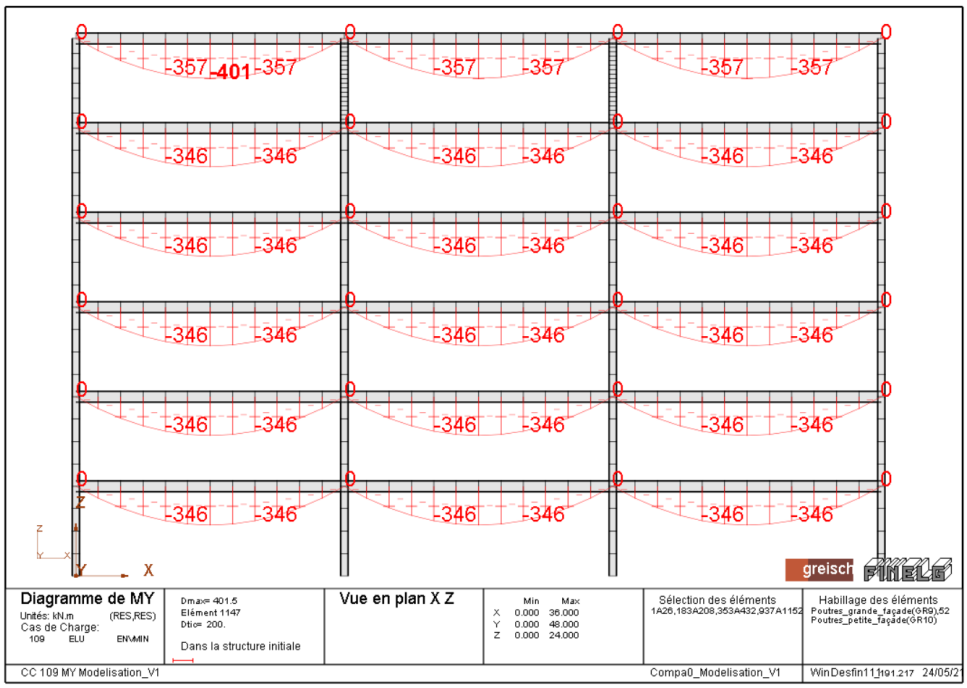

Figure A.4: Bending moment in the IPE500 beams of the short frame facade (envelope diagram at ULS).

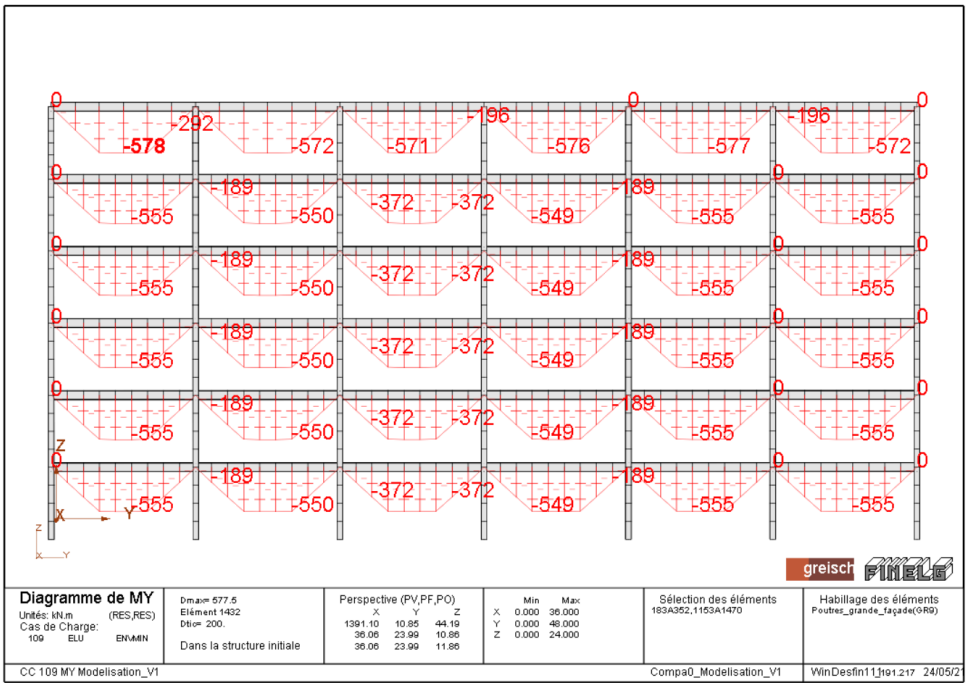

Figure A.5: Bending moment in the IPE500 beams of the long frame facade (envelope diagram at ULS).

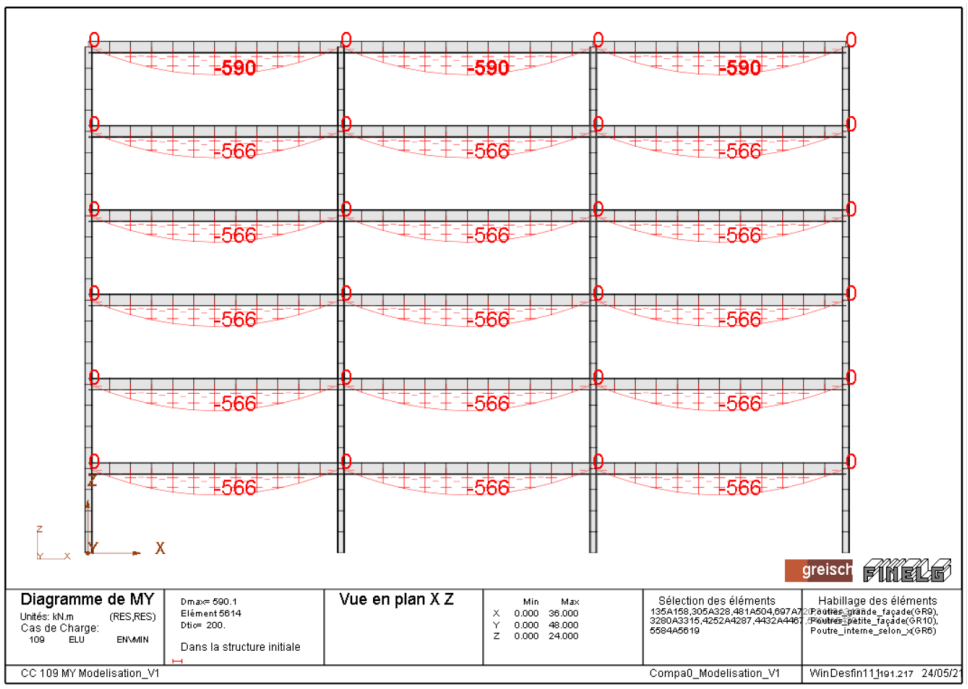

Figure A.6: Bending moment in the IPE550 beams (envelope diagram at ULS).

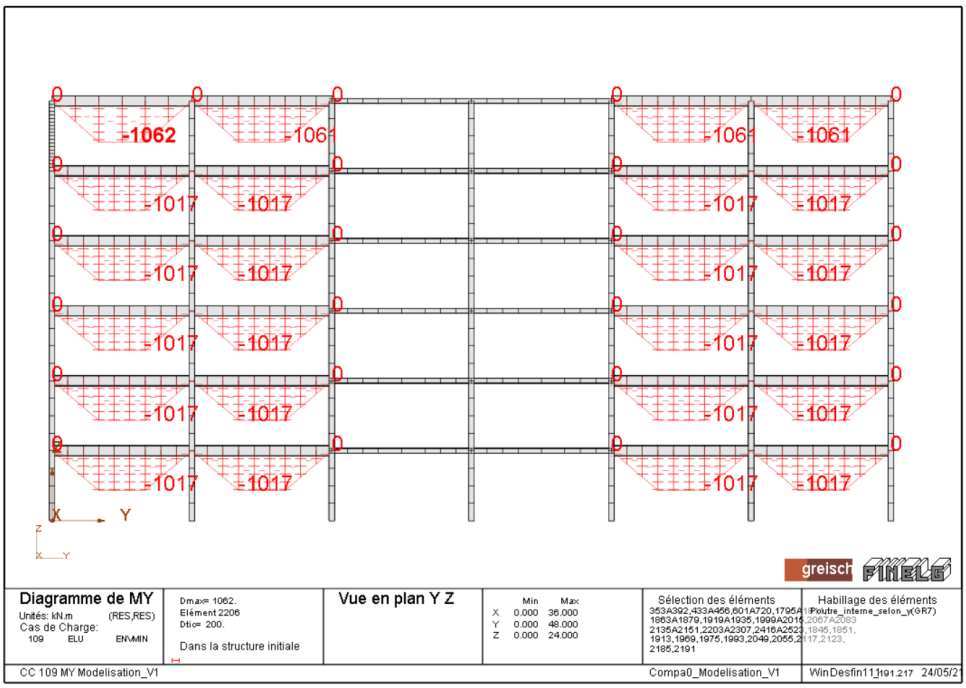

Figure A.7: Bending moment in the IPE600 beams (envelope diagram at ULS).

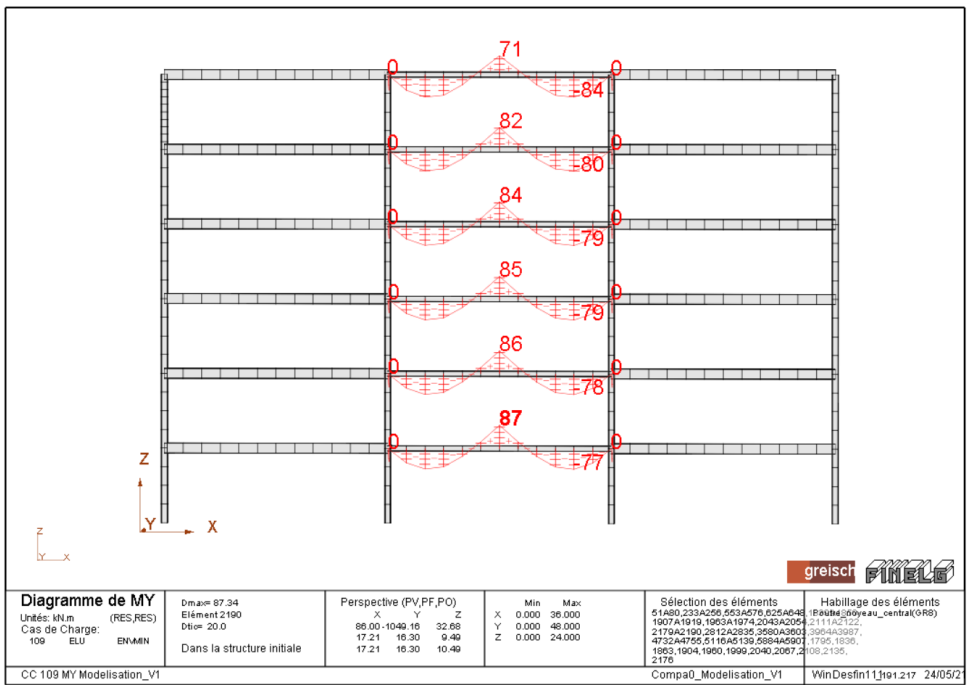

Figure A.8: Bending moment in the HEA300 beams (envelope diagram at ULS).

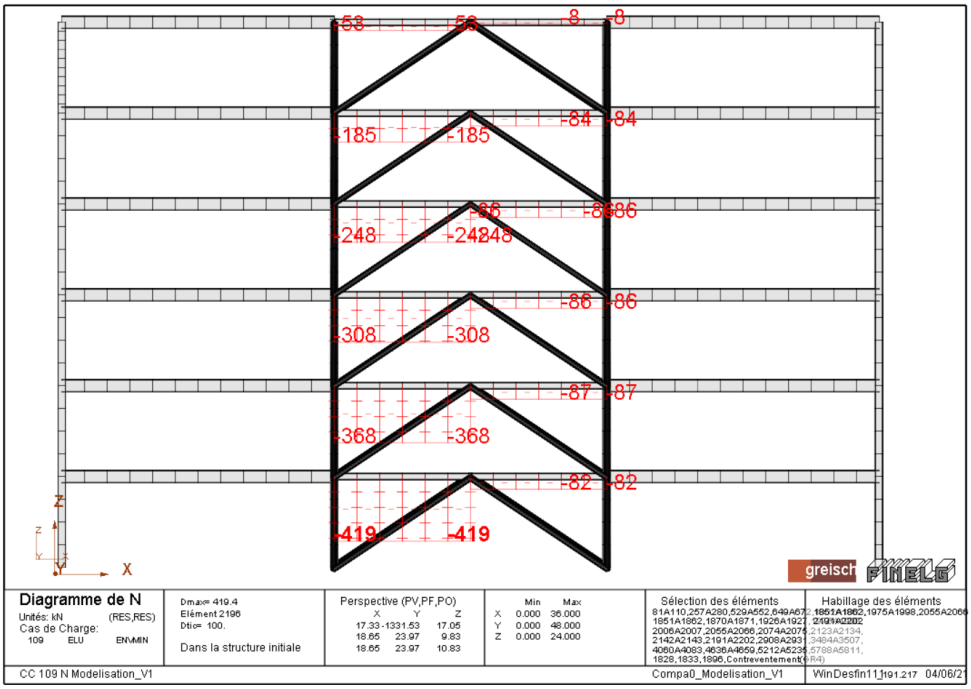

Figure A.9: Normal forces in the HEA300 beams (envelope diagram at ULS).

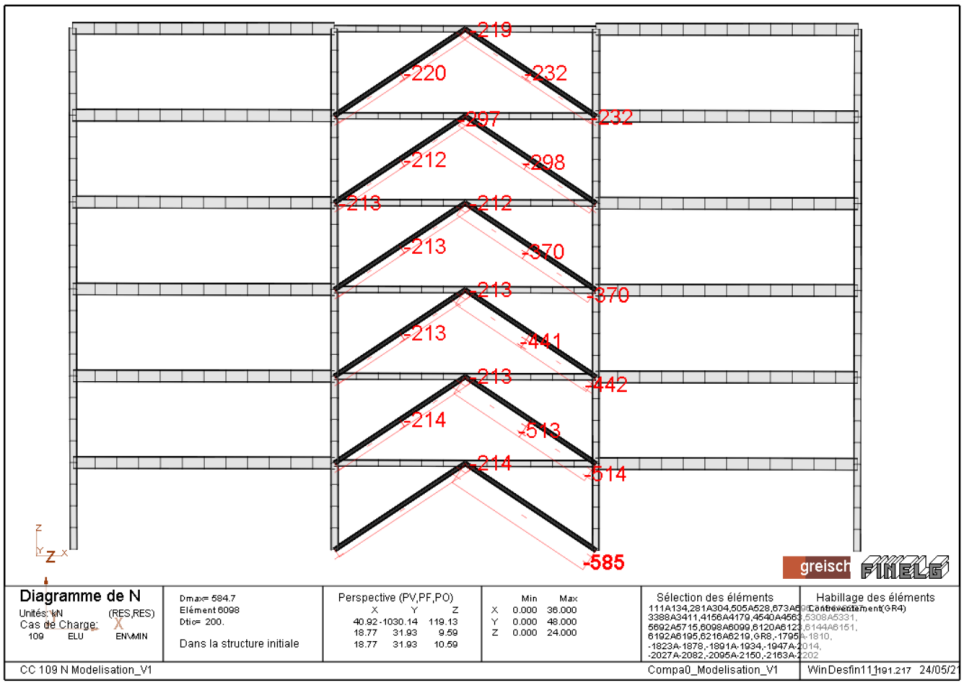

Figure A.10: Normal forces in the long bracing (short frame) (envelope diagram at ULS).

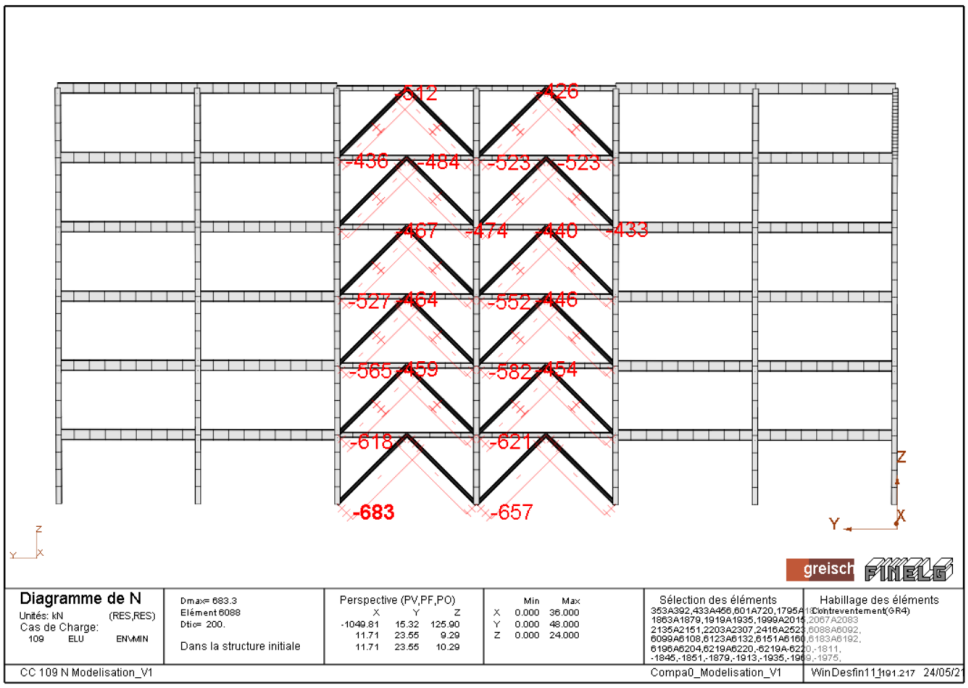

Figure A.11: Normal forces in the short bracing (long frame) (envelop diagram at ULS).

B Appendix : Ultimate tensile resistance for the connection A1w

Note : As the connections have been designed to resist shear, this design is not detailed here. Only the tensile strength part is explained.

1 Datas

1. HEB340

$$h_c = 340\ mm$$
$$b_c = 300\ mm$$
$$t_{fc} = 21.5\ mm$$
$$t_{wc} = 12\ mm$$
$$f_{yc} = 355\ MPa$$
$$f_{uc} = 490\ MPa$$
$$A_c = 17,090\ mm^2$$

2. IPE500

$$h_b = 500\ mm$$
$$b_b = 200\ mm$$
$$t_{fb} = 16\ mm$$
$$t_{wb} = 10.2\ mm$$
$$r_b = 21\ mm$$
$$d_b = 426\ mm$$
$$f_{yb} = 355\ MPa$$
$$f_{ub} = 490\ MPa$$
$$A_b = 11,550\ mm^2$$

3. Fin plate

$$h_p = 225\ mm$$
$$b_p = 150\ mm$$
$$t_p = 10\ mm$$
$$f_{yb} = 355\ MPa$$
$$f_{ub} = 490\ MPa$$
$$a = 6\ mm$$

4. Bolt patern

$M20$ 10.9
$d = 20\ mm$
$d_0 = 22\ mm$
$A_s = 245\ mm^2$
$f_{yb} = 355\ MPa$
$f_{ub} = 490\ MPa$
$n_1 = 4$
$n_2 = 2$

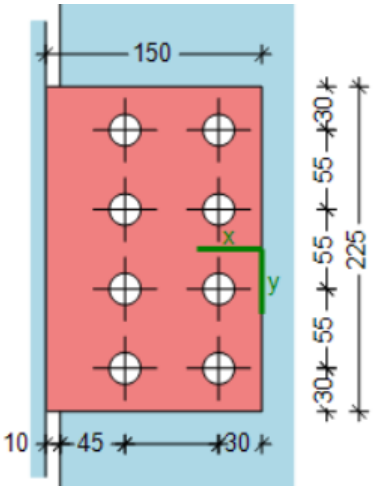

Figure B.1: View of the connection

2 Requirement to allow a plastic redistribution of internal forces

1. $V_{Rd} < \min(V_{Rd,1}; V_{Rd,7}) \rightarrow 255.1 < \min(359.8; 342.3) \rightarrow$ Ok
2. Note for this point, the value of the parameter are taken from the software COP
$$\max\left(\frac{1}{F_{v,Rd}^2} \cdot (\alpha^2 + \beta^2); \frac{1}{V_{Rd,7}^2}\right) \leq \left(\frac{\alpha}{F_{b,ver,Rd}}\right)^2 + \left(\frac{\beta}{F_{b,hor,Rd}}\right)^2$$
For the beam web
$$\Leftrightarrow \max\left(\frac{1}{98000^2} \cdot (0.0735^2 + 0.1865^2); \frac{1}{342300^2}\right) \leq \left(\frac{0.0735}{113700}\right)^2 + \left(\frac{0.1865}{98140}\right)^2$$
$$\Leftrightarrow \max\left(4.18 \cdot 10^{-12}; 8.53 \cdot 10^{-12}\right) \leq 4.03 \cdot 10^{-12} \rightarrow \text{NOK}$$
For the fin plate
$$\Leftrightarrow \max\left(\frac{1}{98000^2} \cdot (0.0735^2 + 0.1865^2); \frac{1}{342300^2}\right) \leq \left(\frac{0.0735}{75480}\right)^2 + \left(\frac{0.1865}{64150}\right)^2$$
$$\Leftrightarrow \max\left(4.18 \cdot 10^{-12}; 8.53 \cdot 10^{-12}\right) 9.4 \cdot 10^{-12} \rightarrow \text{OK}$$

3 Requirements to ensure sufficient rotation capacity

1. $h_p \leq d_b \Leftrightarrow 225\ mm \leq 426\ mm \rightarrow$ Ok
2. $\phi_{available} > \phi_{required}$
where,

$$\phi_{available} = \left(\frac{z}{\sqrt{(z-g_h)^2 + \left(\frac{h_p}{2} + h_e\right)^2}} \right) - \arctan\left(\frac{z-g_h}{\frac{h_p}{2} + h_e} \right)$$

where,
$z = g_h + e_{2b} + p_{21}/2$
$h_e = (h_b - h_p)/2$

$$\phi_{available} = \left(\frac{87.5}{\sqrt{(87.5-10)^2 + \left(\frac{225}{2} + 137.5\right)^2}} \right) - \arctan\left(\frac{87.5-10}{\frac{225}{2} + 137.5} \right) = 0.0403\ rad$$

$\phi_{required} = 0.003$ coming from Finelg

$0.0403 > 0.003 \rightarrow$ Ok

4 Requirement to ensure the ductility

$$a > \frac{\beta_w \cdot f_{yp} \cdot \gamma_{M2} \cdot t_p}{\sqrt{2} \cdot f_{up} \cdot \gamma_{M0}}$$

$$6\ mm > \frac{0.9 \cdot 355 \cdot 1.25 \cdot 10}{\sqrt{2} \cdot 490 \cdot 1.0} = 5.76\ mm$$

5 Computation of the resistance to tying forces

1. Bolts in shear

$$\begin{aligned} N_{u,1} &= n \cdot F_{v,u} \\ &= n \cdot \alpha_v \cdot f_{ub} \cdot A/\gamma_{Mu} \\ &= 8 \cdot 0.5 \cdot 245 \cdot 1000/1.1 = 890.91\ kN \end{aligned}$$

2. Fin plate in bearing

$$\begin{aligned} N_{u,2} &= n \cdot F_{b,u,hor} \\ &= n \cdot k_1 \cdot \alpha_b \cdot f_{up} \cdot d \cdot t_p/\gamma_{Mu} \\ &= 8 \cdot 1.8 \cdot 0.454 \cdot 490 \cdot 20 \cdot 10/1.1 = 583.14\ kN \end{aligned}$$

where,

$$\alpha_b = \min\left(\frac{e_2}{3 \cdot d_0}; \frac{p_2}{3 \cdot d_0} - 0.25; \frac{f_{ub}}{f_{up}}\right)$$
$$= \min\left(\frac{30}{66}; \frac{65}{66} - 0.25; 1\right) = 0.454$$

$$k_1 = \min\left(\frac{2.8 \cdot e_1}{d_0} - 1.7; 1.4 \cdot \frac{p_1}{d_0} - 1.7; 2.5\right)$$
$$= \min\left(\frac{2.8 \cdot 30}{22} - 1.7; 1.4 \cdot \frac{55}{22} - 1.7; 2.5\right) = 1.8$$

3. Fin plate in tension, gross section

$$N_{u,3} = t_p \cdot h_p \cdot f_{up}/\gamma_{Mu}$$
$$= 10 \cdot 225 \cdot 490/1.1 = 1,002.27\ kN$$

4. Fin plate in tension, net section

$$N_{u,4} = 0.9 \cdot A_{net,p} \cdot f_{up}/\gamma_{Mu}$$
$$= 0.9 \cdot (10 \cdot 225 - 22 \cdot 4 \cdot 10) \cdot 490/1.1 = 549.25\ kN$$

5. Beam web in bearing

$$N_{u,5} = n \cdot F_{b,u,hor}$$
$$= n \cdot k_1 \cdot \alpha_b \cdot f_{up} \cdot d \cdot t_{bw}/\gamma_{Mu}$$
$$= 8 \cdot 1.8 \cdot 0.68 \cdot 490 \cdot 20 \cdot 10.2/1.1 = 892.2\ kN$$

where,

$$\alpha_b = \min\left(\frac{e_{2b}}{3 \cdot d_0}; \frac{p_2}{3 \cdot d_0} - 0.25; \frac{f_{ub}}{f_{up}}\right)$$
$$= \min\left(\frac{45}{66}; \frac{65}{66} - 0.25; 1\right) = 0.68$$

$$k_1 = \min\left(1.4 \cdot \frac{p_1}{d_0} - 1.7; 2.5\right)$$
$$= \min\left(1.4 \cdot \frac{55}{22} - 1.7; 2.5\right) = 1.8$$

6. Beam web in tension, gross section

$$N_{u,6} = t_{bw} \cdot h_{bw} \cdot f_{ubw}/\gamma_{Mu}$$
$$= 10.2 \cdot 426 \cdot 490/1.1 = 1,935.59\ kN$$

7. Beam web in tension, net section

$$N_{u,7} = 0.9 \cdot A_{net,bw} \cdot f_{ubw}/\gamma_{Mu}$$
$$= 0.9 \cdot (10.2 \cdot 426 - 22 \cdot 4 \cdot 11.1) \cdot 490/1.1 = 1,382.17\ kN$$

8. Supporting member in bending

$$N_{u,8} = k_m \cdot f_{u,c} \cdot t_{w,c}^2 \cdot \left[\frac{2 \cdot h_p}{d_c} + 4 \cdot \sqrt{1 - \frac{t_p}{d_c}}\right] /\gamma_{Mu}$$
$$= 1.0 \cdot 490 \cdot 12^2 \left[\frac{2 \cdot 225}{243} + 4 \cdot \sqrt{1 - \frac{10}{243}}\right] /1.1 = 370.03\ kN$$

C Appendix : Ultimate tensile resistance for the connection A1S

Note : As the connections have been designed to resist shear, this design is not detailed here. Only the tensile strength part is explained.

1 Datas

1. HEB340

$$h_c = 340\ mm$$
$$b_c = 300\ mm$$
$$t_{fc} = 21.5\ mm$$
$$t_{wc} = 12\ mm$$
$$f_{yc} = 355\ MPa$$
$$f_{uc} = 490\ MPa$$
$$A_c = 17,090\ mm^2$$

2. IPE500

$$h_b = 500\ mm$$
$$b_b = 200\ mm$$
$$t_{fb} = 16\ mm$$
$$t_{wb} = 10.2\ mm$$
$$r_b = 21\ mm$$
$$d_b = 426\ mm$$
$$f_{yb} = 355\ MPa$$
$$f_{ub} = 490\ MPa$$
$$A_b = 11,550\ mm^2$$

3. Fin plate

$$h_p = 180\ mm$$
$$b_p = 140\ mm$$
$$t_p = 10\ mm$$
$$f_{yb} = 355\ MPa$$
$$f_{ub} = 490\ MPa$$
$$a = 6\ mm$$

4. Bolt patern

$M20$ 10.9
$d = 20\ mm$
$d_0 = 22\ mm$
$a_s = 245\ mm^2$
$f_{yb} = 355\ MPa$
$f_{ub} = 490\ MPa$
$n_1 = 3$
$n_2 = 2$

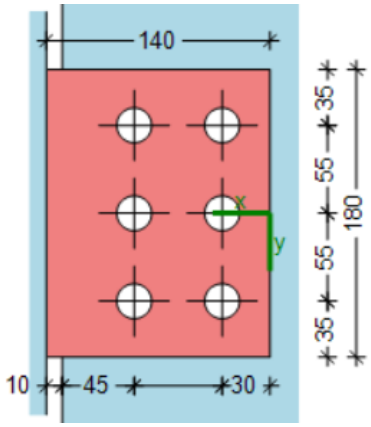

Figure C.1: View of the connection

2 Requirement to allow a plastic redistribution of internal forces

1. $V_{Rd} < \min(V_{Rd,1}; V_{Rd,7}) \rightarrow 170.3 < \min(240.4; 232.4) \rightarrow$ Ok
2. Note for this point, the value of the parameter are taken from the software COP
$$\max\left(\frac{1}{F_{v,Rd}^2} \cdot (\alpha^2 + \beta^2); \frac{1}{V_{Rd,7}^2}\right) \leq \left(\frac{\alpha}{F_{b,ver,Rd}}\right)^2 + \left(\frac{\beta}{F_{b,hor,Rd}}\right)^2$$

For the beam web

$$\Leftrightarrow \max\left(\frac{1}{98000^2} \cdot (0.1364^2 + 0.2727^2); \frac{1}{232400^2}\right) \leq \left(\frac{0.1364}{83970}\right)^2 + \left(\frac{0.2727}{83970}\right)^2$$

$$\Leftrightarrow \max\left(9.68 \cdot 10^{-12}; 1.85 \cdot 10^{-11}\right) \leq 1.31 \cdot 10^{-11} \rightarrow \text{NOK}$$

For the fin plate

$$\Leftrightarrow \max\left(\frac{1}{98000^2} \cdot (0.1364^2 + 0.2727^2); \frac{1}{232400^2}\right) \leq \left(\frac{0.1364}{74840}\right)^2 + \left(\frac{0.2727}{64150}\right)^2$$

$$\Leftrightarrow \max\left(9.68 \cdot 10^{-12}; 1.85 \cdot 10^{-11}\right) \leq 2.13 \cdot 10^{-11} \rightarrow \text{OK}$$

3 Requirements to ensure sufficient rotation capacity

1. $h_p \leq d_b \Leftrightarrow 180\ mm \leq 426\ mm \rightarrow$ Ok
2. $\phi_{available} > \phi_{required}$
where,

$$\phi_{available} = \left(\frac{z}{\sqrt{(z-g_h)^2 + \left(\frac{h_p}{2} + h_e\right)^2}} \right) - \arctan\left(\frac{z-g_h}{\frac{h_p}{2} + h_e} \right)$$

where,
$z = g_h + e_{2b} + p_{21}/2$
$h_e = (h_b - h_p)/2$

$$\phi_{available} = \left(\frac{82.5}{\sqrt{(82.5-10)^2 + \left(\frac{180}{2} + 160\right)^2}} \right) - \arctan\left(\frac{82.5-10}{\frac{180}{2} + 160} \right) = 0.0402\ rad$$

$\phi_{required} = 0.003$ coming from Finelg

$0.0402 > 0.003 \rightarrow$ Ok

4 Requirement to ensure the ductility

$$a > \frac{\beta_w \cdot f_{yp} \cdot \gamma_{M2} \cdot t_p}{\sqrt{2} \cdot f_{up} \cdot \gamma_{M0}}$$

$$6\ mm > \frac{0.9 \cdot 355 \cdot 1.25 \cdot 10}{\sqrt{2} \cdot 490 \cdot 1.0} = 5.76\ mm$$

5 Computation of the resistance to tying forces

1. Bolts in shear

$$\begin{aligned} N_{u,1} &= n \cdot F_{v,u} \\ &= n \cdot \alpha_v \cdot f_{ub} \cdot A/\gamma_{Mu} \\ &= 6 \cdot 0.5 \cdot 245 \cdot 1000/1.1 = 668.18\ kN \end{aligned}$$

2. Fin plate in bearing

$$\begin{aligned} N_{u,2} &= n \cdot F_{b,u,hor} \\ &= n \cdot k_1 \cdot \alpha_b \cdot f_{up} \cdot d \cdot t_p/\gamma_{Mu} \\ &= 6 \cdot 1.8 \cdot 0.454 \cdot 490 \cdot 20 \cdot 10/1.1 = 437.36\ kN \end{aligned}$$

where,

$$\alpha_b = \min\left(\frac{e_2}{3 \cdot d_0}; \frac{p_2}{3 \cdot d_0} - 0.25; \frac{f_{ub}}{f_{up}}\right)$$
$$= \min\left(\frac{30}{66}; \frac{55}{66} - 0.25; 1\right) = 0.454$$

$$k_1 = \min\left(\frac{2.8 \cdot e_1}{d_0} - 1.7; 1.4 \cdot \frac{p_1}{d_0} - 1.7; 2.5\right)$$
$$= \min\left(\frac{2.8 \cdot 35}{22} - 1.7; 1.4 \cdot \frac{55}{22} - 1.7; 2.5\right) = 1.8$$

3. Fin plate in tension, gross section

$$N_{u,3} = t_p \cdot h_p \cdot f_{up}/\gamma_{Mu}$$
$$= 10 \cdot 180 \cdot 490/1.1 = 801.8\ kN$$

4. Fin plate in tension, net section

$$N_{u,4} = 0.9 \cdot A_{net,p} \cdot f_{up}/\gamma_{Mu}$$
$$= 0.9 \cdot (10 \cdot 180 - 22 \cdot 3 \cdot 10) \cdot 490/1.1 = 457.04\ kN$$

5. Beam web in bearing

$$N_{u,5} = n \cdot F_{b,u,hor}$$
$$= n \cdot k_1 \cdot \alpha_b \cdot f_{up} \cdot d \cdot t_{bw}/\gamma_{Mu}$$
$$= 6 \cdot 1.8 \cdot 0.583 \cdot 490 \cdot 20 \cdot 11.1/1.1 = 572.5\ kN$$

where,

$$\alpha_b = \min\left(\frac{e_{2b}}{3 \cdot d_0}; \frac{p_2}{3 \cdot d_0} - 0.25; \frac{f_{ub}}{f_{up}}\right)$$
$$= \min\left(\frac{45}{66}; \frac{55}{66} - 0.25; 1\right) = 0.583$$

$$k_1 = \min\left(1.4 \cdot \frac{p_1}{d_0} - 1.7; 2.5\right)$$
$$= \min\left(1.4 \cdot \frac{55}{22} - 1.7; 2.5\right) = 1.8$$

6. Beam web in tension, gross section

$$N_{u,6} = t_{bw} \cdot h_{bw} \cdot f_{ubw}/\gamma_{Mu}$$
$$= 10.2 \cdot 426 \cdot 490/1.1 = 1,935.6\ kN$$

7. Beam web in tension, net section

$$N_{u,7} = 0.9 \cdot A_{net,bw} \cdot f_{ubw}/\gamma_{Mu}$$
$$= 0.9 \cdot (10.2 \cdot 426 - 22 \cdot 3 \cdot 10.2) \cdot 490/1.1 = 1,472.2\ kN$$

8. Supporting member in bending

$$N_{u,8} = +\infty$$

D Appendix : Ultimate tensile resistance for the connection A2

Note : As the connections have been designed to resist shear, this design is not detailed here. Only the tensile strength part is explained.

1 Datas

1. HEB360

$$h_c = 360\ mm$$
$$b_c = 300\ mm$$
$$t_{fc} = 22.5\ mm$$
$$t_{wc} = 12.5\ mm$$
$$f_{yc} = 355\ MPa$$
$$f_{uc} = 490\ MPa$$
$$A_c = 18,060\ mm^2$$

2. IPE500

$$h_b = 500\ mm$$
$$b_b = 200\ mm$$
$$t_{fb} = 16\ mm$$
$$t_{wb} = 10.2\ mm$$
$$r_b = 21\ mm$$
$$d_b = 426\ mm$$
$$f_{yb} = 355\ MPa$$
$$f_{ub} = 490\ MPa$$
$$A_b = 11,550\ mm^2$$

3. Fin plate

$$h_p = 180\ mm$$
$$b_p = 140\ mm$$
$$t_p = 10\ mm$$
$$f_{yb} = 355\ MPa$$
$$f_{ub} = 490\ MPa$$
$$a = 6\ mm$$

4. Bolt patern

$M20$ 10.9
$d = 20\ mm$
$d_0 = 22\ mm$
$a_s = 245\ mm^2$
$f_{yb} = 355\ MPa$
$f_{ub} = 490\ MPa$
$n_1 = 3$
$n_2 = 2$

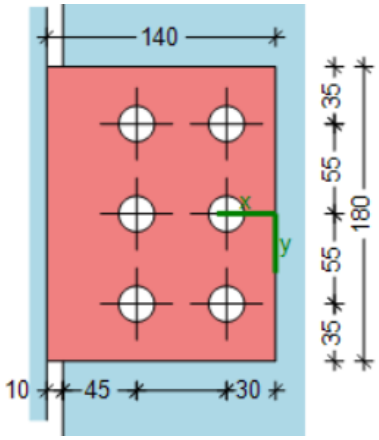

Figure D.1: View of the connection

2 Requirement to allow a plastic redistribution of internal forces

1. $V_{Rd} < \min(V_{Rd,1}; V_{Rd,7}) \rightarrow 255.1 < \min(359.8; 342.3) \rightarrow$ Ok
2. Note for this point, the value of the parameter are taken from the software COP
$$\max\left(\frac{1}{F_{v,Rd}^2}\cdot(\alpha^2+\beta^2); \frac{1}{V_{Rd,7}^2}\right) \leq \left(\frac{\alpha}{F_{b,ver,Rd}}\right)^2 + \left(\frac{\beta}{F_{b,hor,Rd}}\right)^2$$

   For the beam web

$$\Leftrightarrow \max\left(\frac{1}{98000^2}\cdot(0.07348^2+0.1865^2); \frac{1}{342300^2}\right) \leq \left(\frac{0.07348}{113700}\right)^2 + \left(\frac{0.1865}{98140}\right)^2$$

$$\Leftrightarrow \max\left(4.418\cdot10^{-12}; 8.53\cdot10^{-12}\right) \leq 4.03\cdot10^{-12} \rightarrow \text{NOK}$$

   For the fin plate

$$\Leftrightarrow \max\left(\frac{1}{98000^2}\cdot(0.07348^2+0.1865^2); \frac{1}{342300^2}\right) \leq \left(\frac{0.07348}{75480}\right)^2 + \left(\frac{0.1865}{64170}\right)^2$$

$$\Leftrightarrow \max\left(4.418\cdot10^{-12}; 8.53\cdot10^{-12}\right) \leq 9.39\cdot10^{-12} \rightarrow \text{OK}$$

3 Requirements to ensure sufficient rotation capacity

1. $h_p \leq d_b \Leftrightarrow 180\ mm \leq 426\ mm \rightarrow$ Ok
2. $\phi_{available} > \phi_{required}$
   where,

$$\phi_{available} = \left(\frac{z}{\sqrt{(z-g_h)^2 + \left(\frac{h_p}{2} + h_e\right)^2}} \right) - \arctan\left(\frac{z-g_h}{\frac{h_p}{2} + h_e} \right)$$

where,
$z = g_h + e_{2b} + p_{21}/2$
$h_e = (h_b - h_p)/2$

$$\phi_{available} = \left(\frac{82.5}{\sqrt{(82.5-10)^2 + \left(\frac{180}{2} + 160\right)^2}} \right) - \arctan\left(\frac{82.5-10}{\frac{180}{2} + 160} \right) = 0.0402\ rad$$

$\phi_{required} = 0.002$ coming from Finelg

$0.0402 > 0.003 \rightarrow$ Ok

4 Requirement to ensure the ductility

$$a > \frac{\beta_w \cdot f_{yp} \cdot \gamma_{M2} \cdot t_p}{\sqrt{2} \cdot f_{up} \cdot \gamma_{M0}}$$

$$6\ mm > \frac{0.9 \cdot 355 \cdot 1.25 \cdot 10}{\sqrt{2} \cdot 490 \cdot 1.0} = 5.76\ mm$$

5 Computation of the resistance to tying forces

1. Bolts in shear

$$\begin{aligned} N_{u,1} &= n \cdot F_{v,u} \\ &= n \cdot \alpha_v \cdot f_{ub} \cdot A/\gamma_{Mu} \\ &= 6 \cdot 0.5 \cdot 245 \cdot 1000/1.1 = 668.18\ kN \end{aligned}$$

2. Fin plate in bearing

$$\begin{aligned} N_{u,2} &= n \cdot F_{b,u,hor} \\ &= n \cdot k_1 \cdot \alpha_b \cdot f_{up} \cdot d \cdot t_p/\gamma_{Mu} \\ &= 6 \cdot 1.8 \cdot 0.454 \cdot 490 \cdot 20 \cdot 10/1.1 = 437.36\ kN \end{aligned}$$

where,

$$\alpha_b = \min\left(\frac{e_2}{3 \cdot d_0}; \frac{p_2}{3 \cdot d_0} - 0.25; \frac{f_{ub}}{f_{up}}\right)$$
$$= \min\left(\frac{30}{66}; \frac{55}{66} - 0.25; 1\right) = 0.454$$

$$k_1 = \min\left(\frac{2.8 \cdot e_1}{d_0} - 1.7; 1.4 \cdot \frac{p_1}{d_0} - 1.7; 2.5\right)$$
$$= \min\left(\frac{2.8 \cdot 35}{22} - 1.7; 1.4 \cdot \frac{55}{22} - 1.7; 2.5\right) = 1.8$$

3. Fin plate in tension, gross section

$$N_{u,3} = t_p \cdot h_p \cdot f_{up}/\gamma_{Mu}$$
$$= 10 \cdot 180 \cdot 490/1.1 = 801.81\ kN$$

4. Fin plate in tension, net section

$$N_{u,4} = 0.9 \cdot A_{net,p} \cdot f_{up}/\gamma_{Mu}$$
$$= 0.9 \cdot (10 \cdot 180 - 22 \cdot 3 \cdot 10) \cdot 490/1.1 = 457.04\ kN$$

5. Beam web in bearing

$$N_{u,5} = n \cdot F_{b,u,hor}$$
$$= n \cdot k_1 \cdot \alpha_b \cdot f_{up} \cdot d \cdot t_{bw}/\gamma_{Mu}$$
$$= 6 \cdot 1.8 \cdot 0.583 \cdot 490 \cdot 20 \cdot 11.1/1.1 = 572.5\ kN$$

where,

$$\alpha_b = \min\left(\frac{e_{2b}}{3 \cdot d_0}; \frac{p_2}{3 \cdot d_0} - 0.25; \frac{f_{ub}}{f_{up}}\right)$$
$$= \min\left(\frac{55}{66}; \frac{55}{66} - 0.25; 1\right) = 0.583$$

$$k_1 = \min\left(1.4 \cdot \frac{p_1}{d_0} - 1.7; 2.5\right)$$
$$= \min\left(1.4 \cdot \frac{55}{22} - 1.7; 2.5\right) = 1.8$$

6. Beam web in tension, gross section

$$N_{u,6} = t_{bw} \cdot h_{bw} \cdot f_{ubw}/\gamma_{Mu}$$
$$= 10.2 \cdot 426 \cdot 490/1.1 = 1,935.59\ kN$$

7. Beam web in tension, net section

$$N_{u,7} = 0.9 \cdot A_{net,bw} \cdot f_{ubw}/\gamma_{Mu}$$
$$= 0.9 \cdot (10.2 \cdot 426 - 22 \cdot 3 \cdot 10.2) \cdot 490/1.1 = 1,472.1\ kN$$

8. Supporting member in bending

$$N_{u,8} = +\infty$$

E Appendix : Ultimate tensile resistance for the connection B1

Note : As the connections have been designed to resist shear, this design is not detailed here. Only the tensile strength part is explained.

1 Datas

1. HEB340

$$h_c = 340\ mm$$
$$b_c = 300\ mm$$
$$t_{fc} = 21.5\ mm$$
$$t_{wc} = 12\ mm$$
$$f_{yc} = 355\ MPa$$
$$f_{uc} = 490\ MPa$$
$$A_c = 17,090\ mm^2$$

2. IPE550

$$h_b = 550\ mm$$
$$b_b = 210\ mm$$
$$t_{fb} = 17.2\ mm$$
$$t_{wb} = 11.1\ mm$$
$$r_b = 24\ mm$$
$$d_b = 467.6\ mm$$
$$f_{yb} = 355\ MPa$$
$$f_{ub} = 490\ MPa$$
$$A_b = 17,090\ mm^2$$

3. Fin plate

$$h_p = 200\ mm$$
$$b_p = 150\ mm$$
$$t_p = 10\ mm$$
$$f_{yb} = 355\ MPa$$
$$f_{ub} = 490\ MPa$$
$$a = 7\ mm$$

4. Bolt patern

$$
\begin{aligned}
&M20\ 10.9\\
&d = 20\ mm\\
&d_0 = 22\ mm\\
&a_s = 245\ mm^2\\
&f_{yb} = 355\ MPa\\
&f_{ub} = 490\ MPa\\
&n_1 = 3\\
&n_2 = 2
\end{aligned}
$$

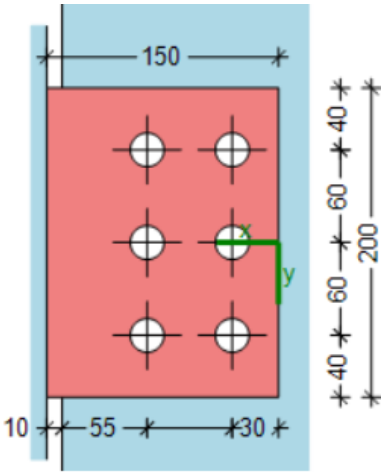

Figure E.1: View of the connection

2 Requirement to allow a plastic redistribution of internal forces

1. $V_{Rd} < \min(V_{Rd,1}; V_{Rd,7}) \rightarrow 190.8 < \min(233.3; 255.9) \rightarrow$ Ok
2. Note for this point, the value of the parameter are taken from the software COP
   $\max\left(\frac{1}{F_{v,Rd}^2} \cdot (\alpha^2 + \beta^2); \frac{1}{V_{Rd,7}^2}\right) \leq \left(\frac{\alpha}{F_{b,ver,Rd}}\right)^2 + \left(\frac{\beta}{F_{b,hor,Rd}}\right)^2$

   For the beam web

   $$\Leftrightarrow \max\left(\frac{1}{98000^2} \cdot (0.1343^2 + 0.2931^2); \frac{1}{255900^2}\right) \leq \left(\frac{0.1343}{103200}\right)^2 + \left(\frac{0.2931}{107500}\right)^2$$

   $$\Leftrightarrow \max\left(1.08 \cdot 10^{-11}; 1.52 \cdot 10^{-11}\right) \leq 9.12 \cdot 10^{-12} \rightarrow \text{NOK}$$

   For the fin plate

   $$\Leftrightarrow \max\left(\frac{1}{98000^2} \cdot (0.1343^2 + 0.2931^2); \frac{1}{255900^2}\right) \leq \left(\frac{0.1343}{85530}\right)^2 + \left(\frac{0.2931}{75480}\right)^2$$

   $$\Leftrightarrow \max\left(1.08 \cdot 10^{-11}; 1.52 \cdot 10^{-11}\right) \leq 1.75 \cdot 10^{-11} \rightarrow \text{OK}$$

3 Requirements to ensure sufficient rotation capacity

1. $h_p \leq d_b \Leftrightarrow 200\ mm \leq 467.6\ mm \rightarrow$ Ok
2. $\phi_{available} > \phi_{required}$
   where,

$$\phi_{available} = \left(\frac{z}{\sqrt{(z-g_h)^2 + \left(\frac{h_p}{2} + h_e\right)^2}} \right) - \arctan\left(\frac{z-g_h}{\frac{h_p}{2} + h_e} \right)$$

where,
$z = g_h + e_{2b} + p_{21}/2$
$h_e = (h_b - h_p)/2$

$$\phi_{available} = \left(\frac{82.5}{\sqrt{(82.5-10)^2 + \left(\frac{200}{2} + 175\right)^2}} \right) - \arctan\left(\frac{82.5-10}{\frac{200}{2} + 175} \right) = 0.037\ rad$$

$\phi_{required} = 0.0065$ coming from Finelg

$0.0402 > 0.0065 \rightarrow$ Ok

4 Requirement to ensure the ductility

$$a > \frac{\beta_w \cdot f_{yp} \cdot \gamma_{M2} \cdot t_p}{\sqrt{2} \cdot f_{up} \cdot \gamma_{M0}}$$

$$6\ mm > \frac{0.9 \cdot 355 \cdot 1.25 \cdot 10}{\sqrt{2} \cdot 490 \cdot 1.0} = 5.76\ mm$$

5 Computation of the resistance to tying forces

1. Bolts in shear

$$\begin{aligned} N_{u,1} &= n \cdot F_{v,u} \\ &= n \cdot \alpha_v \cdot f_{ub} \cdot A/\gamma_{Mu} \\ &= 6 \cdot 0.5 \cdot 245 \cdot 1000/1.1 = 668.18\ kN \end{aligned}$$

2. Fin plate in bearing

$$\begin{aligned} N_{u,2} &= n \cdot F_{b,u,hor} \\ &= n \cdot k_1 \cdot \alpha_b \cdot f_{up} \cdot d \cdot t_p/\gamma_{Mu} \\ &= 6 \cdot 2.12 \cdot 0.454 \cdot 490 \cdot 20 \cdot 10/1.1 = 514.67\ kN \end{aligned}$$

where,

$$\alpha_b = \min\left(\frac{e_2}{3 \cdot d_0}; \frac{p_2}{3 \cdot d_0} - 0.25; \frac{f_{ub}}{f_{up}}\right)$$
$$= \min\left(\frac{30}{66}; \frac{55}{66} - 0.25; 1\right) = 0.454$$

$$k_1 = \min\left(\frac{2.8 \cdot e_1}{d_0} - 1.7; 1.4 \cdot \frac{p_1}{d_0} - 1.7; 2.5\right)$$
$$= \min\left(\frac{2.8 \cdot 40}{22} - 1.7; 1.4 \cdot \frac{60}{22} - 1.7; 2.5\right) = 2.12$$

3. Fin plate in tension, gross section

$$N_{u,3} = t_p \cdot h_p \cdot f_{up}/\gamma_{Mu}$$
$$= 10 \cdot 200 \cdot 490/1.1 = 890.9\ kN$$

4. Fin plate in tension, net section

$$N_{u,4} = 0.9 \cdot A_{net,p} \cdot f_{up}/\gamma_{Mu}$$
$$= 0.9 \cdot (10 \cdot 200 - 22 \cdot 3 \cdot 10) \cdot 490/1.1 = 537.22\ kN$$

5. Beam web in bearing

$$N_{u,5} = n \cdot F_{b,u,hor}$$
$$= n \cdot k_1 \cdot \alpha_b \cdot f_{up} \cdot d \cdot t_{bw}/\gamma_{Mu}$$
$$= 6 \cdot 2.12 \cdot 0.583 \cdot 490 \cdot 20 \cdot 11.1/1.1 = 733.14\ kN$$

where,

$$\alpha_b = \min\left(\frac{e_{2b}}{3 \cdot d_0}; \frac{p_2}{3 \cdot d_0} - 0.25; \frac{f_{ub}}{f_{up}}\right)$$
$$= \min\left(\frac{55}{66}; \frac{55}{66} - 0.25; 1\right) = 0.583$$

$$k_1 = \min\left(1.4 \cdot \frac{p_1}{d_0} - 1.7; 2.5\right)$$
$$= \min\left(1.4 \cdot \frac{60}{22} - 1.7; 2.5\right) = 2.12$$

6. Beam web in tension, gross section

$$N_{u,6} = t_{bw} \cdot h_{bw} \cdot f_{ubw}/\gamma_{Mu}$$
$$= 11.1 \cdot 467.6 \cdot 490/1.0 = 2,312.07\ kN$$

7. Beam web in tension, net section

$$N_{u,7} = 0.9 \cdot A_{net,bw} \cdot f_{ubw}/\gamma_{Mu}$$
$$= 0.9 \cdot (11.1 \cdot 467.6 - 22 \cdot 3 \cdot 11.1) \cdot 490/1.1 = 1,787.16\ kN$$

8. Supporting member in bending

$$N_{u,8} = +\infty$$

F Appendix : Ultimate tensile resistance for the connection B3

Note : As the connections have been designed to resist shear, this design is not detailed here. Only the tensile strength part is explained.

1 Datas

1. HEM300

$$h_c = 340\ mm$$
$$b_c = 310\ mm$$
$$t_{fc} = 39\ mm$$
$$t_{wc} = 21\ mm$$
$$f_{yc} = 355\ MPa$$
$$f_{uc} = 490\ MPa$$
$$A_c = 30,310\ mm^2$$

2. IPE550

$$h_b = 550\ mm$$
$$b_b = 210\ mm$$
$$t_{fb} = 17.2\ mm$$
$$t_{wb} = 11.1\ mm$$
$$r_b = 24\ mm$$
$$d_b = 467.6\ mm$$
$$f_{yb} = 355\ MPa$$
$$f_{ub} = 490\ MPa$$
$$A_b = 17,090\ mm^2$$

3. Fin plate

$$h_p = 200\ mm$$
$$b_p = 150\ mm$$
$$t_p = 10\ mm$$
$$f_{yb} = 355\ MPa$$
$$f_{ub} = 490\ MPa$$
$$a = 7\ mm$$

4. Bolt patern

$$
\begin{aligned}
&M20\ 10.9\\
&d = 20\ mm\\
&d_0 = 22\ mm\\
&a_s = 245\ mm^2\\
&f_{yb} = 355\ MPa\\
&f_{ub} = 490\ MPa\\
&n_1 = 3\\
&n_2 = 2
\end{aligned}
$$

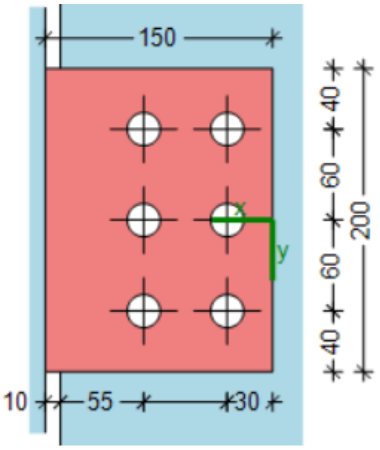

Figure F.1: View of the connection B3

2 Requirement to allow a plastic redistribution of internal forces

1. $V_{Rd} < \min(V_{Rd,1}; V_{Rd,7}) \rightarrow 190.8 < \min(233.3; 255.9) \rightarrow$ Ok
2. Note for this point, the value of the parameter are taken from the software COP

$$\max\left(\frac{1}{F_{v,Rd}^2}\cdot(\alpha^2+\beta^2); \frac{1}{V_{Rd,7}^2}\right) \leq \left(\frac{\alpha}{F_{b,ver,Rd}}\right)^2 + \left(\frac{\beta}{F_{b,hor,Rd}}\right)^2$$

For the beam web

$$\Leftrightarrow \max\left(\frac{1}{98000^2}\cdot(0.1343^2+0.2931^2); \frac{1}{255900^2}\right) \leq \left(\frac{0.1343}{103200}\right)^2 + \left(\frac{0.2931}{107500}\right)^2$$

$$\Leftrightarrow \max\left(1.08\cdot10^{-11}; 1.52\cdot10^{-11}\right) \leq 9.12\cdot10^{-12} \rightarrow \text{NOK}$$

For the fin plate

$$\Leftrightarrow \max\left(\frac{1}{98000^2}\cdot(0.1343^2+0.2931^2); \frac{1}{255900^2}\right) \leq \left(\frac{0.1343}{85530}\right)^2 + \left(\frac{0.2931}{75480}\right)^2$$

$$\Leftrightarrow \max\left(1.08\cdot10^{-11}; 1.52\cdot10^{-11}\right) \leq 1.75\cdot10^{-11} \rightarrow \text{OK}$$

3 Requirements to ensure sufficient rotation capacity

1. $h_p \leq d_b \Leftrightarrow 200\ mm \leq 467.6\ mm \rightarrow$ Ok
2. $\phi_{available} > \phi_{required}$
   where,

$$\phi_{available} = \left(\frac{z}{\sqrt{(z-g_h)^2 + \left(\frac{h_p}{2} + h_e\right)^2}} \right) - \arctan\left(\frac{z-g_h}{\frac{h_p}{2} + h_e} \right)$$

where,
$z = g_h + e_{2b} + p_{21}/2$
$h_e = (h_b - h_p)/2$

$$\phi_{available} = \left(\frac{92.5}{\sqrt{(92.5-10)^2 + \left(\frac{200}{2} + 175\right)^2}} \right) - \arctan\left(\frac{92.5-10}{\frac{200}{2} + 175} \right) = 0.037\ rad$$

$\phi_{required} = 0.0065$ coming from Finelg

$0.0402 > 0.0065 \rightarrow$ Ok

4 Requirement to ensure the ductility

$$a > \frac{\beta_w \cdot f_{yp} \cdot \gamma_{M2} \cdot t_p}{\sqrt{2} \cdot f_{up} \cdot \gamma_{M0}}$$

$$6\ mm > \frac{0.9 \cdot 355 \cdot 1.25 \cdot 10}{\sqrt{2} \cdot 490 \cdot 1.0} = 5.76\ mm$$

5 Computation of the resistance to tying forces

1. Bolts in shear

$$\begin{aligned} N_{u,1} &= n \cdot F_{v,u} \\ &= n \cdot \alpha_v \cdot f_{ub} \cdot A/\gamma_{Mu} \\ &= 6 \cdot 0.5 \cdot 245 \cdot 1000/1.1 = 668.18\ kN \end{aligned}$$

2. Fin plate in bearing

$$\begin{aligned} N_{u,2} &= n \cdot F_{b,u,hor} \\ &= n \cdot k_1 \cdot \alpha_b \cdot f_{up} \cdot d \cdot t_p/\gamma_{Mu} \\ &= 6 \cdot 2.12 \cdot 0.454 \cdot 490 \cdot 20 \cdot 10/1.1 = 514.67\ kN \end{aligned}$$

where,

$$\alpha_b = \min\left(\frac{e_2}{3 \cdot d_0}; \frac{p_2}{3 \cdot d_0} - 0.25; \frac{f_{ub}}{f_{up}}\right)$$
$$= \min\left(\frac{30}{66}; \frac{55}{66} - 0.25; 1\right) = 0.454$$

$$k_1 = \min\left(\frac{2.8 \cdot e_1}{d_0} - 1.7; 1.4 \cdot \frac{p_1}{d_0} - 1.7; 2.5\right)$$
$$= \min\left(\frac{2.8 \cdot 40}{22} - 1.7; 1.4 \cdot \frac{60}{22} - 1.7; 2.5\right) = 2.12$$

3. Fin plate in tension, gross section

$$N_{u,3} = t_p \cdot h_p \cdot f_{up}/\gamma_{Mu}$$
$$= 10 \cdot 200 \cdot 490/1.1 = 890.91\ kN$$

4. Fin plate in tension, net section

$$N_{u,4} = 0.9 \cdot A_{net,p} \cdot f_{up}/\gamma_{Mu}$$
$$= 0.9 \cdot (10 \cdot 200 - 22 \cdot 3 \cdot 10) \cdot 490/1.1 = 537.22\ kN$$

5. Beam web in bearing

$$N_{u,5} = n \cdot F_{b,u,hor}$$
$$= n \cdot k_1 \cdot \alpha_b \cdot f_{up} \cdot d \cdot t_{bw}/\gamma_{Mu}$$
$$= 6 \cdot 2.12 \cdot 0.583 \cdot 490 \cdot 20 \cdot 11.1/1.1 = 733.14\ kN$$

where,

$$\alpha_b = \min\left(\frac{e_{2b}}{3 \cdot d_0}; \frac{p_2}{3 \cdot d_0} - 0.25; \frac{f_{ub}}{f_{up}}\right)$$
$$= \min\left(\frac{55}{66}; \frac{55}{66} - 0.25; 1\right) = 0.583$$

$$k_1 = \min\left(1.4 \cdot \frac{p_1}{d_0} - 1.7; 2.5\right)$$
$$= \min\left(1.4 \cdot \frac{60}{22} - 1.7; 2.5\right) = 2.12$$

6. Beam web in tension gross section

$$N_{u,6} = t_{bw} \cdot h_{bw} \cdot f_{ubw}/\gamma_{Mu}$$
$$= 11.1 \cdot 467.6 \cdot 490/1.1 = 2,312.07\ kN$$

7. Beam web in tension, net section

$$N_{u,7} = 0.9 \cdot A_{net,bw} \cdot f_{ubw}/\gamma_{Mu}$$
$$= 0.9 \cdot (11.1 \cdot 467.6 - 22 \cdot 3 \cdot 11.1) \cdot 490/1.1 = 1,787.16\ kN$$

8. Supporting member in bending

$$N_{u,8} = +\infty$$

G Appendix : Ultimate tensile resistance for the connection C2

Note : As the connections have been designed to resist shear, this design is not detailed here. Only the tensile strength part is explained.

1 Datas

1. HEB360

$$h_c = 360\ mm$$
$$b_c = 300\ mm$$
$$t_{fc} = 22.5\ mm$$
$$t_{wc} = 12.5\ mm$$
$$f_{yc} = 355\ MPa$$
$$f_{uc} = 490\ MPa$$
$$A_c = 18,060\ mm^2$$

2. IPE600

$$h_b = 600\ mm$$
$$b_b = 220\ mm$$
$$t_{fb} = 19\ mm$$
$$t_{wb} = 12\ mm$$
$$r_b = 24\ mm$$
$$d_b = 467.6\ mm$$
$$f_{yb} = 355\ MPa$$
$$f_{ub} = 490\ MPa$$
$$A_b = 15,600\ mm^2$$

3. Fin plate

$$h_p = 300\ mm$$
$$b_p = 150\ mm$$
$$t_p = 10\ mm$$
$$f_{yb} = 355\ MPa$$
$$f_{ub} = 490\ MPa$$
$$a = 6\ mm$$

4. Bolt patern

$$
\begin{aligned}
&M24\ 10.9\\
&d = 24\ mm\\
&d_0 = 26\ mm\\
&a_s = 353\ mm^2\\
&f_{yb} = 355\ MPa\\
&f_{ub} = 490\ MPa\\
&n_1 = 4\\
&n_2 = 2
\end{aligned}
$$

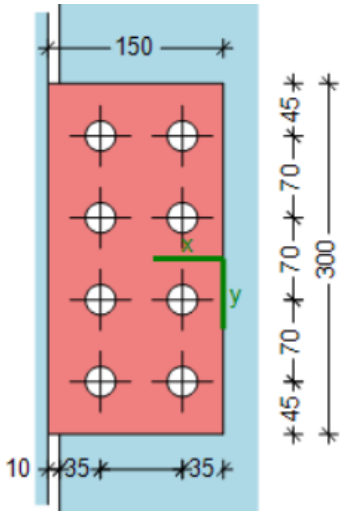

Figure G.1: View of the connection C2

2 Requirement to allow a plastic redistribution of internal forces

1. $V_{Rd} < \min(V_{Rd,1}; V_{Rd,7}) \rightarrow 443.6 < \min(630.2; +\infty) \rightarrow$ Ok
2. Note for this point, the value of the parameter are taken from the software COP
$$\max\left(\frac{1}{F_{v,Rd}^2}\cdot(\alpha^2+\beta^2); \frac{1}{V_{Rd,7}^2}\right) \leq \left(\frac{\alpha}{F_{b,ver,Rd}}\right)^2 + \left(\frac{\beta}{F_{b,hor,Rd}}\right)^2$$

   For the beam web

$$\Leftrightarrow \max\left(\frac{1}{141200^2}\cdot(0.04762^2+0.1429^2); 0\right) \leq \left(\frac{0.04762}{151200}\right)^2 + \left(\frac{0.1429}{104800}\right)^2$$

$$\Leftrightarrow \max\left(1.13\cdot10^{-12}; 0\right) \leq 1.96\cdot10^{-12} \rightarrow \text{NOK}$$

   For the fin plate

$$\Leftrightarrow \max\left(\frac{1}{98000^2}\cdot(0.04762^2+0.1429^2); 0\right) \leq \left(\frac{0.04762}{112300}\right)^2 + \left(\frac{0.1429}{87350}\right)^2$$

$$\Leftrightarrow \max\left(1.13\cdot10^{-12}; 0\right) \leq 2.85\cdot10^{-12} \rightarrow \text{OK}$$

3 Requirements to ensure sufficient rotation capacity

1. $h_p \leq d_b \Leftrightarrow 300\ mm \leq 514\ mm \rightarrow$ Ok
2. $\phi_{available} > \phi_{required}$
   where,

$$\phi_{available} = \left(\frac{z}{\sqrt{(z-g_h)^2 + \left(\frac{h_p}{2} + h_e\right)^2}} \right) - \arctan\left(\frac{z-g_h}{\frac{h_p}{2} + h_e} \right)$$

where,
$z = g_h + e_{2b} + p_{21}/2$
$h_e = (h_b - h_p)/2$

$$\phi_{available} = \left(\frac{85}{\sqrt{(85-10)^2 + \left(\frac{300}{2} + 150\right)^2}} \right) - \arctan\left(\frac{85-10}{\frac{300}{2} + 150} \right) = 0.0335\ rad$$

$\phi_{required} = 0.0071$ coming from Finelg

$0.0335 > 0.0071 \rightarrow$ Ok

4 Requirement to ensure the ductility

$$a > \frac{\beta_w \cdot f_{yp} \cdot \gamma_{M2} \cdot t_p}{\sqrt{2} \cdot f_{up} \cdot \gamma_{M0}}$$

$$6\ mm > \frac{0.9 \cdot 355 \cdot 1.25 \cdot 10}{\sqrt{2} \cdot 490 \cdot 1.0} = 5.76\ mm$$

5 Computation of the resistance to tying forces

1. Bolts in shear

$$\begin{aligned} N_{u,1} &= n \cdot F_{v,u} \\ &= n \cdot \alpha_v \cdot f_{ub} \cdot A/\gamma_{Mu} \\ &= 8 \cdot 0.5 \cdot 353 \cdot 1000/1.1 = 1,283.63\ kN \end{aligned}$$

2. Fin plate in bearing

$$\begin{aligned} N_{u,2} &= n \cdot F_{b,u,hor} \\ &= n \cdot k_1 \cdot \alpha_b \cdot f_{up} \cdot d \cdot t_p/\gamma_{Mu} \\ &= 8 \cdot 2.07 \cdot 0.449 \cdot 490 \cdot 24 \cdot 10/1.1 = 794.12\ kN \end{aligned}$$

where,

$$\alpha_b = \min\left(\frac{e_2}{3 \cdot d_0}; \frac{p_2}{3 \cdot d_0} - 0.25; \frac{f_{ub}}{f_{up}}\right)$$
$$= \min\left(\frac{35}{78}; \frac{80}{78} - 0.25; 1\right) = 0.449$$

$$k_1 = \min\left(\frac{2.8 \cdot e_1}{d_0} - 1.7; 1.4 \cdot \frac{p_1}{d_0} - 1.7; 2.5\right)$$
$$= \min\left(\frac{2.8 \cdot 45}{26} - 1.7; 1.4 \cdot \frac{70}{26} - 1.7; 2.5\right) = 2.07$$

3. Fin plate in tension, gross section

$$N_{u,3} = t_p \cdot h_p \cdot f_{up}/\gamma_{Mu}$$
$$= 10 \cdot 300 \cdot 490/1.1 = 1,336.4\ kN$$

4. Fin plate in tension, net section

$$N_{u,4} = 0.9 \cdot A_{net,p} \cdot f_{up}/\gamma_{Mu}$$
$$= 0.9 \cdot (10 \cdot 300 - 26 \cdot 4 \cdot 10) \cdot 490/1.1 = 785.78\ kN$$

5. Beam web in bearing

$$N_{u,5} = n \cdot F_{b,u,hor}$$
$$= n \cdot k_1 \cdot \alpha_b \cdot f_{up} \cdot d \cdot t_{bw}/\gamma_{Mu}$$
$$= 8 \cdot 2.07 \cdot 0.449 \cdot 490 \cdot 24 \cdot 12/1.1 = 952.95\ kN$$

where,

$$\alpha_b = \min\left(\frac{e_{2b}}{3 \cdot d_0}; \frac{p_2}{3 \cdot d_0} - 0.25; \frac{f_{ub}}{f_{up}}\right)$$
$$= \min\left(\frac{35}{78}; \frac{80}{78} - 0.25; 1\right) = 0.449$$

$$k_1 = \min\left(1.4 \cdot \frac{p_1}{d_0} - 1.7; 2.5\right)$$
$$= \min\left(1.4 \cdot \frac{70}{26} - 1.7; 2.5\right) = 2.07$$

6. Beam web in tension gross section

$$N_{u,6} = t_{bw} \cdot h_{bw} \cdot f_{ubw}/\gamma_{Mu}$$
$$= 12 \cdot 514 \cdot 490/1.1 = 2,747.6\ kN$$

7. Beam web in tension, net section

$$N_{u,7} = 0.9 \cdot A_{net,bw} \cdot f_{ubw}/\gamma_{Mu}$$
$$= 0.9 \cdot (12 \cdot 514 - 26 \cdot 4 \cdot 12) \cdot 490/1.1 = 1,972.47\ kN$$

8. Supporting member in bending

$$N_{u,8} = k_m \cdot f_{u,c} \cdot t_{w,c}^2 \cdot \left[\frac{2 \cdot h_p}{d_c} + 4 \cdot \sqrt{1 - \frac{t_p}{d_c}}\right] / \gamma_{Mu}$$
$$= 1.0 \cdot 490 \cdot 12.5^2 \left[\frac{2 \cdot 300}{261} + 4 \cdot \sqrt{1 - \frac{10}{261}}\right] / 1.1 = 433.03\ kN$$

H Appendix : Ultimate tensile resistance for the original connection C3

Note : As the connections have been designed to resist shear, this design is not detailed here. Only the tensile strength part is explained.

1 Datas

1. HEM300

$$h_c = 340\ mm$$
$$b_c = 310\ mm$$
$$t_{fc} = 39\ mm$$
$$t_{wc} = 21\ mm$$
$$f_{yc} = 355\ MPa$$
$$f_{uc} = 490\ MPa$$
$$A_c = 30,310\ mm^2$$

2. IPE600

$$h_b = 600\ mm$$
$$b_b = 220\ mm$$
$$t_{fb} = 19\ mm$$
$$t_{wb} = 12\ mm$$
$$r_b = 24\ mm$$
$$d_b = 467.6\ mm$$
$$f_{yb} = 355\ MPa$$
$$f_{ub} = 490\ MPa$$
$$A_b = 15,600\ mm^2$$

3. Fin plate

$$h_p = 300\ mm$$
$$b_p = 150\ mm$$
$$t_p = 10\ mm$$
$$f_{yb} = 355\ MPa$$
$$f_{ub} = 490\ MPa$$
$$a = 6\ mm$$

4. Bolt patern

$$
\begin{aligned}
&M24\ 10.9\\
&d = 24\ mm\\
&d_0 = 26\ mm\\
&a_s = 353\ mm^2\\
&f_{yb} = 355\ MPa\\
&f_{ub} = 490\ MPa\\
&n_1 = 4\\
&n_2 = 2
\end{aligned}
$$

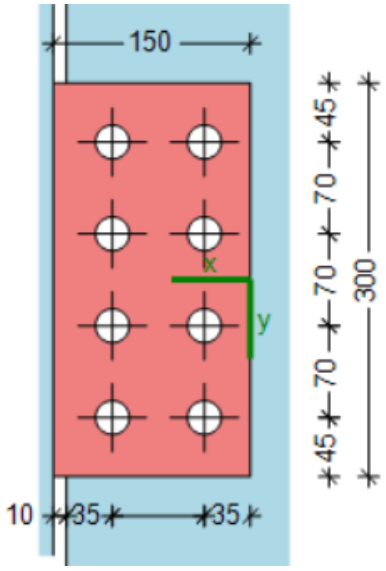

Figure H.1: View of the connection C3

2 Requirement to allow a plastic redistribution of internal forces

1. $V_{Rd} < \min(V_{Rd,1}; V_{Rd,7}) \rightarrow 443.6 < \min(630.2; +\infty) \rightarrow$ Ok
2. Note for this point, the value of the parameter are taken from the software COP
   $$\max\left(\frac{1}{F_{v,Rd}^2}\cdot(\alpha^2+\beta^2); \frac{1}{V_{Rd,7}^2}\right) \leq \left(\frac{\alpha}{F_{b,ver,Rd}}\right)^2 + \left(\frac{\beta}{F_{b,hor,Rd}}\right)^2$$

   For the beam web

   $$\Leftrightarrow \max\left(\frac{1}{141200^2}\cdot(0.04762^2+0.1429^2); 0\right) \leq \left(\frac{0.04762}{151200}\right)^2 + \left(\frac{0.1429}{104800}\right)^2$$

   $$\Leftrightarrow \max\left(1.13\cdot10^{-12}; 0\right) \leq 1.96\cdot10^{-12} \rightarrow \text{NOK}$$

   For the fin plate

   $$\Leftrightarrow \max\left(\frac{1}{98000^2}\cdot(0.04762^2+0.1429^2); 0\right) \leq \left(\frac{0.04762}{112300}\right)^2 + \left(\frac{0.1429}{87350}\right)^2$$

   $$\Leftrightarrow \max\left(1.13\cdot10^{-12}; 0\right) \leq 2.85\cdot10^{-12} \rightarrow \text{OK}$$

3 Requirements to ensure sufficient rotation capacity

1. $h_p \leq d_b \Leftrightarrow 300\ mm \leq 514\ mm \rightarrow$ Ok
2. $\phi_{available} > \phi_{required}$
   where,

$$\phi_{available} = \left(\frac{z}{\sqrt{(z-g_h)^2 + \left(\frac{h_p}{2} + h_e\right)^2}} \right) - \arctan\left(\frac{z-g_h}{\frac{h_p}{2} + h_e} \right)$$

where,
$z = g_h + e_{2b} + p_{21}/2$
$h_e = (h_b - h_p)/2$

$$\phi_{available} = \left(\frac{80}{\sqrt{(80-10)^2 + \left(\frac{300}{2} + 150\right)^2}} \right) - \arctan\left(\frac{80-10}{\frac{300}{2} + 150} \right) = 0.0335\ rad$$

$\phi_{required} = 0.0071$ coming from Finelg

$0.0335 > 0.0071 \rightarrow$ Ok

4 Requirement to ensure the ductility

$$a > \frac{\beta_w \cdot f_{yp} \cdot \gamma_{M2} \cdot t_p}{\sqrt{2} \cdot f_{up} \cdot \gamma_{M0}}$$

$$6\ mm > \frac{0.9 \cdot 355 \cdot 1.25 \cdot 10}{\sqrt{2} \cdot 490 \cdot 1.0} = 5.76\ mm$$

5 Computation of the resistance to tying forces

1. Bolts in shear

$$\begin{aligned} N_{u,1} &= n \cdot F_{v,u} \\ &= n \cdot \alpha_v \cdot f_{ub} \cdot A/\gamma_{Mu} \\ &= 8 \cdot 0.5 \cdot 353 \cdot 1000/1.1 = 1,238.6\ kN \end{aligned}$$

2. Fin plate in bearing

$$\begin{aligned} N_{u,2} &= n \cdot F_{b,u,hor} \\ &= n \cdot k_1 \cdot \alpha_b \cdot f_{up} \cdot d \cdot t_p/\gamma_{Mu} \\ &= 8 \cdot 2.07 \cdot 0.449 \cdot 490 \cdot 24 \cdot 10/1.1 = 794.12\ kN \end{aligned}$$

where,

$$\alpha_b = \min\left(\frac{e_2}{3 \cdot d_0}; \frac{p_2}{3 \cdot d_0} - 0.25; \frac{f_{ub}}{f_{up}}\right)$$
$$= \min\left(\frac{35}{78}; \frac{80}{78} - 0.25; 1\right) = 0.449$$

$$k_1 = \min\left(\frac{2.8 \cdot e_1}{d_0} - 1.7; 1.4 \cdot \frac{p_1}{d_0} - 1.7; 2.5\right)$$
$$= \min\left(\frac{2.8 \cdot 45}{26} - 1.7; 1.4 \cdot \frac{70}{26} - 1.7; 2.5\right) = 2.07$$

3. Fin plate in tension, gross section

$$N_{u,3} = t_p \cdot h_p \cdot f_{up}/\gamma_{Mu}$$
$$= 10 \cdot 300 \cdot 490/1.1 = 1,336.4\ kN$$

4. Fin plate in tension, net section

$$N_{u,4} = 0.9 \cdot A_{net,p} \cdot f_{up}/\gamma_{Mu}$$
$$= 0.9 \cdot (10 \cdot 300 - 26 \cdot 4 \cdot 10) \cdot 490/1.1 = 785.78\ kN$$

5. Beam web in bearing

$$N_{u,5} = n \cdot F_{b,u,hor}$$
$$= n \cdot k_1 \cdot \alpha_b \cdot f_{up} \cdot d \cdot t_{bw}/\gamma_{Mu}$$
$$= 8 \cdot 2.07 \cdot 0.449 \cdot 490 \cdot 24 \cdot 12/1.1 = 952.95\ kN$$

where,

$$\alpha_b = \min\left(\frac{e_{2b}}{3 \cdot d_0}; \frac{p_2}{3 \cdot d_0} - 0.25; \frac{f_{ub}}{f_{up}}\right)$$
$$= \min\left(\frac{35}{78}; \frac{80}{78} - 0.25; 1\right) = 0.449$$

$$k_1 = \min\left(1.4 \cdot \frac{p_1}{d_0} - 1.7; 2.5\right)$$
$$= \min\left(1.4 \cdot \frac{70}{26} - 1.7; 2.5\right) = 2.07$$

6. Beam web in tension gross section

$$N_{u,6} = t_{bw} \cdot h_{bw} \cdot f_{ubw}/\gamma_{Mu}$$
$$= 12 \cdot 514 \cdot 490/1.1 = 2,747.6\ kN$$

7. Beam web in tension, net section

$$N_{u,7} = 0.9 \cdot A_{net,bw} \cdot f_{ubw}/\gamma_{Mu}$$
$$= 0.9 \cdot (12 \cdot 514 - 26 \cdot 4 \cdot 12) \cdot 490/1.1 = 1,972.47\ kN$$

8. Supporting member in bending

$$N_{u,8} = +\infty$$

I Appendix : Ultimate tensile resistance for the original connection D3w

Note : As the connections have been designed to resist shear, this design is not detailed here. Only the tensile strength part is explained.

1 Datas

1. HEM300

$$h_c = 340\ mm$$
$$b_c = 310\ mm$$
$$t_{fc} = 39\ mm$$
$$t_{wc} = 21\ mm$$
$$f_{yc} = 355\ MPa$$
$$f_{uc} = 490\ MPa$$
$$A_c = 30,310\ mm^2$$

2. HEA300

$$h_b = 290\ mm$$
$$b_b = 300\ mm$$
$$t_{fb} = 14\ mm$$
$$t_{wb} = 8.5\ mm$$
$$r_b = 27\ mm$$
$$d_b = 208\ mm$$
$$f_{yb} = 355\ MPa$$
$$f_{ub} = 490\ MPa$$

3. Fin plate

$$h_p = 200\ mm$$
$$b_p = 130\ mm$$
$$t_p = 10\ mm$$
$$f_{yb} = 355\ MPa$$
$$f_{ub} = 490\ MPa$$
$$a = 6\ mm$$

4. Bolt patern

$$
\begin{aligned}
&M20\ 10.9\\
&d = 20\ mm\\
&d_0 = 22\ mm\\
&a_s = 245\ mm^2\\
&f_{yb} = 355\ MPa\\
&f_{ub} = 490\ MPa\\
&n_1 = 3\\
&n_2 = 2
\end{aligned}
$$

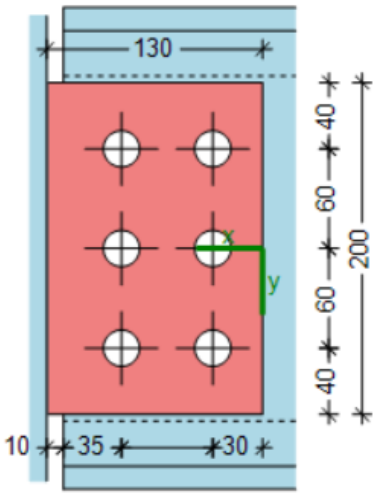

Figure I.1: View of the connection

2 Requirement to allow a plastic redistribution of internal forces

1. $V_{Rd} < \min(V_{Rd,1}; V_{Rd,7}) \rightarrow 216.9 < \min(275.3; +\infty) \rightarrow$ Ok
2. Note for this point, the value of the parameter are taken from the software COP

$$\max\left(\frac{1}{F_{v,Rd}^2}\cdot(\alpha^2+\beta^2); \frac{1}{V_{Rd,7}^2}\right) \leq \left(\frac{\alpha}{F_{b,ver,Rd}}\right)^2 + \left(\frac{\beta}{F_{b,hor,Rd}}\right)^2$$

For the beam web

$$\Leftrightarrow \max\left(\frac{1}{98000^2}\cdot(0.1053^2+0.2297^2); \frac{1}{\infty^2}\right) \leq \left(\frac{0.1053}{79060}\right)^2 + \left(\frac{0.2297}{74860}\right)^2$$

$$\Leftrightarrow \max\left(6.64\cdot10^{-12}; 0\right) \leq 1.11\cdot10^{-11} \rightarrow \text{OK}$$

For the fin plate

$$\Leftrightarrow \max\left(\frac{1}{98000^2}\cdot(0.1053^2+0.2297^2); \frac{1}{\infty^2}\right) \leq \left(\frac{0.1053}{85530}\right)^2 + \left(\frac{0.2297}{75480}\right)^2$$

$$\Leftrightarrow \max\left(6.64\cdot10^{-12}; 0\right) \leq 1.07\cdot10^{-11} \rightarrow \text{OK}$$

3 Requirements to ensure sufficient rotation capacity

1. $h_p \leq d_b \Leftrightarrow 140\ mm \leq 208\ mm \rightarrow$ Ok
2. $\phi_{available} > \phi_{required}$
   where,

$$\phi_{available} = \left(\frac{z}{\sqrt{(z-g_h)^2 + \left(\frac{h_p}{2} + h_e\right)^2}} \right) - \arctan\left(\frac{z-g_h}{\frac{h_p}{2} + h_e} \right)$$

where,
$z = g_h + e_{2b} + p_{21}/2$
$h_e = (h_b - h_p)/2$

$$\phi_{available} = \left(\frac{67.5}{\sqrt{(67.5-10)^2 + \left(\frac{140}{2} + 75\right)^2}} \right) - \arctan\left(\frac{67.5-10}{\frac{140}{2} + 75} \right) = 0.07\ rad$$

$\phi_{required} = 0.002$ coming from Finelg

$0.07 > 0.002 \rightarrow$ Ok

4 Requirement to ensure the ductility

$$a > \frac{\beta_w \cdot f_{yp} \cdot \gamma_{M2} \cdot t_p}{\sqrt{2} \cdot f_{up} \cdot \gamma_{M0}}$$

$$6\ mm > \frac{0.9 \cdot 355 \cdot 1.25 \cdot 10}{\sqrt{2} \cdot 490 \cdot 1.0} = 5.76\ mm$$

5 Computation of the resistance to tying forces

1. Bolts in shear

$$\begin{aligned} N_{u,1} &= n \cdot F_{v,u} \\ &= n \cdot \alpha_v \cdot f_{ub} \cdot A/\gamma_{Mu} \\ &= 6 \cdot 0.5 \cdot 245 \cdot 1000/1.1 = 668.18\ kN \end{aligned}$$

2. Fin plate in bearing

$$\begin{aligned} N_{u,2} &= n \cdot F_{b,u,hor} \\ &= n \cdot k_1 \cdot \alpha_b \cdot f_{up} \cdot d \cdot t_p/\gamma_{Mu} \\ &= 6 \cdot 2.12 \cdot 0.454 \cdot 490 \cdot 20 \cdot 10/1.1 = 514.67\ kN \end{aligned}$$

where,

$$\alpha_b = \min\left(\frac{e_2}{3\cdot d_0}; \frac{p_2}{3\cdot d_0} - 0.25; \frac{f_{ub}}{f_{up}}\right)$$
$$= \min\left(\frac{30}{66}; \frac{55}{66} - 0.25; 1\right) = 0.454$$

$$k_1 = \min\left(\frac{2.8\cdot e_1}{d_0} - 1.7; 1.4\cdot\frac{p_1}{d_0} - 1.7; 2.5\right)$$
$$= \min\left(\frac{2.8\cdot 40}{22} - 1.7; 1.4\cdot\frac{60}{22} - 1.7; 2.5\right) = 2.12$$

3. Fin plate in tension, gross section

$$N_{u,3} = t_p\cdot h_p\cdot f_{up}/\gamma_{Mu}$$
$$= 10\cdot 200\cdot 490/1.1 = 890.9\ kN$$

4. Fin plate in tension, net section

$$N_{u,4} = 0.9\cdot A_{net,p}\cdot f_{up}/\gamma_{Mu}$$
$$= 0.9\cdot(10\cdot 200 - 22\cdot 3\cdot 10)\cdot 490/1.1 = 537.22\ kN$$

5. Beam web in bearing

$$N_{u,5} = n\cdot F_{b,u,hor}$$
$$= n\cdot k_1\cdot\alpha_b\cdot f_{up}\cdot d\cdot t_{bw}/\gamma_{Mu}$$
$$= 6\cdot 2.12\cdot 0.53\cdot 490\cdot 20\cdot 8.5/1.1 = 510.38\ kN$$

where,

$$\alpha_b = \min\left(\frac{e_{2b}}{3\cdot d_0}; \frac{p_2}{3\cdot d_0} - 0.25; \frac{f_{ub}}{f_{up}}\right)$$
$$= \min\left(\frac{35}{66}; \frac{55}{66} - 0.25; 1\right) = 0.53$$

$$k_1 = \min\left(1.4\cdot\frac{p_1}{d_0} - 1.7; 2.5\right)$$
$$= \min\left(1.4\cdot\frac{60}{22} - 1.7; 2.5\right) = 2.12$$

6. Beam web in tension, gross section

$$N_{u,6} = t_{bw}\cdot h_{bw}\cdot f_{ubw}/\gamma_{Mu}$$
$$= 18.5\cdot 208\cdot 490/1.1 = 1,714.11\ kN$$

7. Beam web in tension, net section

$$N_{u,7} = 0.9\cdot A_{net,bw}\cdot f_{ubw}/\gamma_{Mu}$$
$$= 0.9\cdot(8.5\cdot 208 - 22\cdot 3\cdot 8.5)\cdot 490/1.1 = 483.9\ kN$$

8. Supporting member in bending

$$N_{u,8} = +\infty$$

J Appendix : Ultimate tensile resistance for the original connection D3s

Note : As the connections have been designed to resist shear, this design is not detailed here. Only the tensile strength part is explained.

1 Datas

1. HEM300

$$h_c = 340\ mm$$
$$b_c = 310\ mm$$
$$t_{fc} = 39\ mm$$
$$t_{wc} = 21\ mm$$
$$f_{yc} = 355\ MPa$$
$$f_{uc} = 490\ MPa$$
$$A_c = 30,310\ mm^2$$

2. HEA300

$$h_b = 290\ mm$$
$$b_b = 300\ mm$$
$$t_{fb} = 14\ mm$$
$$t_{wb} = 8.5\ mm$$
$$r_b = 27\ mm$$
$$d_b = 208\ mm$$
$$f_{yb} = 355\ MPa$$
$$f_{ub} = 490\ MPa$$

3. Fin plate

$$h_p = 200\ mm$$
$$b_p = 130\ mm$$
$$t_p = 10\ mm$$
$$f_{yb} = 355\ MPa$$
$$f_{ub} = 490\ MPa$$
$$a = 6\ mm$$

4. Bolt patern

$$
\begin{aligned}
&M20\ 10.9\\
&d = 20\ mm\\
&d_0 = 22\ mm\\
&a_s = 245\ mm^2\\
&f_{yb} = 355\ MPa\\
&f_{ub} = 490\ MPa\\
&n_1 = 3\\
&n_2 = 2
\end{aligned}
$$

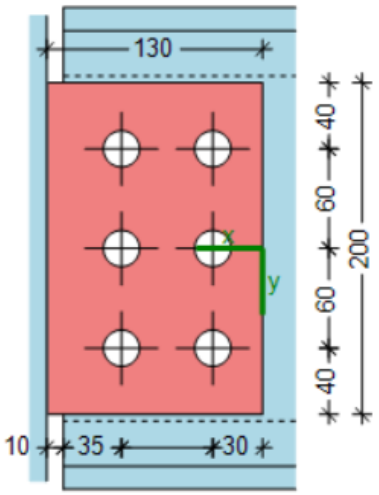

Figure J.1: View of the connection

2 Requirement to allow a plastic redistribution of internal forces

1. $V_{Rd} < \min(V_{Rd,1}; V_{Rd,7}) \rightarrow 216.9 < \min(275.3; +\infty) \rightarrow$ Ok
2. Note for this point, the value of the parameter are taken from the software COP
   $$\max\left(\frac{1}{F_{v,Rd}^2}\cdot(\alpha^2+\beta^2); \frac{1}{V_{Rd,7}^2}\right) \leq \left(\frac{\alpha}{F_{b,ver,Rd}}\right)^2 + \left(\frac{\beta}{F_{b,hor,Rd}}\right)^2$$

   For the beam web

   $$\Leftrightarrow \max\left(\frac{1}{98000^2}\cdot(0.1053^2+0.2297^2); \frac{1}{\infty^2}\right) \leq \left(\frac{0.1053}{79060}\right)^2 + \left(\frac{0.2297}{74860}\right)^2$$

   $$\Leftrightarrow \max\left(6.64\cdot10^{-12}; 0\right) \leq 1.11\cdot10^{-11} \rightarrow \text{OK}$$

   For the fin plate

   $$\Leftrightarrow \max\left(\frac{1}{98000^2}\cdot(0.1053^2+0.2297^2); \frac{1}{\infty^2}\right) \leq \left(\frac{0.1053}{85530}\right)^2 + \left(\frac{0.2297}{75480}\right)^2$$

   $$\Leftrightarrow \max\left(6.64\cdot10^{-12}; 0\right) \leq 1.07\cdot10^{-11} \rightarrow \text{OK}$$

3 Requirements to ensure sufficient rotation capacity

1. $h_p \leq d_b \Leftrightarrow 140\ mm \leq 208\ mm \rightarrow$ Ok
2. $\phi_{available} > \phi_{required}$
   where,

$$\phi_{available} = \left(\frac{z}{\sqrt{(z-g_h)^2 + \left(\frac{h_p}{2} + h_e\right)^2}} \right) - \arctan\left(\frac{z-g_h}{\frac{h_p}{2} + h_e} \right)$$

where,
$z = g_h + e_{2b} + p_{21}/2$
$h_e = (h_b - h_p)/2$

$$\phi_{available} = \left(\frac{82.5}{\sqrt{(82.5-10)^2 + \left(\frac{140}{2} + 75\right)^2}} \right) - \arctan\left(\frac{82.5-10}{\frac{140}{2} + 75} \right) = 0.07\ rad$$

$\phi_{required} = 0.002$ coming from Finelg

$0.07 > 0.002 \rightarrow$ Ok

4 Requirement to ensure the ductility

$$a > \frac{\beta_w \cdot f_{yp} \cdot \gamma_{M2} \cdot t_p}{\sqrt{2} \cdot f_{up} \cdot \gamma_{M0}}$$

$$6\ mm > \frac{0.9 \cdot 355 \cdot 1.25 \cdot 10}{\sqrt{2} \cdot 490 \cdot 1.0} = 5.76\ mm$$

5 Computation of the resistance to tying forces

1. Bolts in shear

$$\begin{aligned} N_{u,1} &= n \cdot F_{v,u} \\ &= n \cdot \alpha_v \cdot f_{ub} \cdot A/\gamma_{Mu} \\ &= 6 \cdot 0.5 \cdot 245 \cdot 1000/1.1 = 668.18\ kN \end{aligned}$$

2. Fin plate in bearing

$$\begin{aligned} N_{u,2} &= n \cdot F_{b,u,hor} \\ &= n \cdot k_1 \cdot \alpha_b \cdot f_{up} \cdot d \cdot t_p/\gamma_{Mu} \\ &= 6 \cdot 2.12 \cdot 0.454 \cdot 490 \cdot 20 \cdot 10/1.1 = 514.67\ kN \end{aligned}$$

where,

$$\begin{aligned}\alpha_b &= \min\left(\frac{e_2}{3\cdot d_0}; \frac{p_2}{3\cdot d_0} - 0.25; \frac{f_{ub}}{f_{up}}\right)\\ &= \min\left(\frac{30}{66}; \frac{55}{66} - 0.25; 1\right) = 0.454\end{aligned}$$

$$\begin{aligned}k_1 &= \min\left(\frac{2.8\cdot e_1}{d_0} - 1.7; 1.4\cdot\frac{p_1}{d_0} - 1.7; 2.5\right)\\ &= \min\left(\frac{2.8\cdot 40}{22} - 1.7; 1.4\cdot\frac{60}{22} - 1.7; 2.5\right) = 2.12\end{aligned}$$

3. Fin plate in tension, gross section

$$\begin{aligned}N_{u,3} &= t_p\cdot h_p\cdot f_{up}/\gamma_{Mu}\\ &= 10\cdot 200\cdot 490/1.1 = 890.9\ kN\end{aligned}$$

4. Fin plate in tension, net section

$$\begin{aligned}N_{u,4} &= 0.9\cdot A_{net,p}\cdot f_{up}/\gamma_{Mu}\\ &= 0.9\cdot(10\cdot 200 - 22\cdot 3\cdot 10)\cdot 490/1.1 = 537.22\ kN\end{aligned}$$

5. Beam web in bearing

$$\begin{aligned}N_{u,5} &= n\cdot F_{b,u,hor}\\ &= n\cdot k_1\cdot\alpha_b\cdot f_{up}\cdot d\cdot t_{bw}/\gamma_{Mu}\\ &= 6\cdot 2.12\cdot 0.583\cdot 490\cdot 20\cdot 11.1/1.1 = 733.14\ kN\end{aligned}$$

where,

$$\begin{aligned}\alpha_b &= \min\left(\frac{e_{2b}}{3\cdot d_0}; \frac{p_2}{3\cdot d_0} - 0.25; \frac{f_{ub}}{f_{up}}\right)\\ &= \min\left(\frac{55}{66}; \frac{55}{66} - 0.25; 1\right) = 0.583\end{aligned}$$

$$\begin{aligned}k_1 &= \min\left(1.4\cdot\frac{p_1}{d_0} - 1.7; 2.5\right)\\ &= \min\left(1.4\cdot\frac{60}{22} - 1.7; 2.5\right) = 2.12\end{aligned}$$

6. Beam web in tension, gross section

$$\begin{aligned}N_{u,6} &= t_{bw}\cdot h_{bw}\cdot f_{ubw}/\gamma_{Mu}\\ &= 8.5\cdot 208\cdot 490/1.1 = 787.56\ kN\end{aligned}$$

7. Beam web in tension, net section

$$\begin{aligned}N_{u,7} &= 0.9\cdot A_{net,bw}\cdot f_{ubw}/\gamma_{Mu}\\ &= 0.9\cdot(8.5\cdot 208 - 22\cdot 3\cdot 8.5)\cdot 490/1.1 = 483.9\ kN\end{aligned}$$

8. Supporting member in bending

$$N_{u,8} = +\infty$$

K Appendix : Ultimate tensile resistance for the header plate connection B1

Note : As the connections have been designed to resist shear, this design is not detailed here. Only the tensile strength part is explained.

1 Datas

1. HEB340

$$
\begin{aligned}
h_c &= 340\ mm \\
b_c &= 300\ mm \\
t_{fc} &= 21.5\ mm \\
t_{wc} &= 12\ mm \\
f_{yc} &= 355\ MPa \\
f_{uc} &= 490\ MPa \\
A_c &= 17,090\ mm^2
\end{aligned}
$$

2. IPE550

$$
\begin{aligned}
h_b &= 550\ mm \\
b_b &= 210\ mm \\
t_{fb} &= 17.2\ mm \\
t_{wb} &= 11.1\ mm \\
r_b &= 24\ mm \\
d_b &= 467.6\ mm \\
f_{yb} &= 355\ MPa \\
f_{ub} &= 490\ MPa \\
A_b &= 17,090\ mm^2
\end{aligned}
$$

3. Header plate

$$h_p = 210\ mm$$
$$b_p = 150\ mm$$
$$t_p = 4\ mm$$
$$f_{yb} = 355\ MPa$$
$$f_{ub} = 490\ MPa$$
$$a = 7\ mm$$

4. Bolt patern

$M20$ 10.9
$$d = 20\ mm$$
$$d_0 = 22\ mm$$
$$A_s = 245\ mm^2$$
$$f_{yb} = 355\ MPa$$
$$f_{ub} = 490\ MPa$$
$$n_1 = 2$$
$$n_2 = 2$$

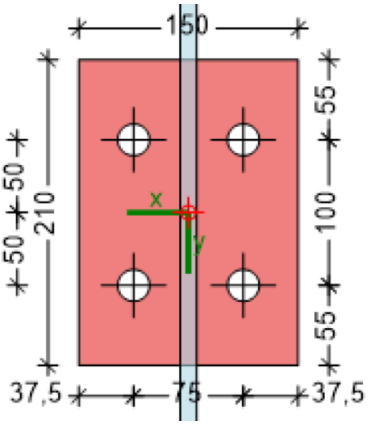

Figure K.1: View of the connection

2 Requirement to allow a plastic redistribution of internal forces

1. $h_p \leq d_b \leftrightarrow 210\ mm \leq 467.6\ mm$

2. $\dfrac{t_p}{h_e} > \phi_{required} \leftrightarrow \dfrac{4}{195} > 0.0065$

3. $\dfrac{d}{t_p} \geq 2.8 \cdot \sqrt{\dfrac{f_{yp}}{f_{ub}}}$ OR $\dfrac{d}{t_{cf}} \geq 2.8 \cdot \sqrt{\dfrac{f_{ycf}}{f_{ub}}}$
$\leftrightarrow \dfrac{20}{4} \geq 2.8 \cdot \sqrt{\dfrac{355}{1000}}$ OR $\dfrac{20}{21.5} \geq 2.8 \cdot \sqrt{\dfrac{355}{1000}}$
$\leftrightarrow 5 \geq 1.67 \rightarrow OK$ OR $0.93 \geq 1.67 \rightarrow NOK$

4. $a \geq \dfrac{\beta_w \cdot f_{ybw} \cdot \gamma_{M2} \cdot t_{bw}}{\sqrt{2} \cdot f_{ubw} \cdot \gamma_{M0}}$
$\leftrightarrow 7 \geq \dfrac{0.9 \cdot 355 \cdot 1.25 \cdot 11.1}{\sqrt{2} \cdot 490 \cdot 1}$
$\leftrightarrow 7 \geq 6.4 \rightarrow OK$

3 Computation of the resistance to tying forces

1. Bolts tension

$$\begin{aligned} N_{u,1} &= n \cdot B_{t,u} \\ &= n \cdot f_{ub} \cdot A_s/\gamma_{Mu} \\ &= 4 \cdot 1000 \cdot 245/1.1 = 890.91\ kN \end{aligned}$$

2. Header plate in bending

$$N_{u,2} = \min(F_{hp,u,1}, F_{hp,u,2})$$

where,

$$F_{hp,u,1} = \frac{(8 \cdot n_p - 2 \cdot e_w) \cdot l_{eff,p,t,1} \cdot m_{u,p}}{2 \cdot m_p \cdot n_p - e_w \cdot (m_p + n_p)}$$

$$F_{hp,u,2} = \frac{2 \cdot l_{eff,p,t,2} \cdot m_{u,p} + n \cdot B_{t,u} \cdot n_p}{m_p + n_p}$$

with,

$$n_p = \min(e_2; 1.25 \cdot m_p) = (37.5; 1.25 \cdot 27.58) = 34.48\ mm$$

$$m_{u,p} = \frac{t_p^2 \cdot f_{up}}{4 \cdot \gamma_{mu}} = \frac{4^2 \cdot 490}{4 \cdot 1.1} = 1,781.81\ N$$

$$l_{eff,pt,1} = l_{eff,pt,2} = h_p = 210\ mm$$

so,

$$F_{hp,u,1} = \frac{(8 \cdot 34.48 - 2 \cdot 9.25) \cdot 210 \cdot 1781.81}{2 \cdot 27.58 \cdot 34.48 - 9.25 \cdot (27.58 + 34.48)} = 75.52\ kN$$

$$F_{hp,u,2} = \frac{2 \cdot 210 \cdot 1781.81 + 4 \cdot 245000 \cdot 34.48}{27.58 + 34.48} = 507.9\ kN$$

and,

$$N_{u,2} = 72.52\ kN$$

3. Supporting member in bending

	Isolated bolt row	
	Circular mecanism	Non circular mecanism
Interior bolt row	$2 \cdot \pi \cdot m = 62.2\ mm$	$4 \cdot m + 1.25 \cdot e = 180.22\ mm$
exterior bolt row	$2 \cdot \pi \cdot m = 62.2\ mm$	$4 \cdot m + 1.25 \cdot e = 180.22\ mm$
Mode 1	$L_{eff,1} = 62.2\ mm$	
Mode 2	$L_{eff,2} = 180.23\ mm$	
	Group bolt row	
Interior bolt row	$2 \cdot p = 200\ mm$	$p = 100\ mm$
exterior bolt row	$\pi \cdot m + p = 131.1\ mm$	$2 \cdot m + 0,625 \cdot e + 0,5 \cdot p = 140.11\ mm$
Mode 1	$L_{eff,1} = 262.2\ mm$	
Mode 2	$L_{eff,2} = 280.23\ mm$	

Table K.1: Effective lengths

with,

$$m = (p_2 - t_{w,c} - 2 \cdot 0.8 \cdot r_c) \cdot 0.5 = (75 - 12 - 2 \cdot 0.8 \cdot 27) \cdot 0.5 = 9.9 \ mm$$
$$e = (b_c - p_2) \cdot 0.5 = (300 - 75) \cdot 0.5 = 112.5 \ mm$$
$$n = \min(e_2; 1.25 \cdot m) = \min(37.5; 1.25 \cdot 9.9) = 12.37 \ mm$$

Resistance for isolated bolt row, no leverage effect
Mode 1 = Mode 2 :

$$F_{T,1-2,u,iso} = \frac{2 \cdot \frac{0.25 \cdot \sum l_{eff,1} \cdot t_f^2 \cdot f_u}{\gamma_{Mu}}}{m} = \frac{2 \cdot \frac{0.25 \cdot 62.2 \cdot 21.5^2 \cdot 490}{1.1}}{9.9} = 646.84 \ kN$$

Mode 3 :

$$F_{T,3,u,iso} = 2 \cdot 1000 \cdot 245/1.1 = 445.45 \ kN$$

Resistance for group bolt, no leverage effect
Mode 1 = Mode 2 :

$$F_{T,1-2,u,iso} = \frac{2 \cdot \frac{0.25 \cdot \sum l_{eff,1} \cdot t_f^2 \cdot f_u}{\gamma_{Mu}}}{m} = \frac{2 \cdot \frac{0.25 \cdot 262.2 \cdot 21.5^2 \cdot 490}{1.1}}{9.9} = 2,726.8 \ kN$$

Mode 3 :

$$F_{T,3,u,goup} = 4 \cdot 1000 \cdot 245/1.1 = 890.9 \ kN$$

Ultimate tensile strength resistant :

$$N_{u,3} = \min\left(\min(2 \cdot F_{T,1-2,u,iso}; 2 \cdot F_{T,3,u,iso}); \min(F_{T,1-2,u,group}; F_{T,3,u,group})\right) = 890.9 \ kN$$

4. Beam web in tension

$$N_{u,4} = t_{w,b} \cdot h_p \cdot f_{ubw}/\gamma_{Mu} = 11.1 \cdot 210 \cdot 490/1.1 = 1,038.35 \ kN$$

L Appendix : Ultimate tensile resistance for the header plate connection B3

Note : As the connections have been designed to resist shear, this design is not detailed here. Only the tensile strength part is explained.

1 Datas

1. HEM300

$$h_c = 340\ mm$$
$$b_c = 310\ mm$$
$$t_{fc} = 39\ mm$$
$$t_{wc} = 21\ mm$$
$$f_{yc} = 355\ MPa$$
$$f_{uc} = 490\ MPa$$
$$A_c = 30,310\ mm^2$$

2. IPE550

$$h_b = 550\ mm$$
$$b_b = 210\ mm$$
$$t_{fb} = 17.2\ mm$$
$$t_{wb} = 11.1\ mm$$
$$r_b = 24\ mm$$
$$d_b = 467.6\ mm$$
$$f_{yb} = 355\ MPa$$
$$f_{ub} = 490\ MPa$$
$$A_b = 17,090\ mm^2$$

3. Header plate

$$h_p = 210\ mm$$
$$b_p = 150\ mm$$
$$t_p = 4\ mm$$
$$f_{yb} = 355\ MPa$$
$$f_{ub} = 490\ MPa$$
$$a = 7\ mm$$

4. Bolt patern

$M20$ 10.9
$$d = 20\ mm$$
$$d_0 = 22\ mm$$
$$A_s = 245\ mm^2$$
$$f_{yb} = 355\ MPa$$
$$f_{ub} = 490\ MPa$$
$$n_1 = 2$$
$$n_2 = 2$$

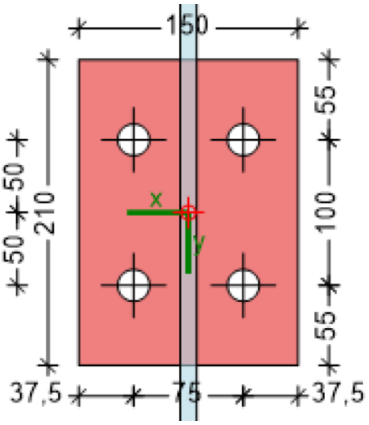

Figure L.1: View of the connection

2 Requirement to allow a plastic redistribution of internal forces

1. $h_p \leq d_b \leftrightarrow 210\ mm \leq 467.6\ mm$

2. $\dfrac{t_p}{h_e} > \phi_{required} \leftrightarrow \dfrac{4}{170} > 0.0065$

3. $\dfrac{d}{t_p} \geq 2.8 \cdot \sqrt{\dfrac{f_{yp}}{f_{ub}}}$ OR $\dfrac{d}{t_{cf}} \geq 2.8 \cdot \sqrt{\dfrac{f_{ycf}}{f_{ub}}}$
$\leftrightarrow \dfrac{20}{4} \geq 2.8 \cdot \sqrt{\dfrac{355}{1000}}$ OR $\dfrac{20}{39} \geq 2.8 \cdot \sqrt{\dfrac{355}{1000}}$
$\leftrightarrow 5 \geq 1.67 \rightarrow OK$ OR $0.51 \geq 1.67 \rightarrow NOK$

4. $a \geq \dfrac{\beta_w \cdot f_{ybw} \cdot \gamma_{M2} \cdot t_{bw}}{\sqrt{2} \cdot f_{ubw} \cdot \gamma_{M0}}$
$\leftrightarrow 7 \geq \dfrac{0.9 \cdot 355 \cdot 1.25 \cdot 11.1}{\sqrt{2} \cdot 490 \cdot 1}$
$\leftrightarrow 7 \geq 6.4 \rightarrow OK$

3 Computation of the resistance to tying forces

1. Bolts tension

$$\begin{aligned} N_{u,1} &= n \cdot B_{t,u} \\ &= n \cdot f_{ub} \cdot A_s/\gamma_{Mu} \\ &= 4 \cdot 1000 \cdot 245/1.1 = 890.91\ kN \end{aligned}$$

2. Header plate in bending

$$N_{u,2} = \min(F_{hp,u,1}, F_{hp,u,2})$$

where,

$$F_{hp,u,1} = \frac{(8 \cdot n_p - 2 \cdot e_w) \cdot l_{eff,p,t,1} \cdot m_{u,p}}{2 \cdot m_p \cdot n_p - e_w \cdot (m_p + n_p)}$$

$$F_{hp,u,2} = \frac{2 \cdot l_{eff,p,t,2} \cdot m_{u,p} + n \cdot B_{t,u} \cdot n_p}{m_p + n_p}$$

with,

$$n_p = \min(e_2; 1.25 \cdot m_p) = (37.5; 1.25 \cdot 27.58) = 34.48\ mm$$

$$m_{u,p} = \frac{t_p^2 \cdot f_{up}}{4 \cdot \gamma_{mu}} = \frac{4^2 \cdot 490}{4 \cdot 1.1} = 1,781.82\ N$$

$$l_{eff,pt,1} = l_{eff,pt,2} = h_p = 210\ mm$$

so,

$$F_{hp,u,1} = \frac{(8 \cdot 34.48 - 2 \cdot 9.25) \cdot 210 \cdot 1,781.82}{2 \cdot 27.58 \cdot 34.48 - 9.25 \cdot (27.58 + 34.48)} = 72.51\ kN$$

$$F_{hp,u,2} = \frac{2 \cdot 210 \cdot 1,781.82 + 4 \cdot 245000 \cdot 34.48}{27.58 + 34.48} = 507.01\ kN$$

and,

$$N_{u,2} = 75.52\ kN$$

3. Supporting member in bending

	Isolated bolt row	
	Circular mecanism	Non circular mecanism
Interior bolt row	$2 \cdot \pi \cdot m = 33.93\ mm$	$4 \cdot m + 1.25 \cdot e = 168.48\ mm$
exterior bolt row	$2 \cdot \pi \cdot m = 33.93\ mm$	$4 \cdot m + 1.25 \cdot e = 168.48\ mm$
Mode 1	$L_{eff,1} = 33.93\ mm$	
Mode 2	$L_{eff,2} = 168.48\ mm$	
	Group bolt row	
Interior bolt row	$2 \cdot p = 200\ mm$	$p = 100\ mm$
exterior bolt row	$\pi \cdot m + p = 116.96\ mm$	$2 \cdot m + 0,625 \cdot e + 0,5 \cdot p = 134.24\ mm$
Mode 1	$L_{eff,1} = 233.93\ mm$	
Mode 2	$L_{eff,2} = 268.48\ mm$	

Table L.1: Effective lengths

with,

$$\begin{aligned} m &= (p_2 - t_{w,c} - 2 \cdot 0.8 \cdot r_c) \cdot 0.5 = (75 - 21 - 2 \cdot 0.8 \cdot 27) \cdot 0.5 = 5.4 \ mm \\ e &= (b_c - p_2) \cdot 0.5 = (310 - 75) \cdot 0.5 = 117.5 \ mm \\ n &= \min(e_2; 1.25 \cdot m) = \min(37.5; 1.25 \cdot 5.4) = 6.75 \ mm \end{aligned}$$

Resistance for isolated bolt row, no leverage effect
Mode 1 = Mode 2 :

$$\begin{aligned} F_{T,1-2,u,iso} &= \frac{2 \cdot \frac{0.25 \cdot \sum l_{eff,1} \cdot t_f^2 \cdot f_u}{\gamma_{Mu}}}{m} \\ &= \frac{2 \cdot \frac{0.25 \cdot 33.93 \cdot 39^2 \cdot 490}{1.1}}{5.4} = 2,128.54 \ kN \end{aligned}$$

Mode 3 :

$$F_{T,3,u,iso} = 2 \cdot 1000 \cdot 245/1.1 = 445.05 \ kN$$

Resistance for group bolt, no leverage effect
Mode 1 = Mode 2 :

$$\begin{aligned} F_{T,1-2,u,group} &= \frac{2 \cdot \frac{0.25 \cdot \sum l_{eff,1} \cdot t_f^2 \cdot f_u}{\gamma_{Mu}}}{m} \\ &= \frac{2 \cdot \frac{0.25 \cdot 233.93 \cdot 39^2 \cdot 490}{1.1}}{5.4} = 14,675.57 \ kN \end{aligned}$$

Mode 3 :

$$F_{T,3,u,goup} = 4 \cdot 1000 \cdot 245/1.1 = 890.91 \ kN$$

Ultimate tensile strength resistant :

$$\begin{aligned} N_{u,3} &= \min\left(\min(2 \cdot F_{T,1-2,u,iso}; 2 \cdot F_{T,3,u,iso}); \min(F_{T,1-2,u,group}; F_{T,3,u,group})\right) \\ &= 890.91 \ kN \end{aligned}$$

4. Beam web in tension

$$\begin{aligned} N_{u,4} &= t_{w,b} \cdot h_p \cdot f_{ubw}/\gamma_{Mu} \\ &= 11.1 \cdot 210 \cdot 490/1.1 = 1,038.35 \ kN \end{aligned}$$

M Appendix : Ultimate tensile resistance for the header plate connection C2

Note : As the connections have been designed to resist shear, this design is not detailed here. Only the tensile strength part is explained.

1 Datas

1. HEB360

$$h_c = 360\ mm$$
$$b_c = 300\ mm$$
$$t_{fc} = 22.5\ mm$$
$$t_{wc} = 12.5\ mm$$
$$f_{yc} = 355\ MPa$$
$$f_{uc} = 490\ MPa$$
$$A_c = 18,060\ mm^2$$

2. IPE600

$$h_b = 600\ mm$$
$$b_b = 220\ mm$$
$$t_{fb} = 19\ mm$$
$$t_{wb} = 12\ mm$$
$$r_b = 24\ mm$$
$$d_b = 467.6\ mm$$
$$f_{yb} = 355\ MPa$$
$$f_{ub} = 490\ MPa$$
$$A_b = 15,600\ mm^2$$

3. Header plate

$$h_p = 210\ mm$$
$$b_p = 150\ mm$$
$$t_p = 8\ mm$$
$$f_{yb} = 355\ MPa$$
$$f_{ub} = 490\ MPa$$
$$a = 7\ mm$$

4. Bolt patern

$$M20\ 10.9$$
$$d = 20\ mm$$
$$d_0 = 22\ mm$$
$$A_s = 245\ mm^2$$
$$f_{yb} = 355\ MPa$$
$$f_{ub} = 490\ MPa$$
$$n_1 = 3$$
$$n_2 = 2$$

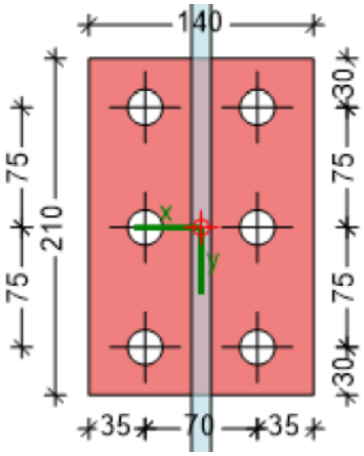

Figure M.1: View of the connection

2 Requirement to allow a plastic redistribution of internal forces

1. $h_p \leq d_b \leftrightarrow 210\ mm \leq 514\ mm$

2. $\frac{t_p}{h_e} > \phi_{required} \leftrightarrow \frac{8}{195} > 0.01$

3. $\frac{d}{t_p} \geq 2.8 \cdot \sqrt{\frac{f_{yp}}{f_{ub}}}$ OR $\frac{d}{t_{cf}} \geq 2.8 \cdot \sqrt{\frac{f_{ycf}}{f_{ub}}}$
$\leftrightarrow \frac{20}{8} \geq 2.8 \cdot \sqrt{\frac{355}{1000}}$ OR $\frac{20}{12.5} \geq 2.8 \cdot \sqrt{\frac{355}{1000}}$
$\leftrightarrow 2.5 \geq 1.67 \rightarrow OK$ OR $1.6 \geq 1.67 \rightarrow NOK$

4. $a \geq \frac{\beta_w \cdot f_{ybw} \cdot \gamma_{M2} \cdot t_{bw}}{\sqrt{2} \cdot f_{ubw} \cdot \gamma_{M0}}$
$\leftrightarrow 7 \geq \frac{0.9 \cdot 355 \cdot 1.25 \cdot 12}{\sqrt{2} \cdot 490 \cdot 1}$
$\leftrightarrow 7 \geq 6.92 \rightarrow OK$

3 Computation of the resistance to tying forces

1. Bolts tension

$$\begin{aligned} N_{u,1} &= n \cdot B_{t,u} \\ &= n \cdot f_{ub} \cdot A_s/\gamma_{Mu} \\ &= 6 \cdot 1000 \cdot 245/1.1 = 1,336.36\ kN \end{aligned}$$

2. Header plate in bending

$$N_{u,2} = \min(F_{hp,u,1}, F_{hp,u,2})$$

where,

$$\begin{aligned} F_{hp,u,1} &= \frac{(8 \cdot n_p - 2 \cdot e_w) \cdot l_{eff,p,t,1} \cdot m_{u,p}}{2 \cdot m_p \cdot n_p - e_w \cdot (m_p + n_p)} \\ F_{hp,u,2} &= \frac{2 \cdot l_{eff,p,t,2} \cdot m_{u,p} + n \cdot B_{t,u} \cdot n_p}{m_p + n_p} \end{aligned}$$

with,

$$\begin{aligned} n_p &= \min(e_2; 1.25 \cdot m_p) = (35; 1.25 \cdot 23.08) = 28.85\ mm \\ m_{u,p} &= \frac{t_p^2 \cdot f_{up}}{4 \cdot \gamma_{mu}} = \frac{8^2 \cdot 490}{4 \cdot 1.1} = 7,127.27\ N \\ l_{eff,pt,1} &= l_{eff,pt,2} = h_p = 210\ mm \end{aligned}$$

so,

$$\begin{aligned} F_{hp,u,1} &= \frac{(8 \cdot 28.85 - 2 \cdot 9.25) \cdot 210 \cdot 7,127.27}{2 \cdot 23.08 \cdot 28.85 - 9.25 \cdot (23.08 + 28.85)} = 373.22\ kN \\ F_{hp,u,2} &= \frac{2 \cdot 210 \cdot 7,127.27 + 6 \cdot 245000 \cdot 28.85}{23.08 + 28.85} = 800.07\ kN \end{aligned}$$

and,

$$N_{u,2} = 373.22\ kN$$

3. Supporting member in bending

$$\begin{aligned} N_{u,3} &= \frac{k_n \cdot f_{u,c} \cdot t_{w,c}^2}{\left(1 - \frac{p_2}{d_c}\right)} \cdot \left[2 \cdot \frac{p_2}{d_c} + 4 \cdot \sqrt{1 - \frac{p_2}{d_c}}\right] \\ &= \frac{1.0 \cdot 490 \cdot 12.5^2}{\left(1 - \frac{70}{360}\right)} \cdot \left[2 \cdot \frac{70}{360} + 4 \cdot \sqrt{1 - \frac{70}{360}}\right] = 378.18\ kN \end{aligned}$$

4. Beam web in tension

$$\begin{aligned} N_{u,4} &= t_{w,b} \cdot h_p \cdot f_{ubw}/\gamma_{Mu} \\ &= 12 \cdot 210 \cdot 490/1.1 = 1,122.55\ kN \end{aligned}$$

N Appendix : Ultimate tensile resistance for the header plate connection C3

Note : As the connections have been designed to resist shear, this design is not detailed here. Only the tensile strength part is explained.

1 Datas

1. HEM300

$$h_c = 340\ mm$$
$$b_c = 310\ mm$$
$$t_{fc} = 39\ mm$$
$$t_{wc} = 21\ mm$$
$$f_{yc} = 355\ MPa$$
$$f_{uc} = 490\ MPa$$
$$A_c = 30,310\ mm^2$$

2. IPE600

$$h_b = 600\ mm$$
$$b_b = 220\ mm$$
$$t_{fb} = 19\ mm$$
$$t_{wb} = 12\ mm$$
$$r_b = 24\ mm$$
$$d_b = 467.6\ mm$$
$$f_{yb} = 355\ MPa$$
$$f_{ub} = 490\ MPa$$
$$A_b = 15,600\ mm^2$$

3. Header plate

$$
\begin{aligned}
h_p &= 210\ mm \\
b_p &= 150\ mm \\
t_p &= 8\ mm \\
f_{yb} &= 355\ MPa \\
f_{ub} &= 490\ MPa \\
a &= 7\ mm
\end{aligned}
$$

4. Bolt patern

$$
\begin{aligned}
&M20\ 10.9 \\
d &= 20\ mm \\
d_0 &= 22\ mm \\
A_s &= 245\ mm^2 \\
f_{yb} &= 355\ MPa \\
f_{ub} &= 490\ MPa \\
n_1 &= 3 \\
n_2 &= 2
\end{aligned}
$$

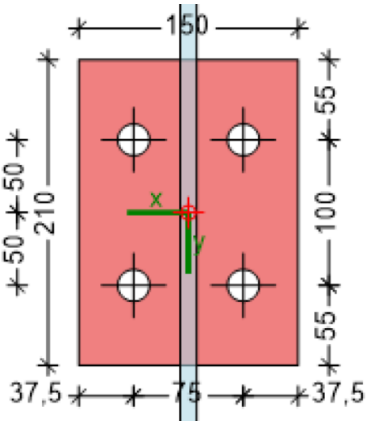

Figure N.1: View of the connection

2 Requirement to allow a plastic redistribution of internal forces

1. $h_p \leq d_b \leftrightarrow 210\ mm \leq 514\ mm$

2. $\dfrac{t_p}{h_e} > \phi_{required} \leftrightarrow \dfrac{8}{195} > 0.01$

3. $\dfrac{d}{t_p} \geq 2.8 \cdot \sqrt{\dfrac{f_{yp}}{f_{ub}}}$ OR $\dfrac{d}{t_{cf}} \geq 2.8 \cdot \sqrt{\dfrac{f_{ycf}}{f_{ub}}}$
$\leftrightarrow \dfrac{20}{8} \geq 2.8 \cdot \sqrt{\dfrac{355}{1000}}$ OR $\dfrac{20}{12.5} \geq 2.8 \cdot \sqrt{\dfrac{355}{1000}}$
$\leftrightarrow 2.5 \geq 1.67 \rightarrow OK$ OR $1.6 \geq 1.67 \rightarrow NOK$

4. $a \geq \dfrac{\beta_w \cdot f_{ybw} \cdot \gamma_{M2} \cdot t_{bw}}{\sqrt{2} \cdot f_{ubw} \cdot \gamma_{M0}}$
$\leftrightarrow 7 \geq \dfrac{0.9 \cdot 355 \cdot 1.25 \cdot 12}{\sqrt{2} \cdot 490 \cdot 1}$
$\leftrightarrow 7 \geq 6.92 \rightarrow OK$

3 Computation of the resistance to tying forces

1. Bolts tension

$$\begin{aligned} N_{u,1} &= n \cdot B_{t,u} \\ &= n \cdot f_{ub} \cdot A_s / \gamma_{Mu} \\ &= 6 \cdot 1000 \cdot 245 / 1.1 = 1,336.4 \ kN \end{aligned}$$

2. Header plate in bending

$$N_{u,2} = \min(F_{hp,u,1}, F_{hp,u,2})$$

where,

$$\begin{aligned} F_{hp,u,1} &= \frac{(8 \cdot n_p - 2 \cdot e_w) \cdot l_{eff,p,t,1} \cdot m_{u,p}}{2 \cdot m_p \cdot n_p - e_w \cdot (m_p + n_p)} \\ F_{hp,u,2} &= \frac{2 \cdot l_{eff,p,t,2} \cdot m_{u,p} + n \cdot B_{t,u} \cdot n_p}{m_p + n_p} \end{aligned}$$

with,

$$\begin{aligned} n_p &= \min(e_2; 1.25 \cdot m_p) = (35; 1.25 \cdot 23.08) = 28.85 \ mm \\ m_{u,p} &= \frac{t_p^2 \cdot f_{up}}{4 \cdot \gamma_{mu}} = \frac{8^2 \cdot 490}{4 \cdot 1.1} = 7,127.27 \ N \\ l_{eff,pt,1} &= l_{eff,pt,2} = h_p = 210 \ mm \end{aligned}$$

so,

$$\begin{aligned} F_{hp,u,1} &= \frac{(8 \cdot 28.85 - 2 \cdot 9.25) \cdot 210 \cdot 7,127.27}{2 \cdot 23.08 \cdot 28.85 - 9.25 \cdot (23.08 + 28.85)} = 373.22 \ kN \\ F_{hp,u,2} &= \frac{2 \cdot 210 \cdot 7,127.27 + 6 \cdot 245000 \cdot 28.85}{23.08 + 28.85} = 800.07 \ kN \end{aligned}$$

and,

$$N_{u,2} = 373.22 \ kN$$

3. Supporting member in bending

$$N_{u,3} = +\infty$$

4. Beam web in tension

$$\begin{aligned} N_{u,4} &= t_{w,b} \cdot h_p \cdot f_{ubw} / \gamma_{Mu} \\ &= 12 \cdot 210 \cdot 490 / 1.1 = 1,122.55 \ kN \end{aligned}$$

O Appendix : Design of the slab

As a reminder, the design office imposed a slab thickness of 0.2 m.

The load combination to design the slab is

$$\begin{aligned} q_{slab} &= 1.35 \cdot \text{Dead load} + 1.5 \cdot \text{Live load} + 1.5 \cdot 0.5 \cdot \text{Snow} + 1.5 \cdot 0.6 \cdot \text{Wind} \\ &= 1.35 \cdot 5 + 1.5 \cdot 3 + 1.5 \cdot 0.5 \cdot 0.68 \\ &= 11.76 \ kN/m^2 \end{aligned} \tag{O.1}$$

As seen previously, the slab rests on beams spaced at 2.66 m. In order to design the slab, a 1 m wide section is studied. The static scheme is therefore summarised as a 1 m wide slab supported on 19 supports with 18 spans of 2.66 m.
The maximum bending moment can be calculated by tables,

$$\begin{aligned} \text{at support} \ : M_{Ed,support} &= 0.1053 \cdot q \cdot L^2 \\ &= 0.1053 \cdot 11.76 \cdot 2.66^2 \\ &= 8.76 \ kN.m \end{aligned}$$

$$\begin{aligned} \text{in span} : M_{Ed,support} &= 0.0777 \cdot q \cdot L^2 \\ &= 0.077 \cdot 11.76 \cdot 2.66^2 \\ &= 6.41 \ kN.m \end{aligned}$$

Thus, the slab is designed to sustain the bending moment $M_{Ed,support} = 8.76 \ kN.m$.

Assuming that the reinforcement yields before the concrete has reached failure, the bending moment resistant is

$$M_{Rd} = A_s \cdot f_{yd} \cdot z$$

In order to control cracks in the slab, the bars should be spaced a maximum of 200 mm apart. In the 1 m portion of the slab there should be at least 5 bars.
Moreover, the concrete cover is $c = 20 \ mm$.

Assuming the bars are 8 mm in diameter, and the steel grade S500, the resistance is,

$$M_{Rd} = (5 \cdot 4^2 \cdot \pi) \cdot 435 \cdot (0.9 \cdot (200 - 20 - 4)) = 17.31 \ kN.m$$

which is higher than the applied bending moment.

To comply with the second principle of reinforced concrete, the area of the steel must be greater than a minimum value $A_{s,min}$. Assuming a concrete of class C30/37, it gives

$$A_{s,min} = 0.26 \cdot \frac{f_{ctm}}{f_{yk}} \cdot b \cdot d = 0.26 \cdot \frac{2.9}{500} \cdot 1000 \cdot (200 - 20 - 4) = 265.41 \ mm^2 \tag{O.2}$$

But the area of steel $A_s = 5 \cdot 4^2 \cdot \pi = 250\ mm^2$ is lower than the minimal value. So the reinforcement has to be increased to $\phi 10$.

The new resistant bending moment is,

$$M_{Rd} = (5 \cdot 5^2 \cdot \pi) \cdot 435 \cdot (0.9 \cdot (200 - 20 - 5)) = 26.9\ kN.m$$

The same reinforcement is provided in the other direction.

The details of the section is given in Figure O.1.

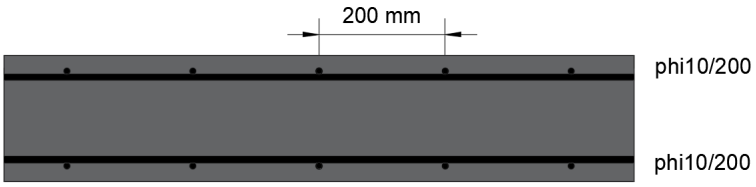

Figure O.1: Design of the slab.

The last verification to be made is to check if the failure appears by yielding of the reinforcements and not by crushing of the concrete. For this purpose, the height of the concrete zone in compression is first sought. It can be obtained by means of a horizontal equilibrium in section, see Figure O.2.

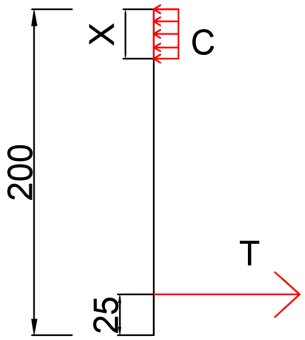

Figure O.2: Horizontal equilibrium in section

The horizontal equilibrium when the reinforcement yield is,

$$\begin{aligned} T &= C \\ 5 \cdot A_s \cdot f_{yd} &= \lambda \cdot \eta \cdot b \cdot x \cdot f_{cd} \\ 5 \cdot (\pi \cdot 5^{2)} \cdot 435 &= 0.8 \cdot 1 \cdot 1000 \cdot x \cdot 17 \\ x &= 12.56\ mm \end{aligned} \tag{O.3}$$

The stress in the concrete is

$$\begin{aligned} \sigma_c &= \frac{5 \cdot A_s \cdot f_{yd}}{b \cdot x} \\ &= \frac{5 \cdot (\pi \cdot 5^{2)} \cdot 435}{1000 \cdot 12.56} \\ &= 13.6\ Mpa \end{aligned} \tag{O.4}$$

Since the compression stress in concrete is lower than f_{cd}, the concrete doesn't crush and the bending resistance is governed by the yielding of the reinforcement.